



**EXPERIMENTAL INVESTIGATION OF THE WIND
ENERGY GENERATION FROM VEHICLE
MOVEMENT ON HIGHWAYS USING THE
DOUBLE TURBINE SYSTEM**

**2023
MASTER THESIS
MECHANICAL ENGINEERING**

Osama Ahmed Kazal KAZAL

**Thesis Advisor
Assist. Prof. Dr. Mehmet BAKIRCI**

**EXPERIMENTAL INVESTIGATING OF THE WIND ENERGY
GENERATION FROM VEHICLE MOVEMENT ON HIGHWAYS USING
THE DOUBLE TURBINE SYSTEM**

Osama Ahmed Kazal KAZAL

Thesis Advisor

Assist. Prof. Dr. Mehmet BAKIRCI

T.C.

Karabük University

Institute of Graduate Programs

Department of Mechanical Engineering

Prepared as

Master Thesis

KARABÜK

December 2023

I certify that in my opinion, the thesis submitted by Osama Ahmed Kazal KAZAL titled “EXPERIMENTAL INVESTIGATING OF THE WIND ENERGY GENERATION FROM VEHICLE MOVEMENT ON HIGHWAYS USING THE DOUBLE TURBINE SYSTEM” is fully adequate in scope and in quality as a thesis for the degree of Master of Science.

Assist. Prof. Dr. Mehmet BAKIRCI
Thesis Advisor, Department of Mechanical Engineering

This thesis is accepted by the examining committee with unanimous vote in the Department of Mechanical Engineering as a Master of Science thesis.7/12/2023

Examining Committee Members (Institutions) Signature

Chairman : Assoc. Prof. Dr. Okan ÜNAL (KBU)

Member : Assoc. Prof. Dr. Battal DOĞAN (GU)

Member : Assist. Prof. Dr. Mehmet BAKIRCI (KBU)

The degree of Master of Science by the thesis submitted is approved by the Administrative Board of the Institute of Graduate Programs, Karabük University.

Assoc. Prof. Dr. Zeynep ÖZCAN
Director of the Institute of Graduate Programs

“This thesis contains information that I have gathered and presented in a manner that is consistent with academic regulations and ethical principles, and I affirm that I have appropriately cited any and all sources that are not my own work.”

Osama Ahmed Kazal KAZAL

ABSTRACT

M.Sc. Thesis

EXPERIMENTAL INVESTIGATING OF THE WIND ENERGY GENERATION FROM VEHICLE MOVEMENT ON HIGHWAYS USING THE DOUBLE TURBINE SYSTEM

Osama Ahmed Kazal KAZAL

**Karabük University
Institute of Graduate Programs
Department of Mechanical Engineering**

Thesis Advisor:

Assist. Prof. Dr. Mehmet BAKIRCI

December 2023, 103 pages

Renewable energy has seen significant development in the past decade, with a focus on methods of displacing fossil fuels and providing clean energy through horizontal and vertical axis turbines. This study investigates the potential to harvest and save energy from highways, a largely untapped source that could contribute to reducing reliance on fossil fuels and grid-based electricity. The study proposes the double turbine model that combines the Savonius and Darrieus vertical wind turbines to maximize energy generation. The model was designed using SolidWorks 2023 software and manufactured using a 3D printer with environmentally friendly PLA material. Experiments were conducted to evaluate the performance of the double turbine under different conditions. Internal tests compared the double turbine to the Savonius and Darrieus turbines, and explored different distances between the Savonius and Darrieus blades. External tests evaluated the performance of the double turbine at

different heights and distances from the highway. Final tests investigated the power generated by the double turbine in response to different types of vehicles. The results of the internal tests showed that the double turbine outperformed the Savonius and Darrieus turbines in terms of power generation. The double turbine also generated more power when the distance between the Savonius and Darrieus blades was 15 cm. The results of the external tests showed that the double turbine performed best at a height of 100 cm from the ground and a distance of 100 cm from the highway. The double turbine also generated the most power when trucks passed in front of it, reaching a maximum power of 50 W. The results of this study demonstrate the potential of the double turbine model to generate clean and renewable energy from highways. The double turbine outperformed traditional turbines, and its versatility suggests that it could be used in a variety of applications.

Keywords : Double turbine, highway energy harvesting, renewable energy, wind turbine, Savonius turbine, Darrieus turbine

Science Code : 91441

ÖZET

Yüksek Lisans Tezi

ÇİFT TÜRBİN SİSTEMİ KULLANILARAK KARAYOLLARINDA ARAÇ HAREKETİNDEN RÜZGAR ENERJİSİ ÜRETİMİNİN DENEYSEL OLARAK İNCELENMESİ

Osama Ahmed Kazal KAZAL

Karabük Üniversitesi

Lisansüstü Eğitim Enstitüsü

Makine Mühendisliği Anabilim Dalı

Tez Danışmanı:

Dr. Öğr. Üyesi Mehmet BAKIRCI

Aralık 2023,103 sayfa

Yenilenebilir enerji, fosil yakıtların yerini alma ve yatay ve dikey eksenli türbinler aracılığıyla temiz enerji sağlama yöntemlerine odaklanılarak son on yılda önemli bir gelişme kaydetti. Bu tez, fosil yakıtlara ve şebekeye dayalı elektriğe olan bağımlılığın azaltılmasına katkıda bulunabilecek, büyük ölçüde kullanılmayan bir kaynak olan otoyollardan enerji toplama ve tasarruf etme potansiyelini ele aldı. Çalışma, enerji üretimini maksimuma çıkarmak için Savonius ve Darrieus dikey rüzgar türbinlerini birleştiren bir Çift türbin modelini önermektedir. Model, SolidWorks 2023 yazılımı kullanılarak tasarlanmış ve çevre dostu PLA malzemesinden 3D yazıcı kullanılarak üretilmiştir. Çift türbinin performansını farklı koşullar altında değerlendirmek için deneyler yapıldı. Dahili testler, Çift türbin performansını, Savonius ve Darrieus türbinleriyle karşılaştırdı ve Savonius ve Darrieus kanatları arasındaki farklı mesafelerin güç performansına etkileri araştırıldı. Harici testler, çift türbinin

performansını, otoyoldan farklı yüksekliklerde ve mesafelerde değerlendirildi. Son testler ile, araç türünün Çift türbin modeli ile üretilen enerji miktarı üzerindeki etkisi hesaplandı. Dahili testlerin sonuçları, çift türbinin enerji üretimi açısından Savonius ve Darrieus türbinlerinden daha iyi performansa sahip olduğunu ortaya koydu. Çift türbin, Savonius ve Darrieus kanatları arasındaki mesafe 15 cm olduğunda da daha fazla güç ürettiyordu. Harici testlerin sonuçları, çift türbinin yerden 100 cm yükseklikte ve otoyoldan 100 cm mesafede en iyi performansı gösterdiğini gösterdi. Çift türbin, kamyonların önünden geçtiğinde de en fazla gücü üreterek maksimum 50 W güce ulaştı. Bu çalışmanın sonuçları, çift türbin modelinin otoyollardan temiz ve yenilenebilir enerji üretme potansiyelini ortaya koyuyor. Bu çalışmada önerilen Çift türbin, geleneksel türbinlerden daha iyi performans gösterdi ve çok yönlülüğü ile çeşitli uygulamalarda kullanılabileceğini dair ipuçları veriyor.

Anahtar Kelimeler: Çift türbin, karayolu enerji hasadı, yenilenebilir enerji, rüzgar türbini, Savonius türbini, Darrieus türbini

Bilim Kodu : 91441

ACKNOWLEDGMENT

In conclusion, I would like to begin my journey in advanced science with the following honourable hadith of our Prophet Muhammad, may God's prayers and peace be upon him, his family, and his companions: "He who does not thank people does not thank God."

I am grateful to everyone who has supported me on this path, especially my family, my mother, father, brothers, and wife, who have provided me with unwavering support. I am also grateful to my second country, Turkey, for providing me with the opportunity to pursue a master's degree and for their continued support. I am particularly indebted to my thesis supervisor, Dr. Mehmet BAKIRCI, for his knowledge, guidance, and constant encouragement. I also extend my sincere thanks and appreciation to all the professors in the Mechanics Department at the College of Engineering, led by Dr. Kamil ARSLAN.

I am grateful to the beautiful city of Karabük for its warmth and hospitality. I also thank everyone who has helped me in any way, whether with a letter, a word, or advice. I am especially grateful to Dr. Mustafa Ali Al-Maliki and Dr. Saud Tamim Al-Jader for their guidance and support.

As I embark on this new chapter, I am reminded of the following quote by the English writer Ernest Hemingway: "Wisdom comes from knowing what we learn, and science is learning what we do not know."

Finally, I pray to Almighty God to grant me health, safety, and inspiration to advance my scientific mission and pursue doctoral studies with determination and strength, after trusting in God.

CONTENTS

	<u>Page</u>
APPROVAL.....	ii
ABSTRACT.....	iv
ÖZET.....	vi
ACKNOWLEDGMENT.....	viii
CONTENTS.....	ix
LIST OF FIGURES	xii
LIST OF TABLES	xiv
LIST OF SYMBOLS AND ABBREVIATIONS	xv
PART 1	1
INTRODUCTION	1
1.1. BACKGROUND.....	1
1.2. EVOLUTION OF WIND TURBINE TECHNOLOGY	2
1.3. VERTICAL AXIS WIND TURBINES (VAWTS)	3
1.3.1. Matching Power to Wind Speed for Savonius and Darrieus VAWT.....	5
1.3.2. Savonius Vertical Wind Turbines	5
1.3.3. Darrieus Vertical Wind Turbines	6
1.4. RESEARCH GAP AND THE NEED FOR STUDY.....	7
1.5. GOALS OF THIS STUDY	8
1.6. THESIS OUTLINE	8
PART 2	10
LITERATURE SURVEY	10
2.1. INTRODUCTION.....	10
2.2. PREVIOUS STUDIES OF SAVONIUS TURBINE	11
2.2.1. The Theoretical Studies for Savonius.....	11
2.2.2. The Experimental Studies for Savonius	14
2.3. PREVIOUS STUDIES OF DARRIEUS TURBINE.....	16
2.3.1. The theoretical studies for Darrieus.....	16

	<u>Page</u>
2.3.2. The Experimental Studies for Darrieus	20
2.4. PREVIOUS STUDIES OF COMPOSITE AND HYBRID TURBINES.....	24
2.5. PREVIOUS STUDIES OF WIND TURBINES ON HIGHWAYS.....	27
2.6. SUMMARY	31
PART 3	33
EXPERIMENTAL PART	33
3.1. INTRODUCTION.....	33
3.2. EXPERIMENTAL SETUP	34
3.3.1. Manufacturing of Savonius Turbine.....	35
3.3.2. Manufacturing of Darrieus Turbine.....	37
3.3.3. The Chord	38
3.3.4. The Rotary Central Shaft.....	39
3.3.5. The Link Connection	40
3.3.6. The Electric Motor.....	41
3.3.7. The Structural Frame	41
3.4. MEASURING DEVICES	43
3.4.1. Current and Voltage Measuring Device	43
3.4.2. The Tachometer	44
3.4.3. The Anemometer	45
3.5. EXPERIMENTAL TESTING PROCEDURE.....	46
3.5.1. Internal Test.....	47
3.5.1.1. Savonius Test.....	48
3.5.1.2. Darrieus Test.....	48
3.5.1.3. Double Turbine Test	49
3.5.2. External Test.....	51
3.5.2.1. Distance Tests	53
3.5.2.2. Height Tests	54
3.5.3. Type of Single Vehicle	56
3.6. GOVERNING EQUATIONS	58
PART 4	61
RESULTS AND DISCUSSION	61

	<u>Page</u>
4.1. INTRODUCTION.....	61
4.2. RESULTS OF INTERNAL TESTS.....	61
4.2.1. Savonius Turbine Results	62
4.2.2. Darrieus Turbine Results	63
4.2.3. Double Turbine Results	65
4.2.4. Comparison Between Double Turbine Tests	69
4.2.5. Comparing the Best Double Turbine with Savonius and Darrieus Turbines.....	70
4.3. RESULT OF EXTERNAL TESTS	72
4.3.1. Effect of Turbine Distance Results.....	73
4.3.2. Comparison Between Distance Tests	77
4.3.3. Effect of Turbine Height Results.....	78
4.3.4. Comparison Between Height Tests	83
4.4. RESULTS OF SINGLE TYPE VEHICLE	84
 PART 5	 87
CONCLUSION AND RECOMMENDATIONS.....	87
5.1. CONCLUSION OF DOUBLE TURBINE.....	87
5.2. RECOMMENDATIONS AND SUGGESTION.....	88
 APPENDIX A.....	 97
 CURRICULUM VITAE	 103

LIST OF FIGURES

	<u>Page</u>
Figure 1.1. The percentages of various greenhouse gases in the atmosphere.	2
Figure 1.2. Typical Varieties of Vertical-Axis Wind Turbines: A Comprehensive Overview (a) Darrieus; (b) Savonius; (c)Solarwind; (d) Helical; (e)Noguchi; (f) Maglev; (g) Cochrane.....	4
Figure 1.3. Savonius Vertical Wind Turbine model.	6
Figure 1.4. Darrieus Vertical Wind Turbine model	7
Figure 3.1. Experimental setup chart	34
Figure 3.2. Proposed double turbine parts.	35
Figure 3.3. Savonius wind turbines with dimension.	36
Figure 3.4. Savonius turbine blades.	37
Figure 3.5. Darrieus airfoils design.	37
Figure 3.6. Manufacturing of Darrieus Blades.....	38
Figure 3.7. Chord design by solidworks.	39
Figure 3.8. The model manufactured by the 3D printer.....	39
Figure 3.9. Rotary shaft with dimensions.	40
Figure 3.10. Model of rotary shaft.	40
Figure 3.11. The link connection with dimensions.	40
Figure 3.12. Electric motor used.	41
Figure 3.13. Frame design with all dimensions.	42
Figure 3.14. Frame manufacturing.....	42
Figure 3.15. Current and voltage measuring device.	44
Figure 3.16. Digital tachometer.	45
Figure 3.17. Anemometer.	46
Figure 3.18. The schematic diagram of a steps for double turbine.	47
Figure 3.19. Savonius turbine test.....	48
Figure 3.20. Darrieus turbine test.....	49
Figure 3.21. Double turbine test third hole.	50
Figure 3.22. Double turbine test third hole.	51

	<u>Page</u>
Figure 3.23. The double turbine installation site.....	52
Figure 3.24. Distance test for double turbine at (A): Test D, (B): Test E, (C): Test F.	54
Figure 3.25. Height test for double turbine at (A): Test G, (B): Test H, (C): Test I.	56
Figure 3.26. type of single vehicle test for double turbine at (A): Test J, (B): Test K, (C): Test L, (D): Test M, (E): Test N.....	58
Figure 4.1. Schematic diagram of procedures.....	61
Figure 4.2. Comparison of different resistances of a $C_p - \lambda(TSR)$ for Savonius turbine.	63
Figure 4.3. Comparison of different resistances of a $C_p - \lambda(TSR)$ for Darrieus turbine.	64
Figure 4.4. Comparison of different resistances of a $C_p - \lambda(TSR)$ for double turbine (15cm).	66
Figure 4.5. Comparison of different resistances of a $C_p - \lambda(TSR)$ for double turbine (10cm).....	67
Figure 4.6. Comparison of different resistances of a $C_p - \lambda(TSR)$ for double turbine (5 cm).	68
Figure 4.7. Comparison the relationship of a $C_p - \lambda(TSR)$ for double turbine tests.	70
Figure 4.8. Comparison the relationship of a $C_p - \lambda(TSR)$ for double turbine and Savonius and Darrieus.	71
Figure 4.9. Flow Chart of The External Test.	73
Figure 4.10. $C_p - \lambda(TSR)$ for double turbine in Test D.....	74
Figure 4.11. Relation between C_p and $\lambda(TSR)$ for double turbine in Test E.....	75
Figure 4.12. Relation between C_p and $\lambda(TSR)$ for double turbine in Test F.	76
Figure 4.13. Comparison the relationship of a C_p and $\lambda(TSR)$ for double turbine in distance tests.	78
Figure 4.14. Relation between C_p and $\lambda(TSR)$ for double turbine in Test G.	79
Figure 4.15. Relation between C_p and $\lambda(TSR)$ for double turbine in Test H.	81
Figure 4.16. Relation between C_p and $\lambda(TSR)$ for double turbine in Test I.....	82
Figure 4.17. Comparison the relationship of a C_p and $\lambda(TSR)$ for double turbine in height tests.	83
Figure 4.18. Comparison of the relationship of the wind speed and test time for the double turbine in single vehicle tests.....	85
Figure 4.19. Comparison of the relationship of the power and test time for the double turbine in single vehicle tests.....	86

LIST OF TABLES

	<u>Page</u>
Table 4.1. Results and values of double turbine tests.	69
Table 4.2. Results and values of the best double turbine and Savonius and Darrieus	71
Table 4.3. Results and values of distance tests of the double turbine.....	77
Table 4.4. Results and values of height tests of the double turbine.....	83
Table 4.5. Data results of the vehicle types test.	85

LIST OF SYMBOLS AND ABBREVIATIONS

SYMBOL

P_{max}	: The maximum wind power
ω	: Angular velocity of the rotor
P_e	: Output electric power for the turbine
ρ	: The air density
r	: Radius of the turbine
A	: The turbine swept area
V	: The wind velocity or wind speed
D	: The diameter of the turbine
H	: The height of the turbine
$\lambda(TSR)$: The tip speed ratio
I	: The output current
V	: The output voltage difference
C_p	: The power coefficient of the wind turbine

ABBREVIATIONS

VAWT	: Vertical axis wind turbine
HAWT	: Horizontal axis wind turbine
RPM	: Revolution per minute
CFD	: Computational fluid dynamic
DNS	: Direct numerical simulation
SST	: Shear stress transfer

PART 1

INTRODUCTION

1.1. BACKGROUND

Wind energy has emerged as a vital and sustainable renewable energy source in response to the global need for clean and eco-friendly power generation. As the world confronts the challenges of climate change and the depletion of finite fossil fuel resources, wind energy technology has become a viable solution to reduce greenhouse gas emissions and provide a reliable source of electricity [1].

Wind energy has long been harnessed for various purposes, including milling grain, pumping water, and providing mechanical power for industrial processes. However, its importance in the contemporary energy landscape is underscored by the following factors [2]. Wind energy is a renewable resource that relies on the Earth's natural wind patterns. Unlike fossil fuels, it is inexhaustible and can play a pivotal role in reducing our dependence on finite energy sources[3]. Wind power generates electricity without the release of harmful pollutants or carbon emissions. Its deployment contributes significantly to mitigating climate change and reducing air pollution [4]. In addition to economic growth, the wind energy industry has witnessed significant growth in recent years, creating job opportunities, attracting investments, and promoting economic development in many countries. However, the high costs of fossil fuels and the associated financial market, making fuel a difficult currency that is not easy to obtain [5]. Figure 1.1 shows the percentages of greenhouse gases emitted due to human activities on a worldwide [6].

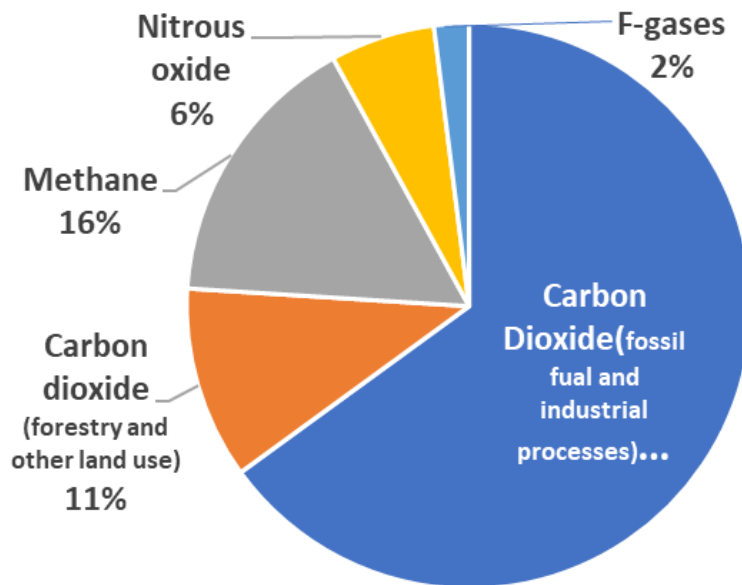


Figure 1.1. The percentages of various greenhouse gases in the atmosphere [6]

1.2. EVOLUTION OF WIND TURBINE TECHNOLOGY

Wind turbine technology has evolved significantly over the years. Traditionally, horizontal axis wind turbines (HAWTs) have been the dominant choice, characterized by their large, three-blade rotors mounted on a horizontal shaft. However, vertical axis wind turbines (VAWTs) have gained attention for their unique design and advantages [7].

Vertical Axis Wind Turbines (VAWTs) offer several benefits and advantages. Their omnidirectional capability allows them to capture wind from any direction, making them suitable for areas with variable or turbulent wind patterns. VAWTs tend to have a lower height profile than traditional horizontal axis wind turbines (HAWTs), which is advantageous in regions with height restrictions or aesthetic concerns. Additionally, VAWTs are known for their simplicity in design, often resulting in lower manufacturing and maintenance costs. Moreover, some VAWT designs, such as the Savonius, are capable of operating efficiently at low wind speeds, expanding the range of locations where wind energy can be harnessed. Furthermore, VAWTs can be used in both urban and rural environments, offering flexibility in deployment [7-9]. but they also come with certain disadvantages. One of the primary challenges is their relatively

lower efficiency compared to HAWTs, which means they may require a larger installation to generate the same amount of energy. VAWTs may also be less reliable in high wind speeds and turbulent conditions, leading to potential issues with durability. The unique design of VAWTs can result in increased drag, which impacts their overall performance. Additionally, the variability in the torque produced during the rotation of the vertical axis can pose challenges in terms of power generation stability [10].

1.3. VERTICAL AXIS WIND TURBINES (VAWTS)

Vertical Axis Wind Turbines (VAWTs) represent a distinctive and innovative approach to harnessing wind energy. These turbines exhibit a set of characteristics that set them apart from traditional horizontal axis wind turbines (HAWTs). One of the primary advantages of VAWTs is their omnidirectional capability, enabling them to capture wind from any direction, which makes them particularly well-suited for sites with unpredictable or turbulent wind patterns. Additionally, VAWTs are characterized by a low-profile design, a feature that proves advantageous in regions with height limitations or aesthetic considerations. This architectural adaptability also allows for discreet integration in urban and densely populated areas. The simplicity of VAWT design, exemplified by the Savonius model, contributes to cost-effectiveness in manufacturing and maintenance. Furthermore, certain VAWTs, like the Savonius, excel at generating power in low wind conditions, thus expanding the range of viable wind energy deployment sites. However, it's worth noting that VAWTs do have their challenges, including relatively lower overall efficiency compared to HAWTs, susceptibility to high winds, and variations in torque during rotation. Despite these limitations, the unique characteristics of VAWTs make them a compelling option in the diverse landscape of wind energy technologies, with the potential to address specific energy needs and spatial constraints in various applications. Vertical-axis wind turbines (VAWTs) come in various designs as shown in Fig 1.2, each with unique characteristics and advantages. The Darrieus VAWT, characterized by vertically oriented airfoil blades, is known for its high efficiency. The Savonius VAWT, with its simple half-cylinder blade design, excels at low-speed wind capture. The Solar Wind VAWT integrates solar panels with its vertical-axis design, offering a

dual energy generation solution. Helical VAWTs employ twisted blades to maximize wind capture efficiency. The Noguchi VAWT, with its helical twist and multiple blades, aims for enhanced power production. Maglev VAWTs utilize magnetic levitation for reduced friction and noise. Lastly, the Cochrane VAWT incorporates a unique blade design to enhance energy capture. These diverse VAWT designs cater to various wind conditions and site-specific requirements, providing flexibility and innovation in the field of wind energy. Figure 1.2 shows various shapes of vertical wind turbines [11].

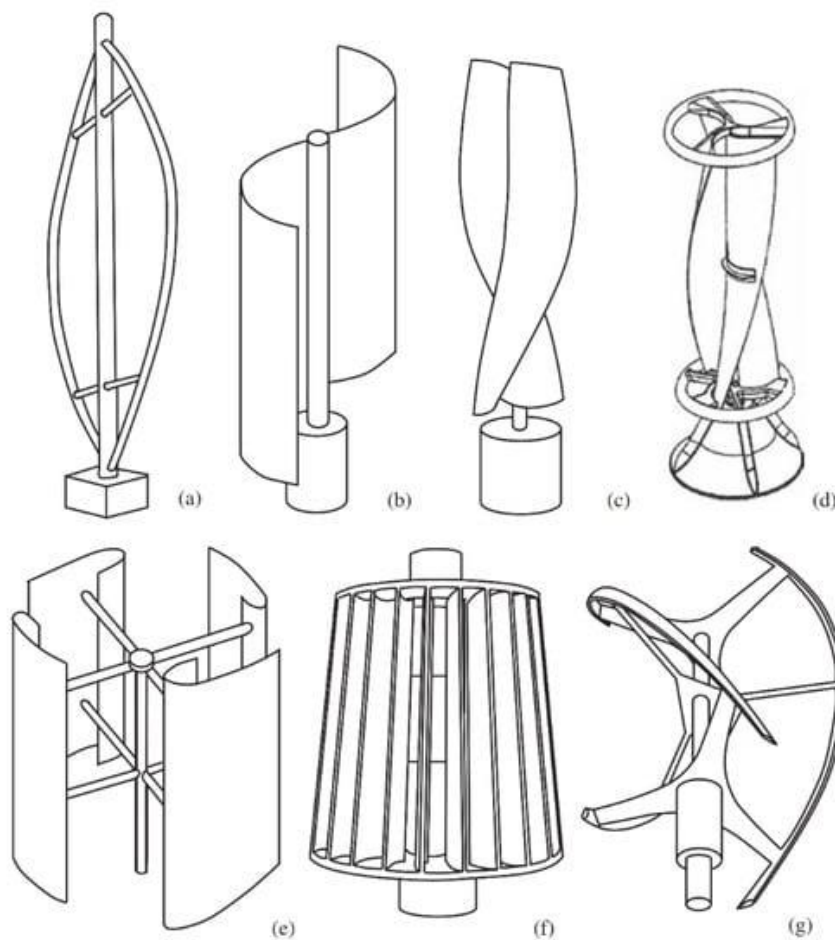


Figure 1.2. Typical Varieties of Vertical-Axis Wind Turbines: A Comprehensive Overview (a) Darrieus; (b) Savonius; (c)Solarwind; (d) Helical; (e)Noguchi; (f) Maglev; (g) Cochrane[11].

1.3.1. Matching Power to Wind Speed for Savonius and Darrieus VAWT

Tip speed ratio and maximum power coefficient (C_p) values vary significantly between Savonius and Darrieus wind turbines, impacting their suitability for different wind regimes. Savonius turbines excel at low wind speeds, with tip speed ratios typically ranging from 1 to 2 and a maximum C_p of 0.2 to 0.35. Their simple design and performance at low, constant speeds make them advantageous in low-wind environments. While increasing blade count can lower the starting threshold, it minimally impacts overall performance. Darrieus turbines, on the other hand, thrive in higher wind speeds, with typical tip speed ratios of 3 to 5 and a maximum C_p of 0.35 to 0.45. Their higher efficiency at higher speeds makes them a preferred choice for high-wind applications. Additionally, increasing blade count can improve starting performance at lower speeds and enhance overall efficiency in such conditions. When comparing power output, Darrieus turbines generally offer higher power coefficients and are more efficient at higher speeds. However, Savonius turbines can outperform at lower speeds and boast simpler constructions. Ultimately, the optimal turbine choice depends on the specific wind conditions, energy requirements, and environmental factors of the intended application.

1.3.2. Savonius Vertical Wind Turbines

Savonius Vertical Wind Turbines, named after their inventor Sigurd J. Savonius, represent a distinct and time-tested class of vertical-axis wind turbines (VAWTs) renowned for their simplicity and efficiency. Characterized by their robust and uncomplicated design, Savonius turbines consist of two or more curved, S-shaped blades forming a half-cylinder shape. This unique configuration allows them to capture wind energy even at low wind speeds, making them highly reliable in areas with variable or intermittent winds. Savonius VAWTs exhibit a low starting speed, which is advantageous for energy generation in urban and remote locations. However, it's important to note that their efficiency tends to be lower than some other wind turbine designs. Nevertheless, their durability and ability to operate in turbulent wind conditions, combined with the relatively low manufacturing and maintenance costs, have made them a compelling choice in various applications, including powering

small-scale devices, water pumping, and experimental wind energy research. As the push for renewable energy solutions intensifies, Savonius VAWTs continue to draw attention for their unique ability to capture wind energy efficiently and cost-effectively. Figure 1.3 shows one form of the Savonius vertical wind turbine [12].

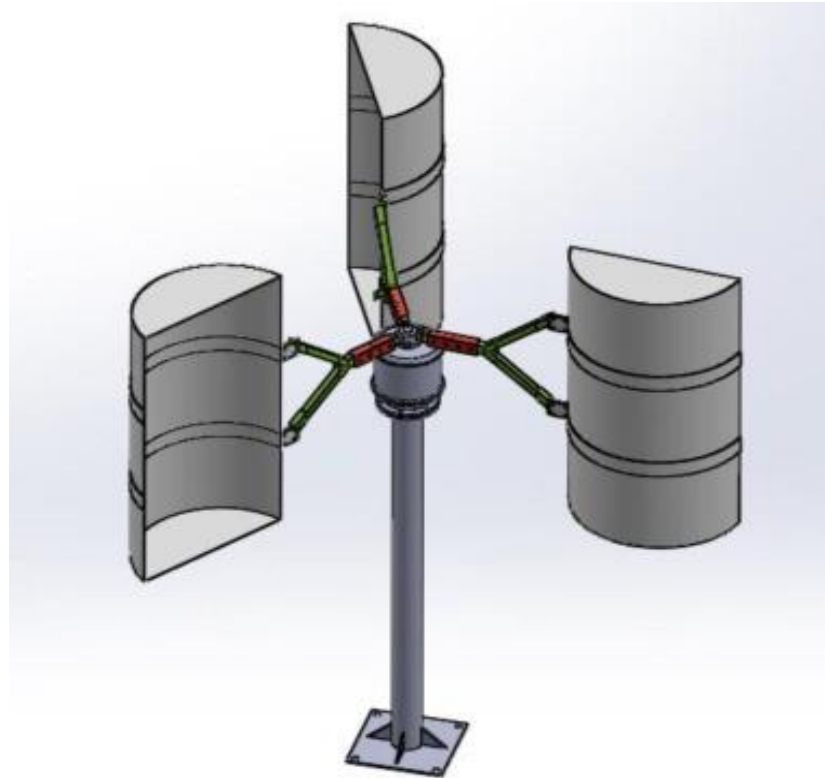


Figure 1.3. Savonius Vertical Wind Turbine model [12].

1.3.3. Darrieus Vertical Wind Turbines

Darrieus Vertical Wind Turbines, developed by Georges Jean Marie Darrieus, represent a notable category of vertical-axis wind turbines (VAWTs) celebrated for their exceptional efficiency and distinct design. These turbines feature vertically oriented airfoil blades, typically in a helical arrangement, which allows them to capture wind energy with high effectiveness across a wide range of wind speeds. Darrieus VAWTs are well-suited for urban environments, research, and residential applications, where aesthetics and compact design are essential considerations. While their complexity can make them more challenging to manufacture and maintain compared to simpler VAWTs, their superior energy conversion capabilities, reduced noise, and

scalability make them an attractive choice. Additionally, Darrieus turbines can exhibit self-starting characteristics due to their blade arrangement, ensuring continuous power generation. With their ability to harness wind power efficiently, Darrieus VAWTs contribute significantly to the advancement of renewable energy technologies, offering a promising solution to address the world's growing energy needs while minimizing environmental impact. Figure 1.4 shows one type of Darrieus vertical turbine [13].



Figure 1.4. Darrieus Vertical Wind Turbine model [13].

1.4. RESEARCH GAP AND THE NEED FOR STUDY

While both Savonius and Darrieus vertical-axis wind turbines (VAWTs) have been extensively researched and offer distinct advantages, a significant research gap remains in understanding their comparative performance when combined within a single turbine assembly. This gap extends to the impact of various blade configurations, including geometry, number, type, and spacing. Moreover, the potential for harnessing wind energy on highways through combined VAWT systems has not been explored in previous studies. Existing research often relies solely on theoretical results obtained through simulation studies. These studies frequently lack clear definitions and fail to identify optimal turbine locations. This project aims to bridge this gap by conducting real-world experimental evaluations of combined Savonius-Darrieus VAWT performance.

1.5. GOALS OF THIS STUDY

This study aims to address the critical challenge of providing sustainable energy for highways in remote locations. The current reliance on fossil fuels for both energy generation and transmission to remote highways presents two key issues: environmental damage and substantial cost and energy loss due to power lines. This research delves into the development of a hybrid composite vertical wind turbine, combining Savonius and Darrieus blades, to optimize wind energy harvesting from moving vehicles on highways. It comprises an in-depth investigation of blade geometry, shape, and optimal distance, along with an analysis of ideal turbine placement on highways to maximize energy output. This innovative approach seeks to substantially increase wind energy generation from highway traffic, enabling a self-sufficient power supply for various applications. This includes powering charging stations for electric vehicles, contributing to the burgeoning global shift towards sustainable transportation.

1.6. THESIS OUTLINE

Part 1: Introduction

- Background and Importance of wind energy, then the evolution of wind turbine technology after that the significance of VAWTs

Part 2: Literature Review

- Overview of wind turbine technology
- Vertical Axis Wind Turbines (VAWTs)
- Savonius and Darrieus VAWTs: Design and Characteristics
- Previous Studies on VAWTs
- Mixing VAWTs: Existing Research

Part 3: Methodology

- Experimental Setup
- Data Collection
- Parameters and Variables
- Data Analysis Methods

Part 4: Results and Discussion

- Presentation of Experimental Data
- Performance Comparison of Savonius and Darrieus VAWTs
- Implications for Wind Energy Applications

Part 5: Conclusion and Recommendations

PART 2

LITERATURE SURVEY

2.1. INTRODUCTION

Highways are a treasure for generating energy using large wind vortices that consist of the movement of vehicles on them through the rapid movement of different vehicles during the night and day, which can be exploited to achieve great gains. In this regard, a composite vertical turbine (double VAWT) will be used to exploit this generated wind and convert it into energy useful to humanity. Apart from some designs, concepts and available literature using numerical data, it also works with many assumptions. Many researchers have conducted tests and experiments on the wind turbine. Some have compared the turbine by changing the number of blades or stages, and some have conducted tests on the turbine in different locations. Others went towards changing the turbine's dimensions and the blades' shape. The researchers approached different methods in research. Some used the simulation system through the ANSYS program, the MATLAB program, or other simulation programs. Some relied on the experimental study and conducted laboratory experiments under laboratory conditions, and some adopted the comparison method. Some researchers worked on conducting different experiments on the turbine, as did the researchers Fuglsang, Peter Thomsen, and Kenneth [14]. By conducting experiments on the turbine in different locations on the beach in Denmark. Some scientists tend to evaluate wind resources more scientifically K. Jackson and C. P. van Dam, D. Yen-Nakafuji [15] who used the California Wind Resources District. The goal was to analyze variations in wind energy production for the area and to evaluate changes in these levels over time.

Others worked on studying and evaluating the financial costs and economic resources of wind turbines, as did Westlund, Hans Wilhelmsson, and Mats [16].

Apart from some of the available designs, concepts and literature, as it is clear and in general, this literature has varied between investigating wind turbines' scientific and technical side; some studied economic feasibility, and some worked on studying comparisons in them. It is worth reviewing the literature related to this.

2.2. PREVIOUS STUDIES OF SAVONIUS TURBINE

The available literature and research on Savonius Turbin are not few, but they are characterized by repetition in principle and the main idea. It is possible to divide the previous literature in terms of the study into theoretical and experimental literature.

2.2.1. The Theoretical Studies for Savonius

Some authors use several simulation programs to improve the performance of the Savonius turbine. These programs are characterized by the fact that the results obtained through them are close to reality and may be accurate at times, and this depends on the user's ability to use these programs and the extent of proficiency in them.

Shah et al [17] used MATLAB simulations to develop a mathematical model for modelling a novel small-scale VAWT with curved blades and compared it to conventional Savonius rotor blades. Ahire, Unmesh D Nikumbh, Rushikesh S More, Bhagyesh S Warke, and Jayesh S [18] relied on similar comparisons with previous research and findings by designing the Savonius rotor for wind power capture and power generation in India by Ansys simulation programme.

Damota, Javier Blanco García and others [19] improved the Savonius turbine type by proposing a blade design based on the Fibonacci shape spiral through OPEN FOAM-CFD program simulation.

Meri Al Absi, Salih Hasan Jabbar and others [20] conducted an experiment to improve Savonius turbines by changing the overlay ratio and then modifying the inner surface of the blade in the concave part into a regular zigzag shape by simulating by a series of unsteady 2D simulations (CFD -Fluent version 19.1) using the model k- ω SST

(Shear Stress Transfer) as well as its comparison with model test results in an open wind tunnel.

Nasef , M. H. El-Askary, W. A. and others [21] conducted experiments to find out the dynamic performance of the fixed Savonius rotor, which contains two semi-circular blades, through simulation using the commercial software Fluent 6.3.26 (2006) using four turbulence models and comparing the simulation results with the published laboratory results to find out The appropriate turbulence model using different interference ratios and different angles of the rotor, as this change causes high vibrations and thus mechanical noise in the rotor

Gupta, Rajat Deb, Bachu Misra, R. D.[22] conducted a study on a shaftless, end-plate Savonius helical rotor in a full cycle of rotation and compared it with a conventional Savonius rotor by performing simulations in CFD Flow-3D software (Flow Science, Flow 3D) using the solution of mean Reynolds Navier-Stokes (RANS) equations.

D.Mohamed, M. H. Janiga, G.Pap, E.Thèvenin [23] They improved the design of the Savonius rotor system in which a high power factor and constant torque can be obtained by placing a baffle plate that specifically and partially protects the blade of the chopper and which leads downwind Towards the forward blade, this study was carried out through simulation by pairing the internal optimization library (OPAL) with the synthetic flow simulation code (ANSYS Fluent).

Sobczak, Krzysztof Obidowski et all [24] Proposed a new idea for a Savonius turbine with variable blade geometry to address the problem of low efficiency by continuously deforming the blades made of elastic material during rotation to increase the advancing blade's positive torque and reduce the returning blade's negative torque. This proposal was implemented through simulation using computational fluid dynamics (CFD).

Ducoin, A.Shadloo, M.S.Roy, S.[25] conducted direct numerical simulation (DNS) to study the flow instability and transition to turbulence occurring on the Savonius turbine blade. This study was conducted through simulations using the open-source code Nek5000 to solve the Navier-Stokes equations.

Ferrari, G. Federici, D. et al.[26] conducted a study to describe the dynamic behaviour of Savonius vertical axis wind turbines by simulating 3D and 2D models using the open source code Open FOAM and comparing the results of the 2D models with the results available from experimental studies.

Yaakob, Omar Ahmed, YM Ismail [27] parametric research to determine the ideal rotor for the Savonius turbine was validated. By contrasting the research findings with published experimental data, the study used the computational fluid dynamics (CFD) package RANSE to simulate two- and three-dimensional assessments. This work used parametric analysis to determine the ideal turbine layout.

Kerikous, Emeel Thévenin, and Dominique [28] worked on a study to increase the power output of the Savonius hydraulic turbine by modifying the blade profile by developing the blade shape for the convex and concave sides independently of each other. This study was performed through transient computational fluid dynamics (CFD) simulation using the industrial flow simulation code Star- CCM+.

Didane et al [29]. worked on a study on extending the operational wind speed range of the counter-rotation concept in vertical wind turbines and developing the conversion efficiency of a single-rotor VAWT system. This study used 3D simulations based on the K-omega shear stress transfer (SST) perturbation model.

de Tarapacá Chile Palencia Díaz et al.[30] analyzed four different models of Savonius blades as well as traditional Savonius blades for the purpose of finding the best Power Coefficient (C_p) and the best torque coefficient (C_m) for these models by a CFD computational model that was used, with 3D simulations during transient regime.

Marinić-Kragić, Ivo Vučina, Damir Milas, Zoran[31] who worked on optimizing a blade of Savonius codes consisting of two circular arc parts to improve the power factor for the purpose of finding an improved solution for Savonius blades by applying intelligent numerical optimization. This study was conducted by intelligent digital optimization using 2D CFD, and the results were verified and compared with previous designs using 3D CFD.

2.2.2. The Experimental Studies for Savonius

Some authors work to complete the literature through experimental studies characterized by their accurate results without relying on simulation programs, which are done by making models and conducting tests on them.

Kamoji, M. A. Kedare, S. B. Prabhu, S. V.[32] worked on studying Savonius-type turbines with and without a central shaft, comparing them, and investigating the effect of engineering factors on turbine performance in terms of static torque coefficient, torque coefficient, and power factor. The experiments in this study were conducted in a closed jet wind tunnel.

Wenehenubun, Frederik Saputra et al [33] conducted an experimental study in a wind tunnel to determine the effect of the number of blades on the Savonius turbine. They compared 2, 3, and 4 blades and proved that the Savonius turbine with three blades is the best compared to the rest. They compared these results with simulation results using the ANSYS 13.0 program.

Menet, J.L.[34] worked on manufacturing, developing and testing a prototype of the Savonius turbine through an experimental study with the help of the French Innovation Agency (ANFAR). This model was initially tested in a laboratory and then tested at the work site. The results concluded that the entire design of the prototype was highly efficient and the low efficiency of Savonius rotors in producing electricity locally.

Fujisawa and Nobuyuki [35] studied the aerodynamic performance and investigated the flow fields of Savonius rotors with different overlap ratios by measuring pressure distributions on the blades and visualizing the flow fields in and around the rotors with and without rotation through experimental work. Experiments were conducted on four rotors with two semicircular blades but with different overlap ratios. These experiments were conducted in an open-circuit wind tunnel.

Damak, A. Driss, Z. Abid, M.S.[36] They worked on studying the aerodynamic behavior of the Savonius helical rotors, where the Savonius helical turbine was

proposed at an angle of 180 degrees for the purpose of studying the effect of the Reynolds number and the overlap ratio on the Savonius turbine and comparing the results between the traditional Savonius turbine and the helical one. This experimental study was conducted in a laboratory through an open jet wind tunnel.

Chen, Jian Jan, Kumbernuss Zhang, et al [37] worked on conducting an experimental study of the Savonius turbine on building roofs by studying the effect of the overlap ratio, phase shift, and stage on the performance of the Savonius rotors.

Sheldahl, Robert E. et al.[38] studied the testing of fifteen Savonius vertical wind turbine configurations to determine the turbine's dynamic performance. The study was conducted under laboratory conditions in a low-speed wind tunnel and concluded that increasing the Reynolds number or aspect ratio improves the rotor.

NAKAJIMA, Miyoshi et al. [39] have developed an environmentally friendly nano hydraulic turbine. The test was conducted in a water tunnel as an experimental study to study the distance between the rotor and the tunnel's bottom wall and the rotor's rotation direction. In this study, the researchers found that changing the distance between the rotor, the bottom and the tunnel wall, and the direction of rotation of the rotor affects the performance of the Savonius hydraulic turbine.

Alexander, A. J. Holownia, B. P.[40] They worked on conducting an experimental study of a Savonius-type vertical turbine in a wind tunnel under laboratory conditions to study the effect of the blade aspect ratio, blade overlap, and Gap and effects of adding end accessories, end plates and shielding on Savonius turbines.

Hayashi, Tsutomu Li et al.[41] worked on designing and manufacturing a new type of Savonius rotor, which has three stages with a 120-degree bucket phase shift between the adjacent stages, This study was conducted under laboratory conditions in a wind tunnel, and the researchers concluded that the static and dynamic torque changes in one revolution of this three-stage rotor were greatly smoothed compared to a regular single-stage rotor, which means improved starting characteristics.

Saha, U. K. Rajkumar, M. Jaya[42] explored the feasibility of a Savonius rotor with a twisted blade for power generation by conducting experimental experiments in a wind tunnel under laboratory conditions and comparing the results with a conventional Savonius turbine. The researchers concluded that the Savonius rotor with twisted blades is smooth in operation, has higher efficiency, and has a greater ability to self-operate than the Savonius rotor with traditional blades.

Irabu, Kunio Roy, Jitendro Nath [43] conducted a study to improve and control the power generated by the Savonius rotor under the influence of different types of winds and propose a method of preventing strong wind disasters by using the steering box tunnel. This study included testing the fixed torque of the fixed rotor at any phase angle and testing the torque dynamic rotation when turning. These tests were conducted in a wind tunnel under laboratory conditions.

Mukrimaa, Syifa S. et al.[44] designed and manufactured a Savonius S-rotor and tested it on rooftops to generate electricity for domestic use .The researchers surveyed Savonius rotary wind turbines adapted for home use in this study. They concluded that they obtained an output of 12 volts, which is used to charge a single battery.

2.3. PREVIOUS STUDIES OF DARRIEUS TURBINE

There is a significant number of literatures concerned with the study of vertical axis turbines of the Darrieus type, which deals with Darrieus turbine types and investigates their efficiency and development. This previous literature can be divided in terms of study into theoretical and experimental literature.

2.3.1. The theoretical studies for Darrieus

Also, in the Darrieus turbine, some authors use several simulation programs to test and improve the performance of this turbine.

These programs are characterized by the fact that the results obtained through them are close to reality and may be accurate at times, and this depends on the user's ability to use these programs and the extent of proficiency in them.

In research, Ghiasi, Pedram Najafi, et al.[45] looked at how well Darrieus wind turbines function when the blade tip speed ratio is more than 1, as well as how design elements affect performance when TSRs are lower than 1. The Fluent software and the k-w SST turbulence model were used to perform this investigation using numerical simulation. The researchers found that while lowering the chord length increases turbine performance at lower TSRs, increasing the chord length of symmetrical and asymmetric airfoils from 0.1 to 0.2 meters improves turbine performance in the drag and lift domain.

Zamani, Mahdi Nazari. et al [46] worked on conducting a study of vertical wind turbines of the Darrieus type with straight J-shaped blades in terms of torque and energy output. The airfoil NACA0015 was used in this study as a basic airfoil and was modified to generate the required J-shape profile through simulation by the ANSYS 3D CFD program.

Researchers Rezaeiha, Abdolrahim Kalkman, et al [47] used computational fluid dynamics (CFD) calculations and relied on unsteady Navier-Stokes calculations (URANS) to study the loads and moments on the Darrieus turbine and the differences between them as well as the angle of attack, the shed vortex, and boundary layer events (leading edge and trailing edge separation, and the transition from laminar to turbulent) as a function of the inclination angle.

Lee, Young Tae Lim, and Hee Chang[48] investigated the effects of several factors on vertical Darrieus-type wind turbines, including the influence of string length, helix angle, inclination angle, and rotor diameter. This study investigated the aerodynamic properties, the discrete flow that occurs close to the blade, the interaction between the flow and the blade, and the torque and power characteristics generated from these characteristics, all in accordance with various design criteria. This investigation was carried out utilizing simulation in the Ansys software using a three-dimensional mesh

based on the unsteady Reynolds average Navier-Stokes. Taking into account the rotational impact of the blades utilizing the sliding mesh technique, too.

Lee and Sang-moon [49] worked on conducting a study to test the performance of the small Darrieus rotor on Duckjeok Island in Korea to investigate the effect of local wind speed, wind direction, ambient air, temperature, and atmospheric pressure by storing all readings in a computer and relying on numerical simulation using code Commercial SC/Tetra and SST turbulence model.

Gosselin, Rémi Dumas .et al [50] conducted a parametric study of H-Darrieus vertical axis turbines using computational fluid dynamics (CFD) and k- ω shear Stress Transport RANS model. By studying the effect of stiffness, number of blades, tip speed ratio, Reynolds number, fixed blade inclination angle, and blade thickness on the aerodynamic efficiency of the Darrieus turbine.

Asr, Mahdi Torabi Nezhad et al.[51] investigated the startup behavior of Darrieus H type vertical wind turbines by performing a series of transient exit CFD simulations using ANSYS.

Chen, Chein Chang Kuo, and Cheng Hsiung [52] conducted a study based on building a simulation model via Ansys/Fluent to study the effects of inclination angle and the effect of blade camber on the characteristics of a small Darrieus turbine by using the blade profiles with three different cambers are NACA0012, 2412 and 4412. respectively, and different pitch angles and also, the investigation into the flow structures, vortex fields, performance of the blades, and the ability to self-start and its effect on the turbine.

Lei, Hang Zhou et al.[53] studied the aerodynamic performance of a two-bladed Darrieus-type vertical axis wind turbine using the ANSYS CFD turbulence model for improved delayed discrete vortex simulation and polyhedral mesh .The researchers investigated the validity of limb velocity and wake velocity ratios by comparing them with experimental data from the available literature.

Mohamed, M.H.[54] worked on conducting an investigation into the aerodynamic acoustics of the Darrieus type vertical wind turbine and the extent of the effect of these acoustics produced by the wind turbine. The researcher here worked to conduct a numerical and dynamic study and the effect of the tip speed ratio and hardness on the noise generated by the blades, based on the FW-H equations (Ffowcs Williams and Hawkings) and their integrated solutions in addition to the URANS equations (unsteady Reynolds-average Navier-Stokes). The research concluded that when the stiffness and peripheral velocity ratio are high, the noise in the turbines increases.

Howell, Robert Qin, et al.[55] worked on conducting a study of the aerodynamics of vertical Darrieus-type wind turbines through three-dimensional (CFD) simulations and comparing the results with an experimental study in a wind tunnel. The researchers concluded that the surface roughness on the turbine rotor blades has a significant impact on the performance of the turbine.

Research was done by Weber, Johannes Becker, et al.[56] to anticipate the noise made by H-Darrieus wind turbines using two alternative techniques. Through studies carried out in an anechoic wind tunnel, the researchers got acoustic measurements of the rotor model. Using this information, the researchers calculated the acoustic source terms in accordance with the Lighthill acoustic measurement, which provides the source terms existing on the original CFD model, to confirm the accuracy of the computational atmospheric acoustic simulation. The inhomogeneous Lighthill wave equation is then projected onto a coarser acoustic grid, which is solved using the finite element (FE) method. The Ffowcs Williams Hawkings (FW-H) approach, based on the free green field function, is used by the second network.

Dominy, Robert G.[57] conducted a study of a Blade Element Momentum (BEM) technique and a computational fluid dynamics (CFD) model research to assess the impact of rotor stiffness on the performance of a three-blade H-Darrieus vertical axis wind turbine (VAWT) during the startup phase. The researchers employed the Start-Up model, a cutting-edge BEM that can dynamically simulate the start-up of a turbine under various wind geometry factors. The researchers discovered Better self-starting capacity at the cost of decreased peak performance. Additionally, they point out that

turbines with longer blade chord lengths and wider rotor radii perform better throughout the operating range for a given stiffness.

Rossetti, A. Pavesi, G.[58] They compared the outcomes of two- and three-dimensional CFD simulations using the BEM model to analyze the curves of the maximum speed ratio versus the power factor and the development of forces during the blade rotation of an H-blade Darrieus turbine.

Patil, Rohit Daróczy, et al.[59] created a custom mesh based on blocks to carry out 3D LES simulation using the WALE sub grid model in their work to analyze the flow field around an H-Darrieus wind turbine using Large Eddy Simulation (LES).The turbine's susceptibility to dynamic stall due to poor TSR at a high angle of attack was researched .By comparing the outcomes of the LES simulations with experimental findings in the literature, the researchers further validated the accuracy of the LES computation through turbulence analysis at various points in the simulations.

2.3.2. The Experimental Studies for Darrieus

Many researchers and authors have worked to use the practical approach through experimental studies in their research, relying on designing and manufacturing models and testing them in laboratory conditions or in general conditions to obtain more accurate and realistic results.

Bravo R et al.[60] studied the experimental determination of the nominal power curves and determined the structural integrity, safety, and operating characteristics of the system for a vertical wind turbine of type H-Darrieus that has airfoils with the NACA0015 profile by testing the turbine in a wide, low-speed wind tunnel.

Du, Longhuan Ingram, and colleagues [61] performed an experiment using a three-blade Darrieus vertical wind turbine in a wind tunnel under controlled conditions to investigate the effects of the turbine stiffness, blade shape, surface roughness, inclination angle, and aspect ratio .The researchers concluded that blade extension greatly influences the startup of these turbines and that increasing blade surface

roughness increases the turbine's ability to self-start at low tip speed ratios and with high turbine stiffness.

Batista, N.C. Melício et al.[62] worked on studying and developing an innovative design for the Darrieus turbine with coiled airfoils called EN0005 and testing this design in the laboratory using a wind tunnel in addition to field testing of the model by evaluating the wind behavior across the width of the blade surface and evaluating the aerodynamic behavior of the Darrieus VAWT. Researchers have discovered that the Darrieus VAWT's novel design can self-start at wind speeds of 1.25 m/s, and steady behavior was shown without the need for any extra components at wind speeds of 25 m/s, no audible noise was produced.

Battisti, L. Brighenti et al.[63] carried out a mechanical and dynamic investigation to study the performance and wake measurements of an H-Darrieus vertical axis wind turbine in an experimental study using a high-speed wind tunnel.

Bianchini and Alessandro [64] researched to determine how a tiny, three-blade H-Darrieus rotor behaved when it first started up. Through an experimental investigation in the wind tunnel, determine the impact of the kind of airfoil and blade shape on the rotor start-up capabilities. The researchers found that experimental experience consistently correlates with changes in self-starting behavior induced by airfoil type and blade shape.

Li, Qing'an Maeda, et al.[65] collaborated on research to perform an experimental investigation in wind tunnel trials to analyze the aerodynamic forces operating on a single blade of a Darrieus turbine depending on the varied numbers of blades. The airfoil that was tested has the cross-sectional form NACA0021. The scientists discovered that when stiffness increased, the pressure differential considerably decreased. Additionally, the torque scale and six-component equilibrium values were lower than those predicted by the stress distributions.

Through an experimental study in a wind tunnel under controlled conditions, Mazarbhuiya, Hussain Mahamed, et al.[66] investigated the performance of an

asymmetric blade H-Darrieus rotor with constant relative blade span thickness (RT) and variable thickness (VT) at various low wind speeds. The researchers discovered that while the blade extension (VT) design can result in superior power coefficients in low wind speed settings, the blade extension (RT) design improves the beginning characteristics of the asymmetric blade H-Darrieus rotor.

Molina, A. Carbó Massai, et al.[67] conducted tests in a wind tunnel. They compared the outcomes with those of CFD models to analyze the near wake of an H-Darrieus VAWT turbine under turbulent circumstances. The researchers discovered the reason why VAWTs function better in turbulence to be deeper and more insightful.

Sengupta et al.[68] Experiments on a centrifugal blower test bench to verify the use of high-rigidity asymmetric or convex blades to enhance the starting performance of a three-bladed H-Darrieus rotor using three types of blade designs (two asymmetric blades, S815 and EN0005, and one conventional symmetrical blade, NACA 0018) By low wind currents .Researchers found that the S815 asymmetric blade rotor outperforms the EN0005 asymmetric rotors and the NACA 0018 H-Darrieus blade rotor in dynamic torque .The performance of the Darrieus turbine was explored, and the effects of the blade arrangement in one or two stages, the adjustment angle, and the number of blades were examined by Dumitrescu, H. Dumitrache, and others.[69]Researchers concluded that the torque developed by VAWT at low speeds is greater when the blade adjustment angle is greater. Still, the torque developed by VAWT at higher speeds is greater when the blade adjustment angles are lower, based on the results of the experiments carried out in the wind tunnel of the flexible experimental model.

Nawfal M., Ali Aljabair ,et al.[70] researchers tested six versions of the Darrieus wind turbines to determine the best design for the turbines. They looked at how the performance of the turbines was affected by the number of blades and the tip speed ratio. by using the turbine blades' airfoil form, designated as DU06W200, and their set geometric dimensions. All Darrieus wind turbine types were tested in an open-type test section of a subsonic wind tunnel. The experimental investigation results were compared to numerical simulations performed using the Ansys CFD software. The

researchers concluded that the Darrieus WT two-blade rotor performs better than other models and that the Darrieus WT straight type can self-start at a wind speed of 3 m/s, but the other kinds cannot start at a wind speed of less than 5 m/s. Shiono, Mitsuhiro Suzuki, et al. embarked on research to see if the Darrieus turbine might produce energy by tidal movement on the water. The power, rigidity, number of blades, and initial torque in the water channel were all factors that the researchers looked at. The researchers concluded that the water turbine's efficiency and tip speed ratio are not correlated with flow rate and that the turbine's efficiency is greatest at solidities of 0.179.

Researchers Patel, Vimal Eldho, et al.[71] worked on performing experimental research to evaluate the hydrodynamic performance of the three Darrieus blades NACA0015, NACA0018, and NACA4415 with varied stiffnesses in another study on the Darrieus turbine in water. The experiment was then enlarged to assess the performance of four identical NACA0018 and NACA4415 convex rotors. This study calculated the blockage impact using Maxwell's velocity correction approach. The researchers discovered that at a stiffness of roughly 0.382, the wings NACA0015 and NACA0018 have a maximum energy coefficient of 0.15.

The research was done by Benzerdjeb, Abdelouahab Abed, et al.[72] to determine how the Darrieus water turbine's " i_g " blade inclination affected its performance. Researchers found that the best performance of the turbine tested was obtained when the blades were set at an inclination angle of 1.75 degrees. This was discovered by conducting four main sets of experimental tests using the same model of vertical axis water turbine (VAWT) with four-blade installation angles ($i_g = 1.75^\circ, 4.5^\circ, 1.75^\circ,$ and 4.5°), at different water flow velocities. At a water flow rate of 0.37 m/s, this results in a relative decrease in power and power factor of about 75% and 81%, respectively, while the relative increases in optimal mechanical strength and power factor reach, respectively, 82% and 67%. The worst performance was obtained for a negative blade installation inclination angle of -4.5 degrees.

The research was undertaken by Gharib-Yosry, Ahmed Blanco-Marigorta, et al.[73] to assess the performance of the Darrieus rotor turbine as a small wind or water

generator. Several experiments were carried out in the water streams and wind tunnel using two blockage correction equations in water channel tests carried out under blockage values ranging from 0.2 to 0.35 to predict the operational behavior of the turbine in open water, the researchers concluded that the turbine rotor performs appropriately in open-field circumstances. This study established that the features of the wind turbine are typical of how it would operate in open water settings, so long as the Reynolds number is kept constant between the stream trials and wind tunnel tests.

2.4. PREVIOUS STUDIES OF COMPOSITE AND HYBRID TURBINES

There is little literature dealing with composite turbines or hybrid turbines, as some authors have worked on research in which they studied the installation of different types of turbines to improve turbine performance and obtain more energy through them.

Here we discuss some of these previous studies of composite turbines.

In research, Erwin, Erwin Wiyono, et al.[74] found that adding triangular directing fins that face the wind turbines and point in the same direction as the wind increases the efficiency of the turbines. According to calculations and simulation data, a double blade with a high blade angle has a larger damping response than a single blade. The pentagonal form creates the most force. In summary, the study's findings showed that the optimal fin design, as determined by performance testing, is Type 3b, which leads to improved power factor and produced capacity.

Didane, D.H. Maksud, et al. [75] conducted an experimental study in a wind tunnel using a centrifugal blower for a model consisting of three common blades from Savonius and Darrieus to develop and improve the efficiency of vertical wind turbines using a joint design of Darrieus and Savonius rotors based on counter-rotation technology. The performance of the model is constrained, the researchers concluded. It can be seen from examining the individual rotor performances that the conversion efficiency of the H-type rotor rises with increasing wind speed. Though it tends to

decrease as the working speed increases, it is higher for the S-type rotor when the wind speed is low.

K. Balaji B. Mohan Krishna, et al.[76] worked on conducting a study on installing a wind turbine with solar panels in one model for the purpose of benefiting from wind and solar energy in generating electrical energy .The researchers in this study did not address sufficient information and the resulting energy of this hybrid structure.

Salih, Tasneem Wang, et al.[77] collaborated on research to give electricity to Sudan's wireless communications network using a hybrid system made of a wind turbine and solar panels to do away with diesel engines .The HOMER software was used to acquire the findings reported in this study .Researchers concluded that the suggested hybrid system for the ADLDAN Communications website revealed that it exhibits 100% uptime, high performance, prolonged life (20 years), and is more economical than conventional energy sources.

Trisna Nugraha Priyambodo, Anggara, Dadang [78] They researched by building a hybrid wind turbine prototype with solar panels and a vertical axis.

To maximize the energy produced, the researchers designed a model combining solar panels and Savonius turbines according to the findings of their experimental investigation, the researchers concluded that this model might provide up to (11.5146) watts of electricity.

Prashanth, B. N. Pramod, et al.[79] worked on creating a composite model of HAWT horizontal wind turbines made using PVC pipes with solar panels combined with turbine blades to maximize renewable energy sources and obtain the most electrical energy possible Through an experimental analysis, the researchers concluded that the suggested composite model, which improves wind turbine performance throughout production, has several benefits over the conversion method. The efficiency increased significantly when combined with solar panels and the turbine.

The viability of a novel hybrid system that combines wind turbines with compressed air energy storage was investigated by Sun, Hao Luo, et al.[80] This study involved designing and putting into practice a mechanical transmission mechanism for power

integration within the hybrid system based on the screw expander to function as an "air-machinery energy converter," which can transfer the generalized additional driving energy from the stored compressed air to the turbine shaft to stabilize the fluctuation in wind energy. In this study, the researchers worked on developing a mathematical model of the entire hybrid process and investigating the control scheme for the associated collaborative activities to implement the suggested method and demonstrate the notion. A prototype test platform was also developed. The researchers concluded that the suggested hybrid wind turbine system is technically viable through modelling and experimental testing.

In research by Borowy, Bogdan S., et al.[81] the ideal photovoltaic array size for a standalone hybrid wind/PV system was determined using long-term data on wind speed and radiation that were logged every hour of the day for 30 years.

By creating an algorithm to estimate the ideal size of the PV array in the system, the researchers used the least squares approach to identify the optimum match of the PV array and wind turbine for a certain load. According to the experts, this is the best arrangement of wind turbines with photovoltaic electricity. According to the exact location and load profile, this will enable the battery size to be decreased.

A novel sort of hybrid wind and solar system, presented by Huang, Qunwu Shi, et al.[82] substitutes numerous tiny wind turbines for bigger ones. By building two different types of wind-solar hybrid systems with the same capacity, the researchers worked on this study to evaluate the electrical performance of the multi-turbine solar-wind hybrid system to the conventional system. The TRNSYS program was used to measure and simulate the power output of the two systems. According to the researchers, the multi-wind-solar hybrid system offers a higher power production than the reference system at low wind speeds. The simulated findings and experimental results were in perfect agreement.

Through the use of hydrogen storage, a triple hybrid system was proposed by Haddad, Ahmad Ramadan, et al.[83] in their study. This system included solar energy cells, wind turbines, and fuel cells. The systems were sized for this investigation using the DNI data for the examined site and the average wind speed. There are recognized

mathematical models for the WT, PT, fuel cell, and electrolyzer. the suggested models determine the amount of hydrogen generated as well as the energy output of each system. The researchers concluded that combining a solar thermal system with a wind energy system enables one to overcome the solar thermal system's poor energy output, particularly during the winter.

2.5. PREVIOUS STUDIES OF WIND TURBINES ON HIGHWAYS

According to the novelty of installing wind turbines on roadways to collect energy from this source, there is limited study and literature in this area. With the exception of a few designs and concepts still being developed, the quantity of material that is now accessible in the literature is quite minimal and consists only of a few numerical calculations that have been completed under several assumptions.

The discuss several research in this respect in this section.

Researchers Al-Aqel, A. A. Lim, et al.[84] conducted an experimental study using a four-blade Darrius turbine and three parameters to determine and choose the best location for the turbine with the highest efficiency. The study evaluated the viability of implementing small-scale wind turbines along highways in Malaysia. The researchers concluded that the ideal places for wind turbines are at a distance of one meter from the lateral distance and height from the ground, respectively, by comparing the outcomes of the experimental investigation with simulations performed via the ANSYS Fluent program. Additionally, it was shown that 45 degrees away from the route they are situated is the best direction.

In Bangladesh, Rana, Shoel Roy, et al.[85] have been working on conducting an experimental study by proposing and designing a Savonius-type VAWT in a way that allows the turbine to capture wind from two directions in any busy highway location by positioning these turbines close to moving traffic, such as bridges, ramps, and tunnels. The researchers came to the conclusion that even under less-than-ideal site circumstances, Savonius-type vertical axis wind energy conversion is feasible and can make a substantial contribution to the creation of clean, renewable, and sustainable

wind electricity. The electricity produced might be used to power traffic lights, toll booths, and streetlights.

Researchers Gokul and Manikanda [86] A conducted an experimental study using three-blade Savonius vertical wind turbines in India to recover wind energy from moving vehicles. They compared the findings with simulations performed using the MATLAB Simulink program. testing a variety of variables, such as the turbine's form or the ideal position, would have made this study more thorough. The researchers concluded that generating power at a low cost is feasible without harming the environment.

Researchers Raj, Mithun S., and Ashok [87] conducted an experimental study using a proposed model of a windmill with a spiral vertical axis on the highway to benefit from the wind energy generated by vehicles moving on highways in generating electrical energy that can be stored in a battery and used for many purposes. This was done as part of another study to exploit wind-generated energy from vehicles moving on highways. the experts concluded that it is feasible to produce a significant volume of ecologically friendly and sustainable electrical energy, which may significantly alleviate the issue of the energy crisis.

By designing and making the vertical axis SWT using inexpensive materials and working to measure and calculate the coefficient Savonius turbine torque, Santhakumar, Senthilvel Palanivel, et al.[88] experimented with studying the behavior of the Savonius vertical axis wind turbine (SWT) in four-lane highways during the southwest and northeast monsoons. To understand the behavior of the turbine under various wind directions and to work on analyzing errors in the data obtained by looking at possible measurement errors and instrument accuracy, the researchers carried out these experiments on a four-lane highway by positioning the turbine in two different locations (the middle and sides of the highway). As the nominal rotational speed of SWT fluctuates based on the monsoon, the researchers concluded that wind directions significantly capture the most energy in wind power generation on roads. Positioning SWT in the center of four-lane highways in various monsoons may increase rotational speed up to a maximum of roughly 64% when it is situated on both sides of the road.

Researchers Hussain, Safdar Simeon, et al.[89] created and installed wind turbines on the highway that generate energy using vehicle traffic. They did this by conducting traffic surveys in various locations to determine the best location for the turbine installation while taking into account various factors. The researchers fitted an online system with the turbine and sensors to record voltage, current, and any motor failures, taking into consideration wind speed, vehicle movement, and traffic congestion. Additionally, boosting the voltage has been made possible by the employment of a boost converter. the researchers came to the conclusion that the generated voltage, which depicts the heavy flow of vehicles during this time, is 4 volts through the results of the experimental study. This leads to the conclusion that the more vehicles that are on the road, the more power is generated.

In a different investigation of wind turbines on roads, Kulkarni, Saurabh Kulkarni, et al.[90] designed and produced a vertical wind turbine (VAWT) with eight semicircular blades and a pulley that functions as both a gearbox and bearing mechanism. the researchers discovered that there was a discrepancy between the theoretical and experimental results through experimental study and theoretical calculations because, in the theoretical calculations, the researchers assumed that the wind hits all eight blades of the turbine, but they found that, in practice, this is not true. through their investigation and the conclusions drawn, the researchers were persuaded that employing a vertical turbine to transform wind energy into electricity is feasible and likely to substantially impact the creation of clean, renewable power from wind.

Researchers Ahmed and Arham [91] conducted a study on the use of horizontal wind turbines (HAWT) to harvest wind energy from moving vehicles on the highway. They did this by simulating computational fluid dynamics using the MATLAB program in addition to performing turbine energy calculations using the idea of velocity triangles to calculate the amount of energy harvested. for the purpose of analyzing vehicles moving at different speeds on the highway with the placement of wind turbines on overhead poles (whose height is appropriately determined) and thus capturing the wind generated from the pressure difference, the researchers suggested having a separate place for cars and heavy vehicles, which could be achieved by having separate lanes on the highways. the findings of the simulation, according to the experts, were quite

close to theoretical values. As a result, this method may create a respectable quantity of electricity. This can lessen the existing reliance on conventional fuels, lessen pollution to some extent, and pave the way for the idea of green roads.

Touarbari and other researchers [92] used CFD simulation to examine the performance of the Darrieus three-blade straight wind turbine on roads. They used the k-SST turbulence model to simulate the turbulent flow system. In this study, the researchers used three separate case studies. In the first instance, a model was created for a single car using a one-way street. In the second scenario, a two-way highway with two opposing lanes was simulated, and in the third situation, a one-way highway with two opposing lanes was simulated. The researchers concluded that the third example yielded the greatest outcomes, was more realistic than the first and second cases, and had the highest value for the coefficient of the ability in the third state.

In a different research strategy, Morbiato, et al.[93] conducted a study to characterise the resource index for wind time above the specified speed, analyze the effects of traffic groups and wind drops associated with traffic, and comprehensively analyze the relationship between truck flow and wind speed categories to estimate wind energy resources from transportation traffic on highways. By enhancing the self-operation capabilities of VAWT, this study contained an optimal technology. A straightforward operating speed control uses the optimal power factor in repeating processes with varying speeds. The researchers concluded that the case study for the novel clean technology—a straight stretch of highway operating above a truck flow threshold—is the most typical case study. If wind energy systems with variable speed operation are approved, this opens up a wide range of potential future improvements for highway applications (such as tunnel exits and urban canyons) as well as for transportation systems in general (such as railroads, canals and airside flow at airports). In addition, a comprehensive analysis of the transient behavior of VAWT in potential transportation system applications will provide a better understanding of the implications of wind drops.

2.6. SUMMARY

By reviewing some published literature and studies regarding the operation of wind turbines in general and their operation on highways in particular, and after comparing their results and working methods with the current experimental study, it was clarified to what extent the proposed work was able to make maximum use of energy from highways, especially the double turbines on the highway. Most of the authors used numerical simulation methods to arrive at the results, which relied, as a maximum, on the use of only two vehicles, which does not give sufficient results to reach the desired facts. At the same time, it is impossible to rely entirely on the results of the simulation programs because they are close to the truth and need complete accuracy. It is no secret that a large number of previous researchers work on a limited number of parameters, which may not give an accurate description of the actual work of wind turbines on highways since this type of work requires extensive study and significant depth in obtaining sufficient information that guides the development of the use of clean energy and thus obtaining sustainable roadways. In addition to this, most previous studies assumed a somewhat constant rotation speed for vertical wind turbines, and this does not match the principle of uneven vehicle movement on highways, which produce different wind speeds due to random traffic, which makes it impossible for the turbine blades to rotate at a constant speed. After reviewing much of the previous literature in this field, many authors resorted to using known types of vertical and horizontal wind turbines of all kinds. No study was found that used double turbines in exploiting wind energy from highways, which gives an advantage to the model proposed in the current study, which explains significantly, and through a broad and in-depth experimental study with a significant number of parameters, the extent of obtaining the enormous amount of clean energy on highways, which was not appropriately exploited, was achieved.

To address the gaps in previous literature and to obtain accuracy in results that are closer to the ideal through an experimental study, and to reach the desired goal, the following steps will be followed:

- Accurate dimensions will be adopted for successful models of vertical wind turbines of both types (Savonius and Darrieus), which have been tested and

whose success has been confirmed in previously approved research to obtain the best design.

- Several tests will be compared between the model proposed in the current study and the traditional wind turbine model by comparing the values of power, power factor, and rotational speed of the blades to determine the extent of the preference of the proposed turbine.
- Several tests will be conducted, taking several days, to reach the best location for the wind turbine proposed in this study for the purpose of harvesting the largest amount of energy on highways.
- High-quality measurements will be used in the tests above to obtain real, accurate results and to address fluctuations in V , ω , generator, TSR and the problem of measuring that give a complete visualization of all values to obtain the final results.

PART 3

EXPERIMENTAL PART

3.1. INTRODUCTION

The wind is one of the most important renewable energy sources, which can be effectively harnessed to produce energy through wind turbines [94] and convert mechanical energy into electrical energy [95]. In this chapter, the design and manufacture of the proposed turbine be studied. The extent of benefit and change in the amount of energy that can be obtained from this model be examined, in addition to studying many comparisons and parameters in a practical way to show the extent of preference by comparing the proposed turbine with the traditional turbine, additionally studying the optimal location for installing the turbine proposed on the highway In addition to studying the energy that can be obtained by testing the proposed turbine on different types of vehicles and test one type of vehicle and comparison between them. Experimental studies may require a long time and a high cost to complete the work. Still, they are characterized by giving accurate, realistic, and reliable results that can be used for future studies or commercial companies. To accomplish this work well, an experimental study was used to find the required data and obtain extremely dependable results. Figure 3.1 shows the steps of the experimental work that are relied upon in this chapter.

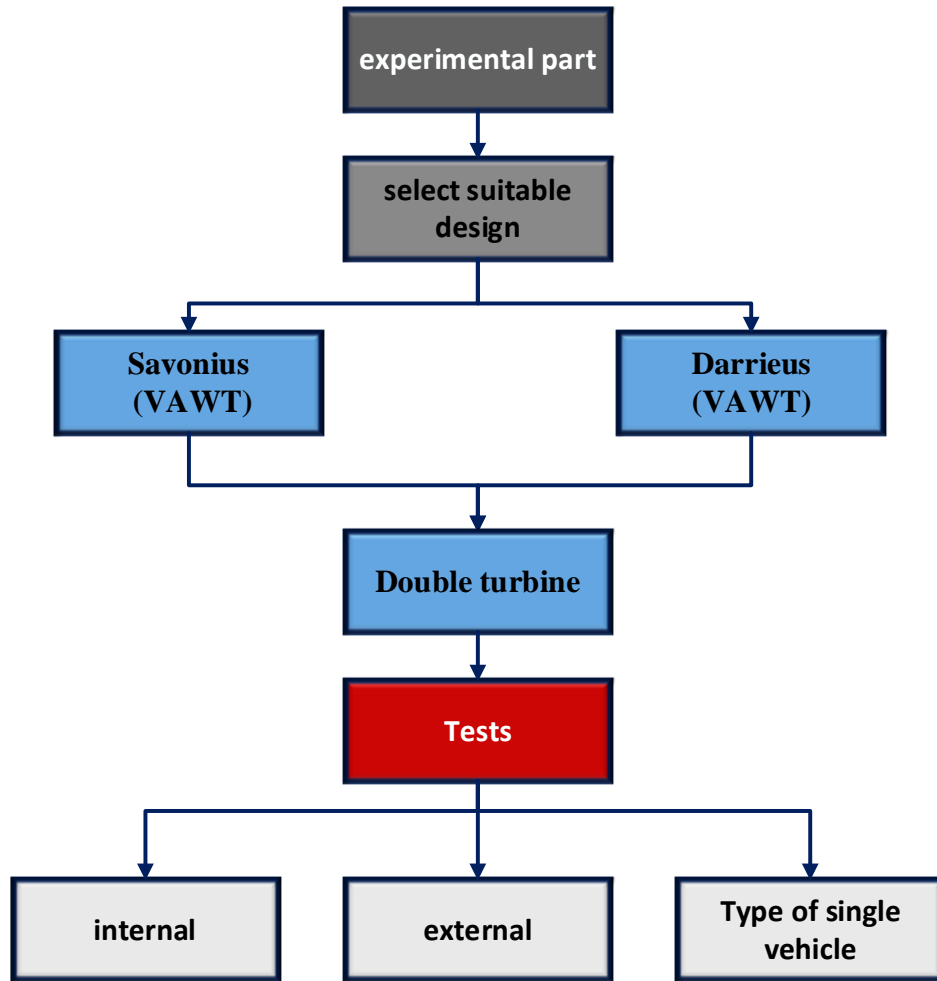


Figure 3.1. Experimental setup chart

3.2. EXPERIMENTAL SETUP

Darrieus gives improved efficiency, and Savonius aids in a self-startup. for this reason, both types be combined in this proposed model at the first design of the proposed model of the wind turbine by using Solidworks software version 2022, then Manufacture and connect all components (shaft, electric motor, chord.etc) for wind turbine fabrication and installation of the appropriate frame for the proposed turbine, finally test the rig and using the necessary measuring devices (tachometer and anemometer.etc). Figure 3.2 shows the all components that were manufactured locally.

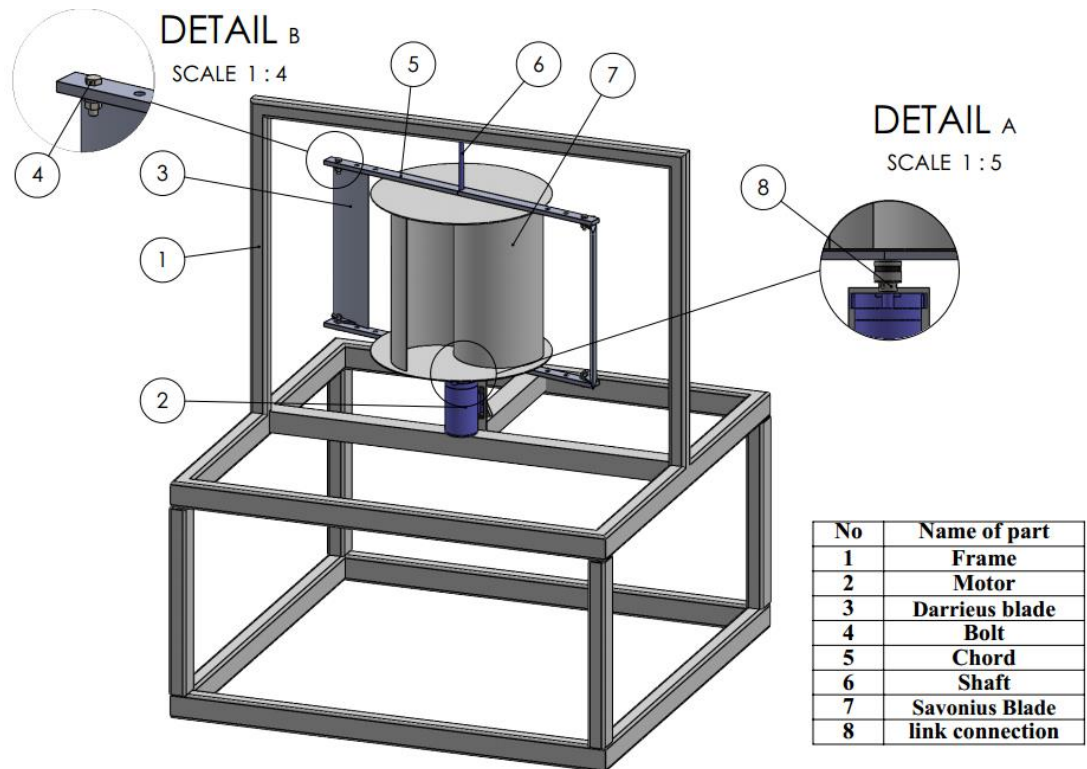


Figure 3.2. Proposed double turbine parts.

3.2.1. Manufacturing of Savonius Turbine

In this study, and after reviewing a large number of research and studies related to the Savonius rotor to choose the appropriate dimensions, one of the studies that proved successful was relied upon through an experimental study conducted by the researcher [Frederikus Wenehenubun] [33], who proved that the Savonius rotor with three blades is the best in terms of the results obtained. at the first step, design the model with all dimensions in cm. With note that this type of rotor depends on the drag force through which the blades are in the shape of the letter (S), as these blades, in the form of scoops, reduce the drag force when they move toward the wind or in the opposite direction of the wind. Figure 3.3 shows the design model of the Savonius turbine with all its dimensions in cm.

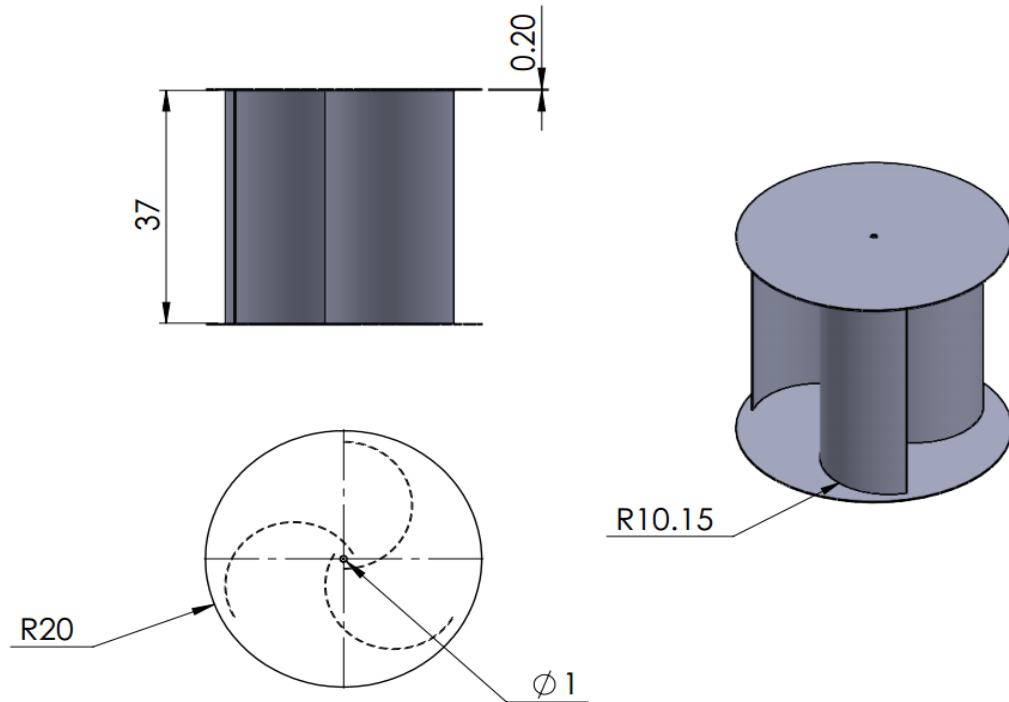


Figure 3.3. Savonius wind turbines with dimension.

The second step after the design is the manufacturing process of the model and it is no less important than its design through the material used in manufacturing the proposed model and its method of manufacture, in addition to the secondary parts used to make the model in the perfect shape, which in turn works to give good results. The manufacturing step is by using a 3D printer type of the Creality (Ender 5 plus) or Creality (Ender 10 Max) to produce the three-bladed Savonius turbine out of material compressed plastic (PLA), and this is a natural material and environmentally friendly where the total weight of the Savonius turbine that was manufactured is (1.695) k.g. Figure 3.4 shows the manufacturing model of the Savonius turbine.

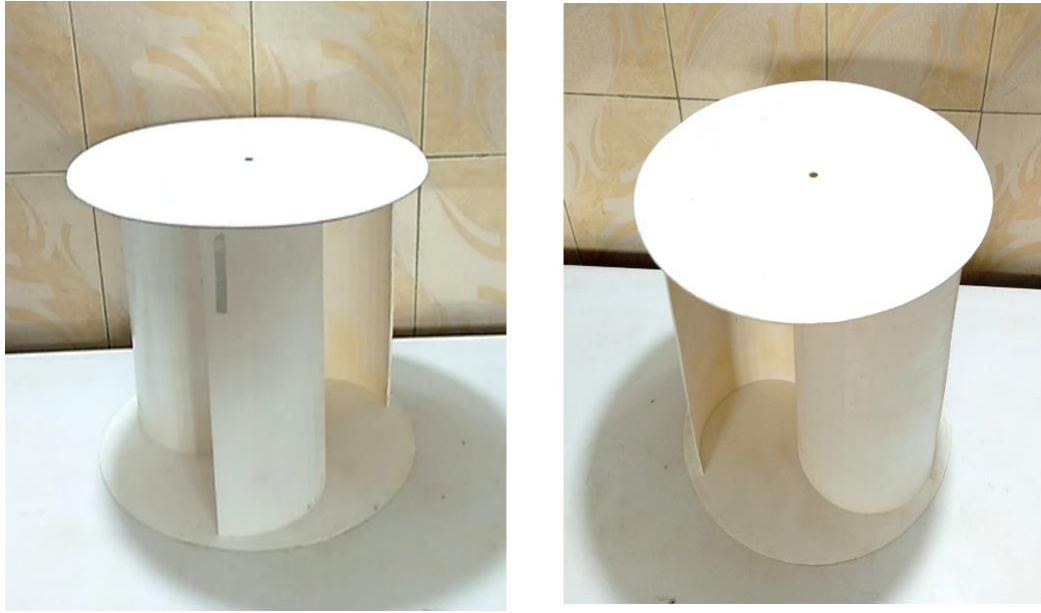


Figure 3.4. Savonius turbine blades.

3.2.2. Manufacturing of Darrieus Turbine

After looking at a large number of research related to the Darrieus turbine and obtaining the optimal design for this turbine, a study was found for a group of researchers who proved the success of their work through the results proven in the conclusions, where the researcher, Proved [Dr. Sattar Aljabair] [70] that the Darrieus two-blade rotor is the best compared to other models, and this design was adopted because of the experimental tests conducted by the researchers with note This type depends on the lifting force, which can rotate several times at the speed of the wind. Fig 3.5 shows the design model with all dimension in cm.

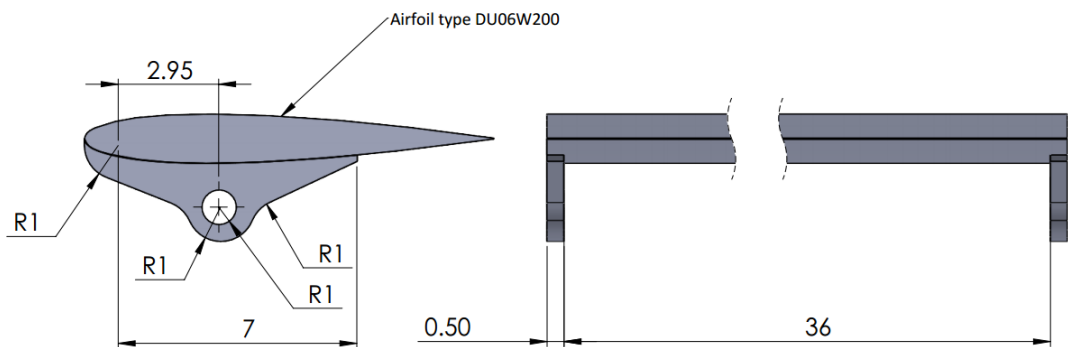


Figure 3.5. Darrieus airfoils design.

After completing the design process for the Darrius turbine, the model-making stage begins. Using the same type of 3D printer mentioned earlier, Darrius's two airfoils are made of the same material used to manufacture the Savonius turbine (compressed plastic PLA). The total weight of the Darrius turbine that was manufactured is (0.660) k.g. Figure 3.6 shows the manufacturing model of the Darrius turbine.



Figure 3.6. Manufacturing of Darrius Blades.

3.2.3. The Chord

In this part of the work, a complete chord was designed that connects the two airfoils of Darrius from the right and left sides by the Solidworks 2022 where the chord is a straight line connecting the Darrius airfoil and the main rotor shaft. It is responsible for transferring the movement of Darrius' blades due to the force of the wind to the main shaft, which rotates it at different speeds. The top and the bottom are in the form of two halves, where the total length of the chord is (72.7 cm) Moreover, the chord contains three holes at both ends, which are added to choose the best distance between the Savonis and Darrius blades. Fig 3.7 shows the design and dimensions of the chord. Additionally, the form was printed with the same printer and material used in printing previous models (PLA). Figure 3.8 shows the manufactured model of the chord.

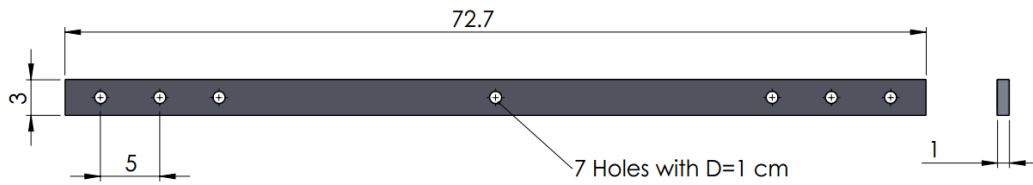


Figure 3.7. Chord design by solidworks.



Figure 3.8. The model manufactured by the 3D printer.

3.2.4. The Rotary Central Shaft

The shaft is the center of the turbine in general and the main center of rotation that combines all parts of the vertical turbine through direct connection with these parts, which transmits the rotational motion to the electric motor. This rotational movement of the shaft is generated due to the rotation of the turbine blades connected to it, which rotate at different speeds due to the wind speed. Choosing and manufacturing the appropriate shaft is important so that the blades are installed from the top and bottom very well. It was purchased because of its availability in the local markets, as the basic design of the Savonius turbine in this work was through which a hole of diameter (1 cm) was placed. The basic design of the chord that connects the two airfoils of Darrieus with the rotating shaft includes a hole with the same diameter in the center of this chord. In this study, a spiral shaft used made of iron with a length of (55 cm), a diameter of (1 cm) and a weight of (253 g) was used. Figure 3.9 shows the design and dimensions of the shaft, and Figure 3.10 shows the manufactured model used.

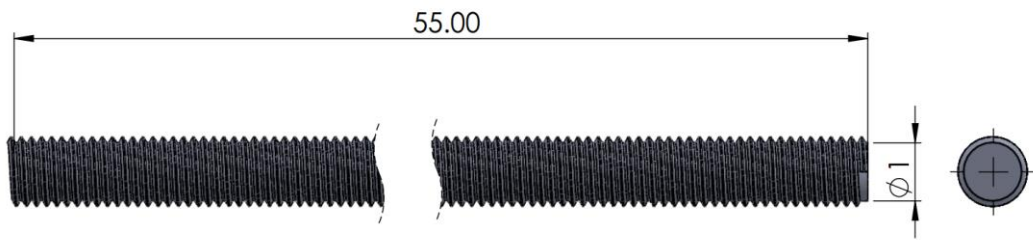


Figure 3.9. Rotary shaft with dimensions.



Figure 3.10. Model of rotary shaft.

3.2.5. The Link Connection

In this work, it was necessary to find a means of connection between the rotating shaft and the electric motor that transmits the rotational motion in the shaft to the motor without any loss of this energy. It is possible to design a specific piece of aluminum, iron, or any other metal that does this work, but after looking at many ideas in this specialty and field, the idea of using the connecting link used in the electric drill is a good idea. Where this link was tested and it was found that the rate of vibration in it is very low, and it is made of stainless steel, and it is worth mentioning that a nut with an internal diameter (1 cm) was added by welding for the purpose of connecting this link to the shaft in a tight way. Figure 3.11 shows the link connection and the dimensions.

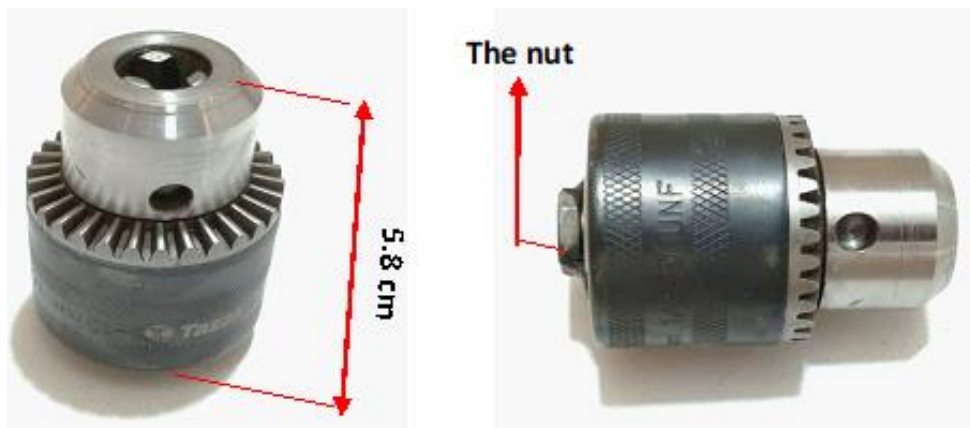


Figure 3.11. The link connection with dimensions.

3.2.6. The Electric Motor

The generator in question operates on the foundational principles of Faraday's electromagnetic induction, effectively converting mechanical energy into electrical power [96]. Have meticulously selected an electric generator designed to deliver voltage at minimal RPM levels, opting for the BOOST PUMP FF-BP-75GPD DC motor, commonly utilized in small residential water purification systems. This motor operates at 24 volts and consumes a current within the range of 0.9 to 1.8 amperes, all while maintaining exceptionally low noise and vibration levels. Additionally, it boasts an environmentally friendly profile, low power dissipation, high efficiency, and shockproof resistance. Constructed with a copper inner coil, it is highly corrosion-resistant and yet remains lightweight at 1.116 kilograms. Figure 3.12 shows the electric motor used.



Figure 3.12. Electric motor used.

3.2.7. The Structural Frame

One crucial aspect in realizing the envisioned model is the construction of a robust frame, integral to its function as a reliable incubator, safeguarding the model's seamless operation under various conditions and climates. This frame necessitates a multitude of exacting specifications to ensure optimal turbine performance. Crafted from iron, it conforms to the dimensions illustrated in Fig. 3.13, meticulously manufactured within a dedicated workshop as depicted in Fig. 3.14. Notably, the frame's key attributes include its capacity to balance the turbine, mitigate energy-draining vibrations, and provide essential protection. The iron frame has been

rigorously tested, with components securely joined through a combination of welding and bolts. It comprises two integral parts: the ground base, forming a stabilizing cube, and the upper section, housing the turbine. The latter includes a bearing mechanism in its upper portion, crucial for stabilizing the rotating shaft and ensuring its smooth operation. The collective weight of this iron structure amounts to 27 kilograms.

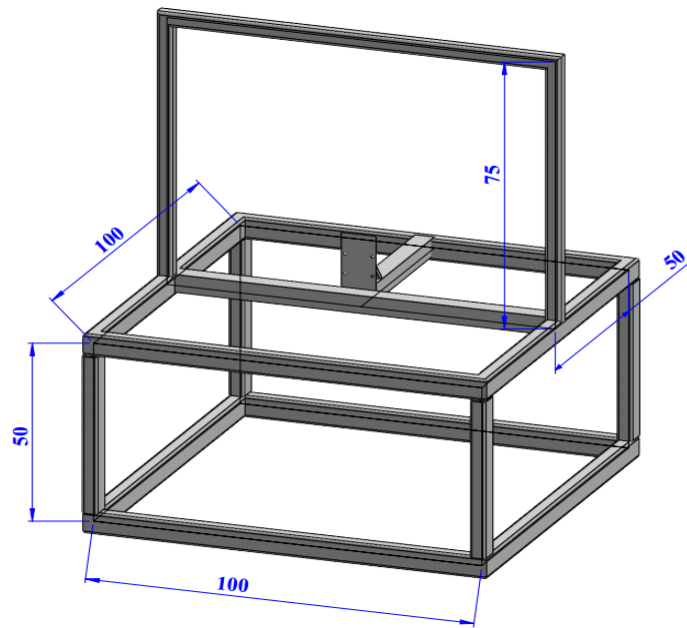


Figure 3.13. Frame design with all dimensions.



Figure 3.14. Frame manufacturing.

3.3. MEASURING DEVICES

In the experimental study, it is important to provide some necessary measurements to complete this study. Results are obtained through these measurements, and the accuracy of these results depends on the type of measurements used. The measurements that were used in our experimental study are:

3.3.1. Current and Voltage Measuring Device

The locally manufactured device comprises a compact box with dimensions of (20 * 20) cm, housing an array of resistors spanning from 1 ohm to 15 ohms, all interconnected to a manual switch for adjustable resistance. It is equipped with two sizable LCD screens: one dedicated to current readings, and the other for voltage measurements. Additionally, two switches are provided for toggling the screens on and off. Each LCD screen is powered by a separate 3-volt battery to prevent any drain on the energy generated by the turbine. The device functions on the premise of a straightforward electrical circuit, enabling the passage of current generated by the turbine and electric motor through the resistor network, simulating a practical load to obtain authentic current and voltage data. Utilizing an external switch, users can manually adjust the resistors to achieve the highest resistance level, facilitating the acquisition of accurate current measurements. This device has undergone examination and testing to ensure its precision in measuring both current and voltage. It serves as a primary tool for evaluating the electrical output resulting from the turbine's mechanical motion, consistently delivering reliable current and voltage readings in tandem during various tests. Figure 3.15 shows the device used to measure current and voltage.



Figure 3.15. Current and voltage measuring device.

3.3.2. The Tachometer

A digital tachometer, a critical instrument for measuring the rotational speed of objects, is defined as an optical encoder that precisely determines the angular velocity of rotational motion. Its applications span a wide spectrum, finding extensive use in automotive, aviation, engineering, and various industrial applications. In our experimental investigation, we employ a digital tachometer of the DT-2234A+ model, which serves the essential function of quantifying the revolutions per minute (RPM) of the turbine blades driven by the wind generated through the rapid motion of vehicles in this research. Notable specifications of this device include its memory feature, capable of storing maximum, minimum, and last recorded values; a large, 5-digit LCD

display with 31mm height; a broad test range measurement spanning from 2.5 to 99,999 RPM; a high-resolution capability of 0.1 RPM (for RPMs from 2.5 to 999.9) and 1 RPM (for RPMs exceeding 1,000); a remarkable accuracy level of $\pm (0.05\% + 1 \text{ digit})$; a swift sampling time of 0.8 seconds per 60 RPM; and an effective measuring range from 50 mm to 500 mm (2" to 20") utilizing a laser light source. Figure 3.16 shows the digital tachometer used in the tests.



Figure 3.16. Digital tachometer.

3.3.3. The Anemometer

The anemometer, specifically the GM 816 model, serves as an essential instrument for quantifying wind speed. In the context of our research, we employ it to gauge the velocity of wind eddies generated by the motion of vehicles on highways. This device boasts a generously sized LCD screen for enhanced data readability and is characterized by its lightweight, user-friendly, and efficient design, delivering rapid response times and precise measurements of various meteorological parameters. Its versatility extends to applications in heating, ventilation, air conditioning, meteorology, agriculture, and numerous other fields. Notable features of the GM 816 anemometer encompass the measurement of air velocity and temperature, as well as the capability to record maximum, average, and current air velocity readings, ensuring comprehensive and accurate wind assessment. Figure 3.17 shows the anemometer used in the tests.



Figure 3.17. Anemometer.

3.4. EXPERIMENTAL TESTING PROCEDURE

This section of the chapter details a comprehensive testing process conducted in three distinct stages: the internal test, the external test, and the single-vehicle test. The internal test involved the evaluation of traditional Savonius and Darrieus turbines, followed by the examination of a double turbine configuration with blade separation distances of 5, 10, and 15 cm. This analysis aimed to identify the optimal distance between blades spacing that would give the best results. The external test focused on determining the optimal positioning of the double turbine relative to the fastest side of the highway in the Baghdad-Mosul corridor. This assessment included tests at various heights above the ground to ascertain the most efficient placement for the double turbine. The final experimental section centered on the single-vehicle test, involving a range of vehicle types such as sedans, trucks, and buses...etc to quantify the total energy output generated by the double turbine across diverse vehicle scenarios. In tests performed at constant wind speed, the resistance applied by the generator must be changed in order to obtain different speed ratio values. In this study, the response of the generator was achieved by using different resistors. However, in the experiments, fluctuations in wind speed on the turbine caused a second reason to arise that affected the tip speed ratio value. The fan used in internal tests could not always provide a homogeneous and constant wind speed and caused slight fluctuations in wind speed. In the tests carried out in the highway area, the same fluctuation in wind speed was

caused by the effect of other vehicles and the natural wind in the environment. Tip speed ratio values were determined by calculations using different resistances and different measured wind speed values. Figure 3.18 illustrates the schematic representation of these procedural steps.

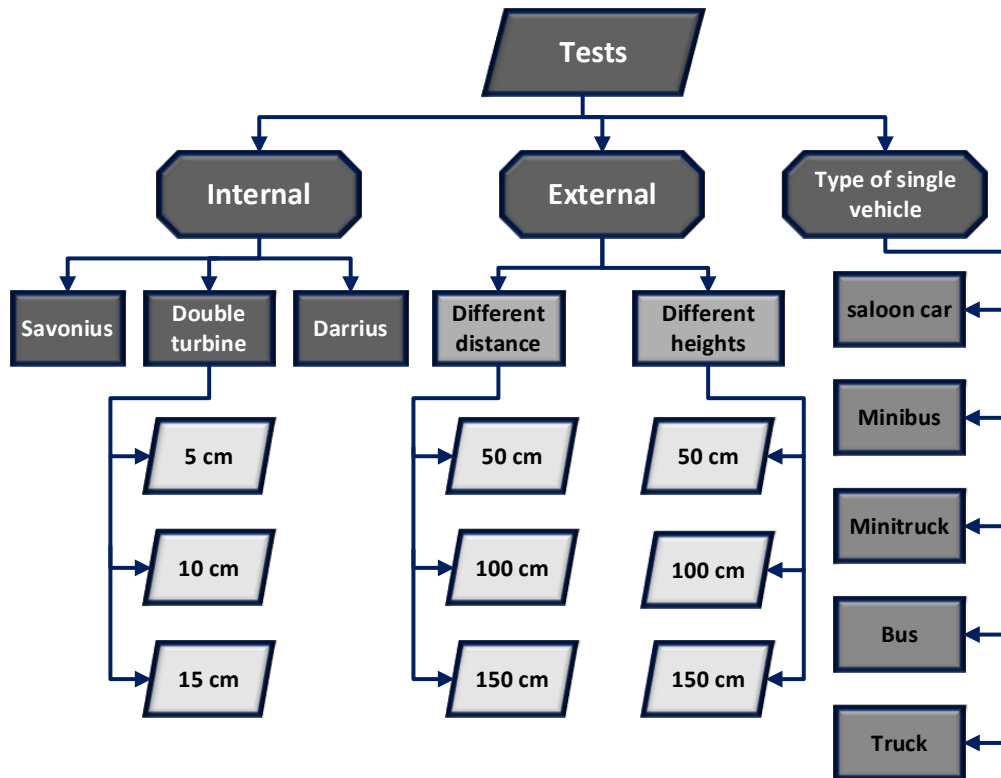


Figure 3.18. The schematic diagram of a steps for double turbine.

3.4.1. Internal Test

This section of study focuses on the assessment of power enhancement through a comparative analysis involving the conventional Savonius and Darrius turbines in contrast to the proposed turbine design. Furthermore, it seeks to determine the optimal spatial configuration between the Darrius and Savonius blades within the proposed turbine, with the ultimate goal of achieving peak performance. These experiments are conducted within a controlled, enclosed environment characterized by consistent wind speeds and a fixed turbine-blower distance. Wind speed measurements are taken using an anemometer positioned 50 centimeters in front of the blower, registering wind speeds ranging from 3.8 to 4.5 meters per second. These meticulously controlled

laboratory tests were executed within the controlled confines of a laboratory at the College of Engineering, Al-Mustansiriya University.

3.4.1.1. Savonius Test

The test procedure can be outlined in a series of steps: Firstly, the Savonius Turbine is tested in isolation, excluding the Darrieus airfoils. An anemometer is then positioned at a 50-centimeter distance in front of the blower, and the blower is operated to measure wind speed at five-minute intervals using the anemometer. Subsequently, the Savonius Turbine is placed at the same 50-centimeter distance in front of the blower, and the blower is re-activated, causing the Savonius blades to rotate due to the wind speed generated by the blower, thereby facilitating an assessment of its performance. Figure 3.19 shows the Savonius turbine test.



Figure 3.19. Savonius turbine test.

3.4.1.2. Darrieus Test

The test methodology can be delineated into a series of steps: Firstly, the Darrieus Turbine undergoes isolated testing. Following this, an anemometer is meticulously positioned at a fixed 50-centimeter distance in front of the blower. Subsequently, the

blower is set into operation, facilitating the periodic measurement of wind speed at five-minute intervals through the employed anemometer. The Darrieus Turbine is then placed at the identical 50-centimeter distance in front of the blower. Finally, the blower is reactivated, inducing the rotation of the Darrieus airfoils as they respond to the wind speed generated by the blower, thus enabling a comprehensive evaluation of the Darrieus Turbine's performance. Figure 3.20 shows the Darrieus turbine test.



Figure 3.20. Darrieus turbine test.

3.4.1.3. Double Turbine Test

This experimental phase is dedicated to increasing the power of double turbine, focusing on identifying the ideal spacing between the Darrieus and Savonius blades. To determine the optimal distance between the Savonius and Darrieus blades, the largest available distance (15 cm) was divided into test sections of 5, 10, and 15 cm. The basis for choosing these distances is that the maximum length of the chord connecting the rotating shaft to the Darrieus blades was designed to maintain the balance of the system and Reduce vibration. The tests are conducted within the same laboratory to evaluate Savonius and Darrieus turbines. In Test A, the process involves affixing Darrieus airfoils to the Savonius turbine's final hole in the chord, establishing a precise

separation of 15 centimeters between the Darrieus and Savonius blades using laser measurement as shown in Fig 3.21. An anemometer, positioned at a fixed distance of 50 centimeters from the blower, records wind speed measurements at five-minute intervals during the test. The proposed double turbine is then installed at the same 50-centimeter distance from the blower. In Test B, the procedures are executed as follows: Initially, the Darrieus airfoils are connected to the Savonius turbine at the middle hole in the chord. The separation between the Darrieus and Savonius blades is precisely set at 10 centimeters. An anemometer is strategically positioned at a distance of 50 centimeters from the blower to facilitate wind speed measurements during the test. In Test C, the procedure is outlined as the test involves attaching Darrieus airfoils to a Savonius turbine at the nearest-first hole in the chord, which is set at a distance of 5 centimeters. Figure 3.22 shows the third hole double turbine test.



Figure 3.21. Double turbine test third hole.

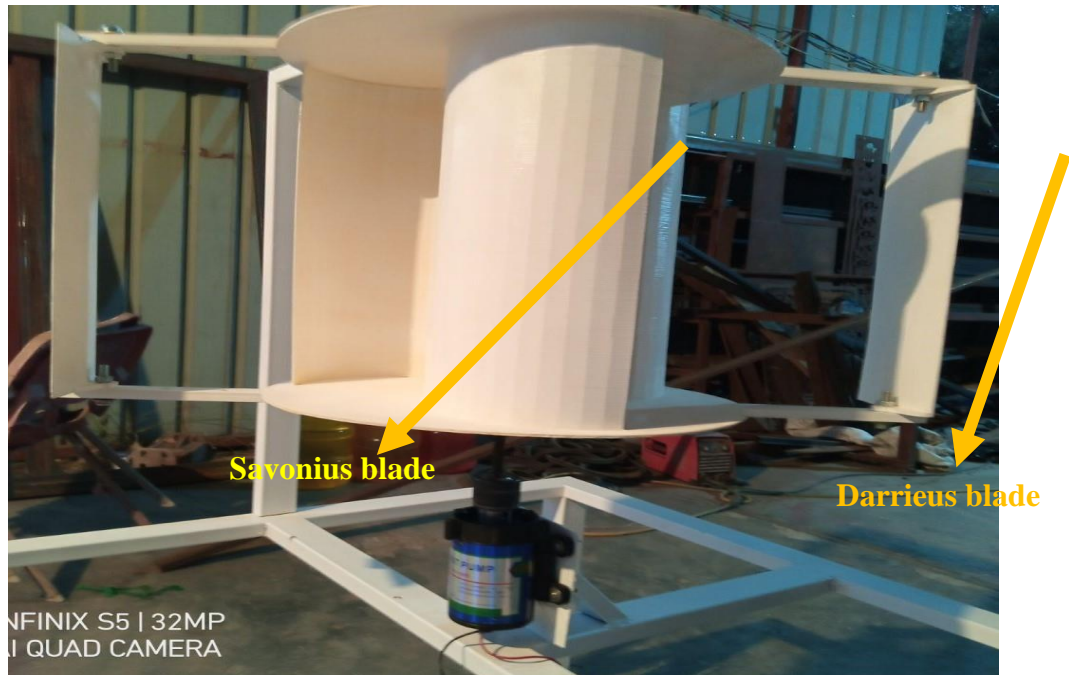


Figure 3.22. Double turbine test third hole.

3.4.2. External Test

To ascertain the optimal real-world performance, testing was conducted by deploying the proposed double turbine model in authentic conditions. This entailed sitting the proposed turbine model on an international highway, a task not devoid of challenges given the substantial risks associated with positioning equipment in the midst of a highway devoid of protective barriers, especially considering the sweltering temperatures characteristic of Iraq during the specific period. Nevertheless, in the pursuit of our objectives, the installation was carried out at the northern entrance to Baghdad, along the prominent International Road Number One (R1) that connects the capital to Mosul as shown in Fig 3.23 This road accommodates a diverse array of vehicles, ranging from trucks and long vehicles to buses, mini buses, mini trucks, SUVs, and saloon cars, all of varying shapes and sizes, and operating at varying speeds. Comprehensive data collection was meticulously conducted under these conditions to fulfil the study's objectives through available measuring devices, an anemometer was placed on top of the double turbine in the middle of the iron frame to accurately measure the speed of the wind controlling the turbine and a laser tachometer was used to measure the number of revolutions of the blades Also, a current and voltage meter was connected to the electric generator to obtain accurate results. The

installation of double turbines at a highway's median, in proximity to the fastest lane, is a conventional practice aimed at harnessing the maximum wind vortices generated by the high-speed movement of vehicles. The distances proposed in the experiment were chosen on the basis that the minimum island width of 3 m, as recommended by various international organizations (AASHTO, European Union, PIARC)[97] , served as the baseline. Since the turbine was designed for testing purposes, only one side of the highway was used. Therefore, half the width of the island was divided into three sections to test the most efficient location. The same dimensions were used to determine the optimal height.

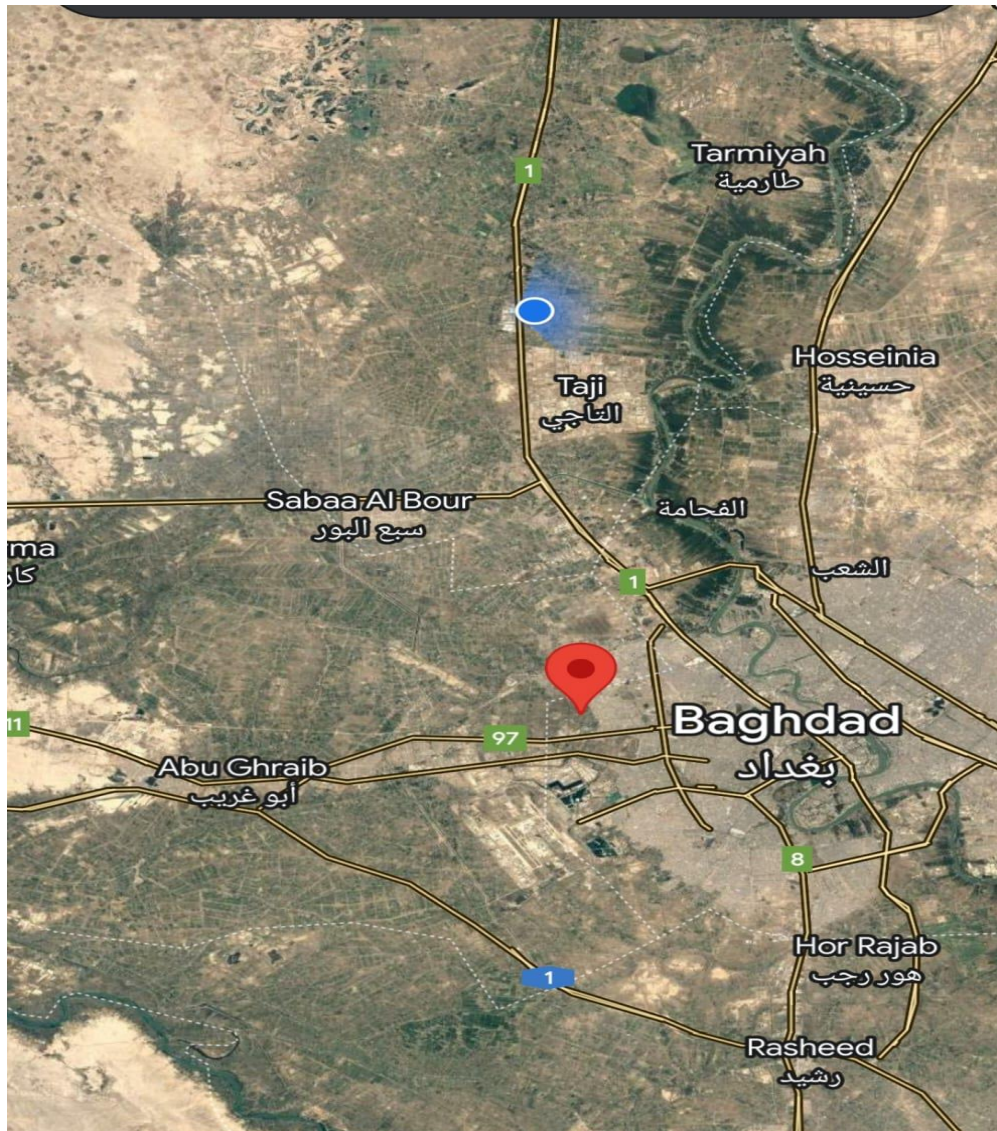


Figure 3.23. The double turbine installation site.

3.4.2.1. Distance Tests

To evaluate the performance of the proposed double turbine, an array of tests was conducted, each focusing on the distance between the double turbine and the highway at a consistent height. These tests were informed by prior assessments and adjustments. The assessments entailed varying the distance between the double turbine and the highway, with the height maintained at 50 centimeters, aiming to attain the most efficient performance. During these evaluations, the resistor settings for current and voltage measurement were standardized at 8 ohms to ensure accurate current readings.

Test D involved situating the double turbine 50 centimeters from the faster side of the highway, with a height of 50 centimeters above the ground, as shown in Fig 3.24, with wind speed measured at five-minute intervals using an anemometer.

Test E saw the double turbine positioned 100 centimeters from the highway's faster side, maintaining a consistent 50-centimeters height, as shown in Fig 3.24 and employing the same anemometer-based wind speed measurements.

In Test F, the distance was extended to 150 centimeters height maintained at 50 centimeters, as shown in Fig 3.24, and wind speed monitored at the same intervals by the anemometer. These systematic tests were crucial for evaluating the impact of varying distances on the turbine's performance.

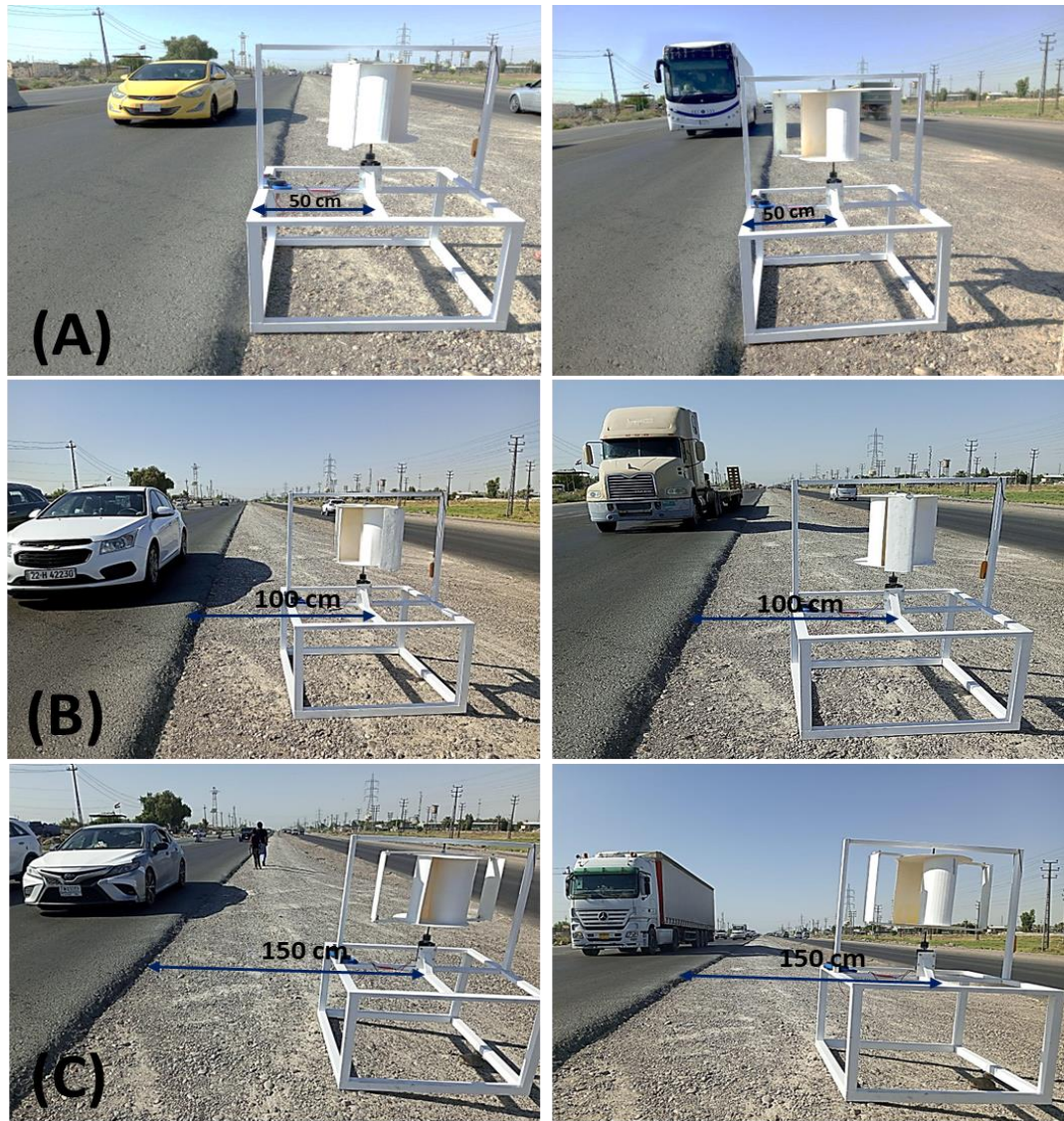


Figure 3.24. Distance test for double turbine at (A): Test D, (B): Test E, (C): Test F.

3.4.2.2. Height Tests

To evaluate the performance of the proposed double turbine, a series of tests were conducted, with a focus on varying the height of the double turbine above the ground. These evaluations built upon previous tests and aimed to determine the most effective height dimension in conjunction with the best distance from the highway for the turbine's optimal operation. In these tests, the resistor settings for the current and voltage measuring device were standardized at 8 ohms to ensure the accurate acquisition of current readings.

Test G involved placing the double turbine at a distance of 100 centimeters from the highway's faster side and maintaining a height of 50 centimeters above the ground, as shown in Fig 3.25, with wind speed monitored at five-minute intervals using an anemometer.

Test H saw the double turbine located at the same 100-centimeter distance from the highway, yet with a height of 100 centimeters above the ground, as shown in Fig 3.25 and wind speed measured by the anemometer at the same intervals.

Test I featured the double turbine positioned 100 centimeters from the highway's faster side, with a height elevated to 150 centimeters above the ground, as shown in Fig 3.25, and wind speed readings taken using the anemometer. These systematic tests were instrumental in evaluating the impact of varying heights on the turbine's performance.

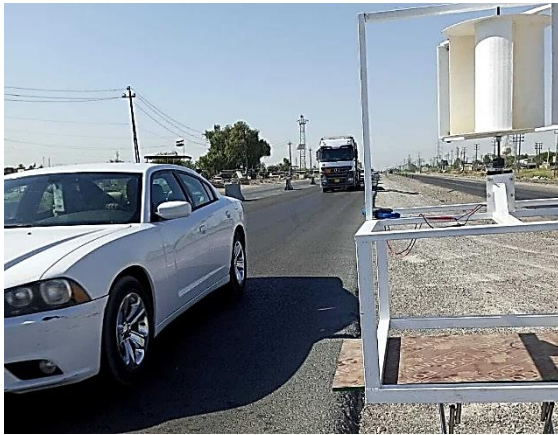


Figure 3.25. Height tests for a double turbine at (A): Test G, (B): Test H, (C): Test I.

3.4.3. Type of Single Vehicle

In this section of the experimental study, following the completion of geometric preference experiments and performance assessments, a focused examination of the proposed double turbine's performance was carried out with various types of vehicles on highways. The objective was to calculate the total energy harnessed by the turbine from each vehicle type. This was achieved by positioning the turbine and passing the respective test vehicles, all traveling at 100 km/h, in front of the proposed double turbine. Readings were taken over a 10-second interval before the vehicle reached the

turbine, as it passed in front of the turbine, and after the vehicle had passed the turbine. To ensure precision, data was recorded through continuous photography of the measurement devices at one-second intervals throughout the vehicle's 10-second passage. A series of tests (Test J to Test N) were conducted, each involving a distinct vehicle type (saloon car, Minibus, Minitruck, Bus, and Truck) all starting on the road at 100 km/h and passing in front of the turbine, with wind speed monitored every second by an anemometer. These meticulously designed tests provided a comprehensive evaluation of the proposed double turbine's performance under real highway conditions, catering to the diversity of vehicle types and their interaction with the turbine. Figure 3.26 shows all tests of type of single vehicle.



(A)



(B)



(C)



(D)



(E)

Figure 3.26. type of single vehicle test for double turbine at (A): Test J, (B): Test K, (C): Test L, (D): Test M, (E): Test N.

3.5. GOVERNING EQUATIONS

In the realm of scientific inquiry and engineering applications, governing equations serve as the fundamental principles that guide the behavior and interactions of physical systems. These equations encapsulate the laws of physics, mathematics, and the relationships that underpin the dynamics of the natural world. In this section, we delve into the essential governing equations at the heart of our exploration and analysis, providing a solid foundation for understanding the phenomena and mechanisms that shape our study where the rotor area is the primary determinant of the energy generated by a wind turbine the power can be calculated as follows [98].

$$P_{max} = \frac{1}{2} \rho A V^3 \quad (3.1)$$

is the maximum power that can be extracted from the wind.

$$A = D * H \quad (3.2)$$

This equation shows that available wind energy increases with the cube of wind speed. It also depends on the air density and the swept area of the turbine blades. Therefore, higher wind speed and larger turbine area result in more power.

Where:

P _{max} : the wind power	D: the diameter of the turbine
ρ : the air density	H: the height of the turbine
A: the turbine swept area	
V: the wind velocity or wind speed	

Can calculate the angular velocity(ω) of the turbine and tip speed ratio(λ), with the equation [98].

$$\omega = \frac{2\pi*n}{60} \tag{3.3}$$

The tip speed ratio is defined as the ratio of the speed of the tips of the wind turbine blades to the speed of the wind that the turbine encounters. Mathematically, it's represented as:

$$\lambda(TSR) = \frac{\omega*r}{v} \tag{3.4}$$

Where:

ω : the angular velocity of the turbine
 r : Turbine radius
 v : The wind velocity or wind speed
 n : the rotation speed.

Electric current and voltage measurements are conducted at five-minute intervals during the test, with fixed parameters meticulously recorded. These measurements are executed through a dedicated current and voltage measuring device, interconnected with the wires emerging from the electric motor. Alterations to the resistors are

facilitated using an external switch, aimed at reaching the maximal load conducive to the generation of electric current. This stage of experimentation allows for the precise computation of electric power (P_e) over a spectrum of resistors, as derived from the obtained electric current and voltage readings [89].

$$P_e = v \times I \quad (3.5)$$

Where:

P_e : the electric power.

I : the output current.

v : the output voltage difference.

The kinetic energy generated from the wind is not fully exploited by the turbine due to the dispersion of the wind to the sides, in addition to part of it remaining behind the turbine. The energy used by the turbine (power coefficient of the wind turbine C_p) can be calculated using the following equation.

$$C_p = \frac{P_{available}}{P_{max}} \quad (3.6)$$

Where:

C_p : The power coefficient of the wind turbine

The total energy produced by the double turbine in this test is calculated using this formula:

$$Energy = \sum_{i=1}^n P_i * \Delta time \quad (3.7)$$

PART 4

RESULTS AND DISCUSSION

4.1. INTRODUCTION

The goal of this chapter is to present the extracted results from the experimental study that was carried out, as well as their analysis and investigation it, and discussion based on all the comparisons. This chapter generally divides the results into internal tests, external tests and single tests results for vehicles with double turbines.

4.2. RESULTS OF INTERNAL TESTS

The results of the internal test are displayed as shown in the Figure 4.1.

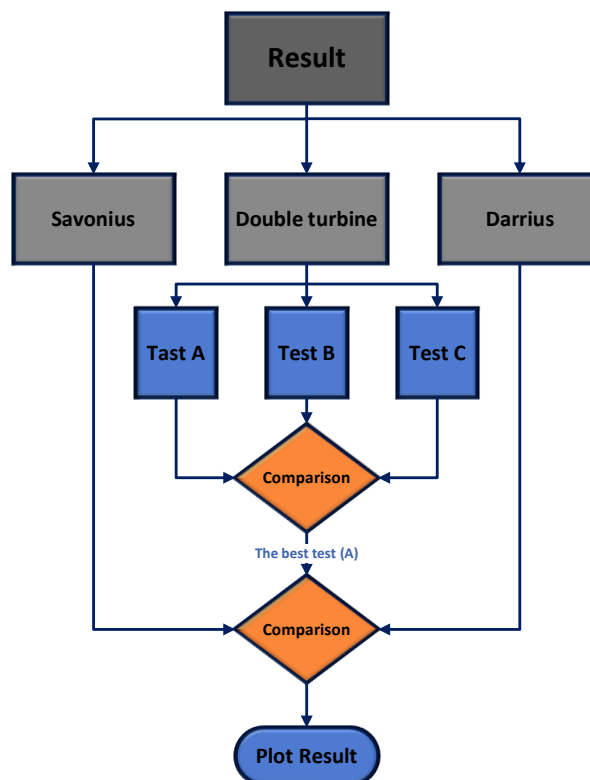


Figure 4.1. Schematic diagram of procedures.

4.2.1. Savonius Turbine Results

The findings derived from the experimental testing of the Savonius turbine in the laboratory, with a consistent wind speed range of (3.8 to 4.5) m/s, manifest a discernible augmentation in the turbine blade rotation speed, quantified in rotations per minute (RPM), during the initial moments of wind vortex capture. This initial acceleration in blade rotation is a distinctive feature of the Savonius turbine, rooted in its capacity for self-starting. The rotational speed of the turbine blades escalates until it culminates at its peak value, with a maximum of (458.8) RPM recorded. Concurrently, as the wind speed range incrementally rises during intermittent measurements throughout the experimental duration, there is a commensurate logical upswing in wind power (P_{max}). The maximum recorded wind power (P_{max}) attained (6.8226) Watts. The tip speed ratio (TSR) was computed based on the turbine blade rotation speed, with the maximum TSR registering at (1.9383). Throughout the test, a series of electrical current and voltage readings were obtained via the designated device, with the peak electrical current reaching (0.66) Amps and the highest turbine voltage measuring (1.96) volts. Subsequently, electrical power was computed to represent the available power in this test, with the highest recorded power standing at (1.2936) Watts. To gauge the turbine's efficiency, the power coefficient (C_p) was calculated, resulting in a maximum C_p of (0.1896), denoting a commendable ratio and high efficiency for the traditional Savonius turbine. For comparative purposes, a resistance of 8 ohms was selected, as it yielded the utmost current and voltage values, as depicted in Figure 4.2.

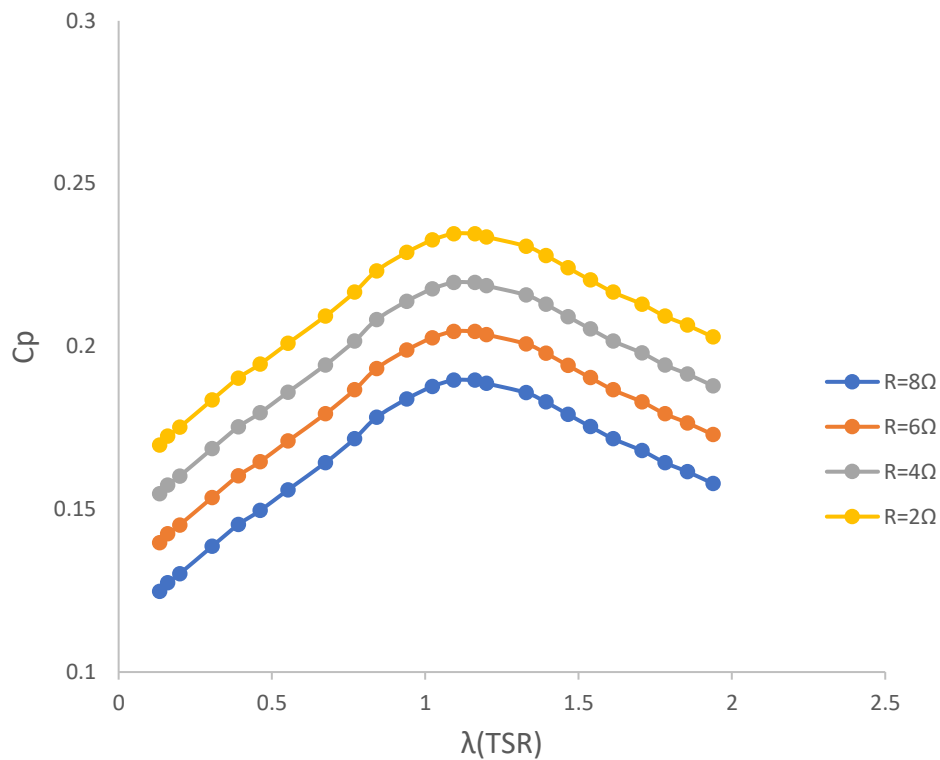


Figure 4.2. Comparison of different resistances of a $C_p - \lambda(\text{TSR})$ for Savonius turbine.

The data also clearly illustrates a noticeable upsurge in the power coefficient at the outset of the test, followed by a continuous ascent until it attains its peak value when the tip speed ratio reaches (1.2). Subsequently, the power coefficient undergoes a gradual decline, ultimately stabilizing by the conclusion of the test. A comparative examination of the curves corresponding to various resistors (8, 6, 4, 2 ohms) reveals significant variations and an increase in the power coefficient. This phenomenon is attributed to the heightened electric current and voltage, stemming from the reduction in resistance, as dictated by the inverse correlation between electric current and load.

4.2.2. Darrieus Turbine Results

The findings derived from the experimental testing of the Darrieus turbine in the laboratory these experiments, conducted under identical laboratory conditions as the Savonius turbine, maintained a constant wind speed range spanning from (3.8 to 4.5) m/s. Throughout the test, the rotational speed of the Darrieus turbine blades exhibited a direct correlation with wind speed, escalating progressively until it reached its zenith.

The maximum recorded turbine blade rotation speed reached (637.39) RPM. Concurrently, observations during the Darrieus turbine experiment underscored the positive correlation between wind power (P_{max}) and wind speed increments, registered intermittently from the onset of operation throughout the test period. The pinnacle wind power (P_{max}) achieved (6.82262) Watts. Tip speed ratio (TSR) calculations, predicated on turbine blade rotation speed, culminated in a maximum TSR of (3.8263). In this test, a series of current and voltage measurements were acquired from the designated device, with the highest recorded electrical current measuring (0.69) Amps and the peak turbine voltage standing at (1.98) Volts. Subsequently, based on the resultant data and the electric current and voltage emanating from the electric motor, electrical power was computed to represent the available power in this test, with the maximum power obtained amounting to (1.3662) Watts. For the assessment of turbine efficiency in this experiment, the power coefficient (C_p) was meticulously calculated. The Darrieus turbine recorded a maximum power coefficient (C_p) of (0.2002), signifying a commendable ratio and impressive efficiency for the Darrieus turbine design, as depicted in Figure 4.3.

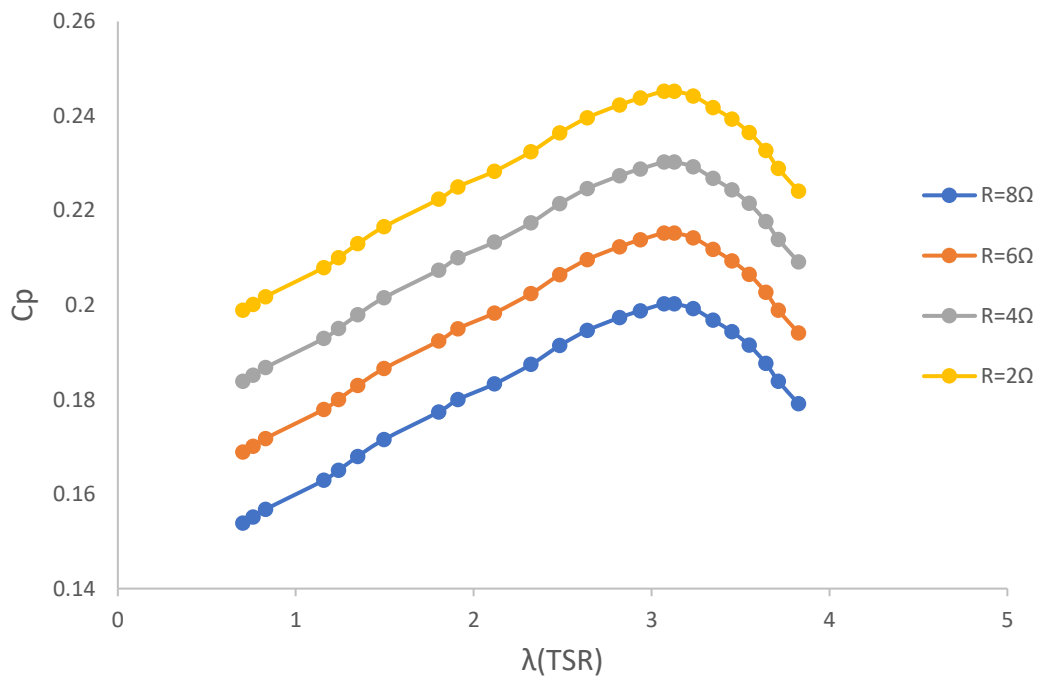


Figure 4.3. Comparison of different resistances of a $C_p - \lambda(TSR)$ for Darrieus turbine.

Figure 4.3 elucidates the intricate relationship between the power coefficient and tip speed ratio within the context of the Darrieus turbine during this specific test. Notably, it becomes evident that the power coefficient undergoes a steady progression from the inception of the test, culminating at its peak value when the tip speed ratio attains (3.1). Subsequently, the power coefficient experiences a gradual descent leading to the test's conclusion. Comparative analysis of the curves associated with various resistors (8, 6, 4, 2 ohms) reveals substantial variations and an augmentation in the power factor. This augmentation is attributable to the amplified electric current and voltage resulting from the electric motor when resistance diminishes, in accordance with the inverse relationship between electric current and load.

4.2.3. Double Turbine Results

Test A: The double turbine system initiates its operation with a rotational motion, achieving a peak turbine blade rotation speed of 554.3 RPM. Moreover, the escalation of the mean wind velocity leads to an augmentation in wind power (P_{max}), which attains a maximum value of 6.8226 watts. This amplification in wind power is attributable to the favorable correlation between wind power and wind speed. The tip speed ratio (TSR) is determined by analyzing the turbine blade's rotational speed, with a peak TSR of 3.8850. The results of this experiment include the recording of electric current and voltage values. The maximum electric current registers at 0.76 Amp, while the maximum voltage reaches 2.66 Volts. By leveraging these outcomes in conjunction with the electrical current and voltage emanating from the electric motor, the electrical power available in this assessment is computed. The highest power output is 2.014 watts. In evaluating the turbine's efficiency, the power coefficient (C_p) is calculated, revealing a peak C_p value of 0.21497, indicative of a favorable efficiency ratio for this specific double-turbine configuration. These findings collectively underscore the success of the turbine within this Darrieus and Savonius blade distance, as the resultant values bear witness to the advantageous impact of increasing the turbine's diameter in enhancing energy production. Furthermore, the cooperative interaction between the Darrieus and Savonius blades further contributes to the observed positive results, as depicted in Figure 4.4.

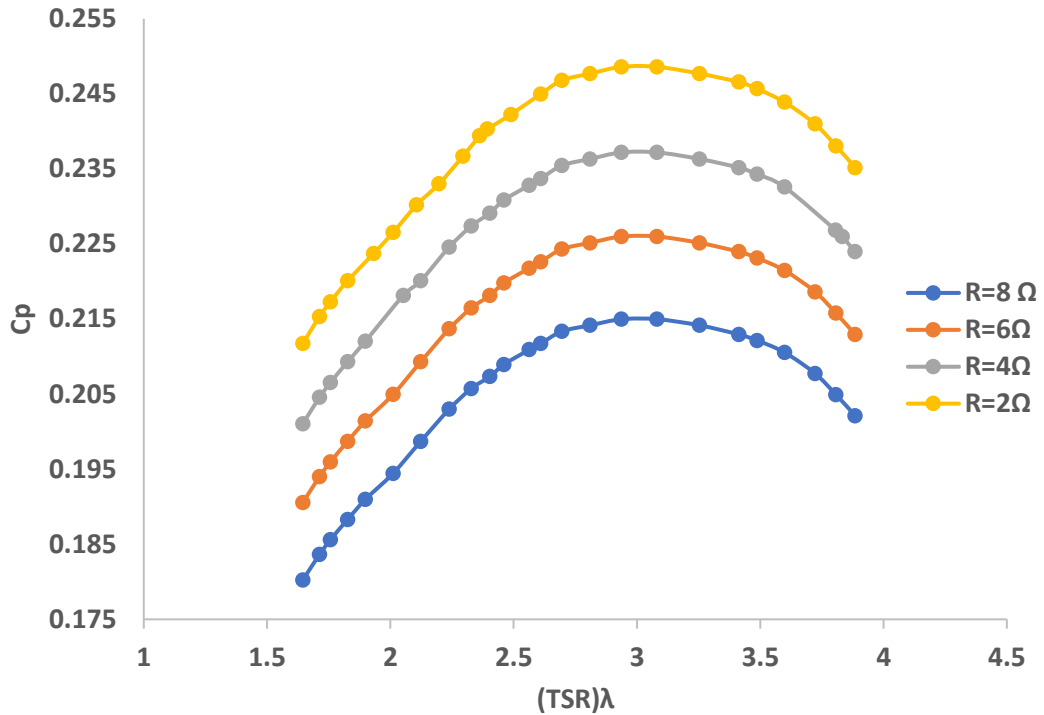


Figure 4.4. Comparison of different resistances of a $C_p - \lambda(\text{TSR})$ for double turbine (15cm).

Figure 4.4 presented herein illustrates the relationship between the power coefficient and tip speed ratio in the dual turbine configuration, where the separation distance between the Savonius and Darrieus blades measures 15 cm. It is evident that there is a noticeable percentage increase in the power coefficient from the outset of the test, culminating at its maximum value, or peak point when the tip speed ratio attains a value of 3. Subsequently, the power coefficient experiences a gradual decline towards the conclusion of the test. When we juxtapose the various curves corresponding to different resistors (8, 6, 4, 2 ohms), a discernible alteration and amplification in the power coefficient become apparent, attributed to the heightened electric current and voltage generated by the electric motor as the resistance diminishes. This phenomenon is a consequence of the inverse relationship between electric current and load.

Test B: This test was conducted with the Darrieus and Savonius blades positioned at a separation distance of 10 cm, maintaining the same laboratory conditions as the preceding experiments. The turbine blades achieved an optimal rotational speed, peaking at 531.45 RPM, while the maximum wind power (P_{max}) reached 6.8226 watts. During this test, the tip speed ratio (TSR) was calculated, with the maximum

TSR recorded at 3.7732. Furthermore, comprehensive readings of electrical current and voltage were obtained, with the highest electric current value registering at 0.6 Amp and the maximum voltage at 2.35 volts. The electrical power was subsequently derived from these measurements, resulting in a peak power output of 1.41 watts. To comprehensively assess the outcomes of this test, the power coefficient (C_p) was computed, revealing a maximum C_p value of 0.2066. It is worth noting that all these results were obtained using the same equipment while employing an 8-ohm resistance, as depicted in Figure 4.5.

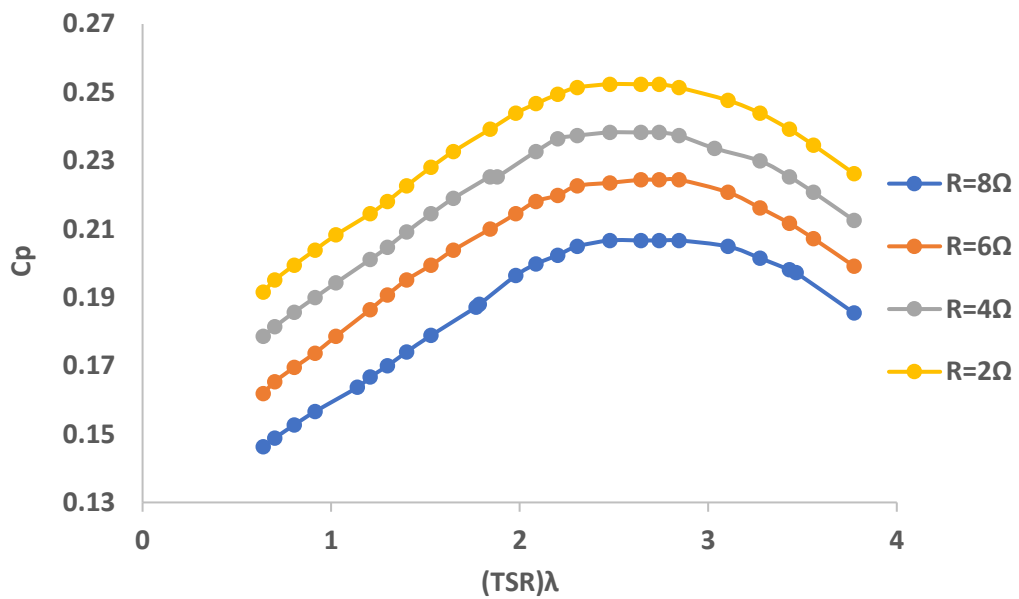


Figure 4.5. Comparison of different resistances of a $C_p - \lambda(TSR)$ for double turbine (10cm).

The depicted Figure 4.5 illustrates the relationship between the power coefficient and tip speed ratio in the dual turbine configuration, with the Darrieus and Savonius blades situated 10 cm apart. Notably, these figures depict the percentage increase in the power coefficient from the test's outset, its ascent to the maximum value (peak point) at a tip speed ratio of 2.8, followed by a subsequent decline in the power coefficient until the conclusion of the test. A comparative analysis of the curves corresponding to different resistors (8, 6, 4, 2 ohms) reveals noticeable alterations and an increase in the power coefficient. This augmentation is attributed to the heightened electric current and voltage resulting from the reduction in resistance, in line with the inverse relationship between electric current and load.

The results of Test C, where the distance between the Darrieus and Savonius blades is 5 cm, conducted under consistent laboratory conditions as in the preceding experiments, reveal a reduced rotational movement of the turbine blades compared to those in the first and second tests with greater blade distance. In line with the earlier tests, the turbine blades exhibited a gradual initiation of rotation at the start of the operation, which then escalated rapidly. The maximum rotation speed of the turbine blades in Test C reached 465.83 RPM, while the maximum wind power (P_{max}) was 6.8226 watts. The tip speed ratio (TSR) was computed, with the highest TSR recorded at 3.2426. Additionally, the maximum electric current reached 0.57 Amp, and the highest voltage measured at 1.94 volts. Electrical power was calculated based on these findings, resulting in a maximum power output of 1.1058 watts. The power coefficient (C_p) was also determined, with the peak C_p value standing at 0.1612, as depicted in Figure 4.6.

The obtained results and values indicate the presence of energy production in this test; however, it does not reach the desired level due to the relatively small distance between the Darrieus and Savonius blades, which impedes the effective capture of wind vortices by the turbine.

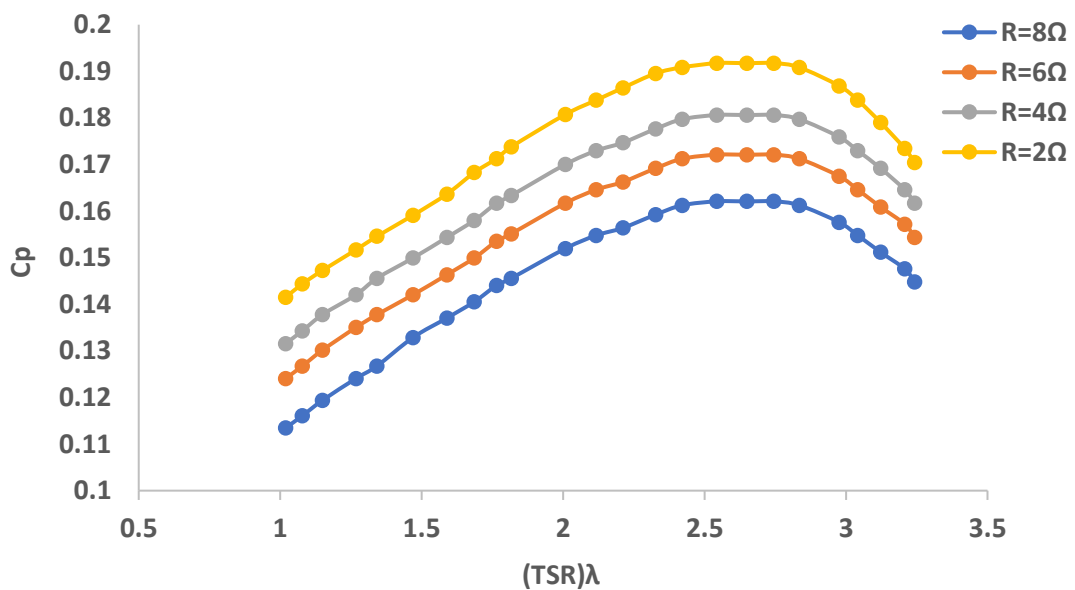


Figure 4.6. Comparison of different resistances of a $C_p - \lambda(TSR)$ for double turbine (5 cm).

The presented Figure 4.6 depicts the correlation between the power coefficient and tip speed ratio in the dual turbine configuration, with the distance between the Savonius and Darrieus blades set at 5 cm. These figures clearly illustrate the percentage increase in the power coefficient from the test's commencement, its ascent to the maximum value (peak point) when the tip speed ratio reaches 2.6, followed by a subsequent decline in the power coefficient until the conclusion of the test. When examining the curves for various resistors (8, 6, 4, 2 ohms), a noticeable alteration and augmentation in the power coefficient become apparent. This phenomenon can be attributed to the increased electric current and voltage generated by the electric motor as the resistance is reduced, in line with the inverse relationship between electric current and load.

4.2.4. Comparison Between Double Turbine Tests

The main purpose of this comparison is to know the best distance between the blades of Savonius and Darrieus in the proposed model to reach the best distance between the blades that can give the best results. By comparing the results and the values obtained in the double turbine tests (A, B, C), this goal can be achieved, which is to achieve geometric improvement of the proposed model. Table 4.1 and Figure 4.7 show the results of the double turbine tests.

Table 4.1. Results and values of double turbine tests.

Test name	The distance between the double turbine blades.cm	Blades rotation speed RPM	The optimum (λ)	Electrical power produced (power available)watt	Power Coefficient Cp
Test A	15	554.3	3	2.014	0.2149
Test B	10	531.45	2.8	1.41	0.2066
Test C	5	465.83	2.6	1.1058	0.1612

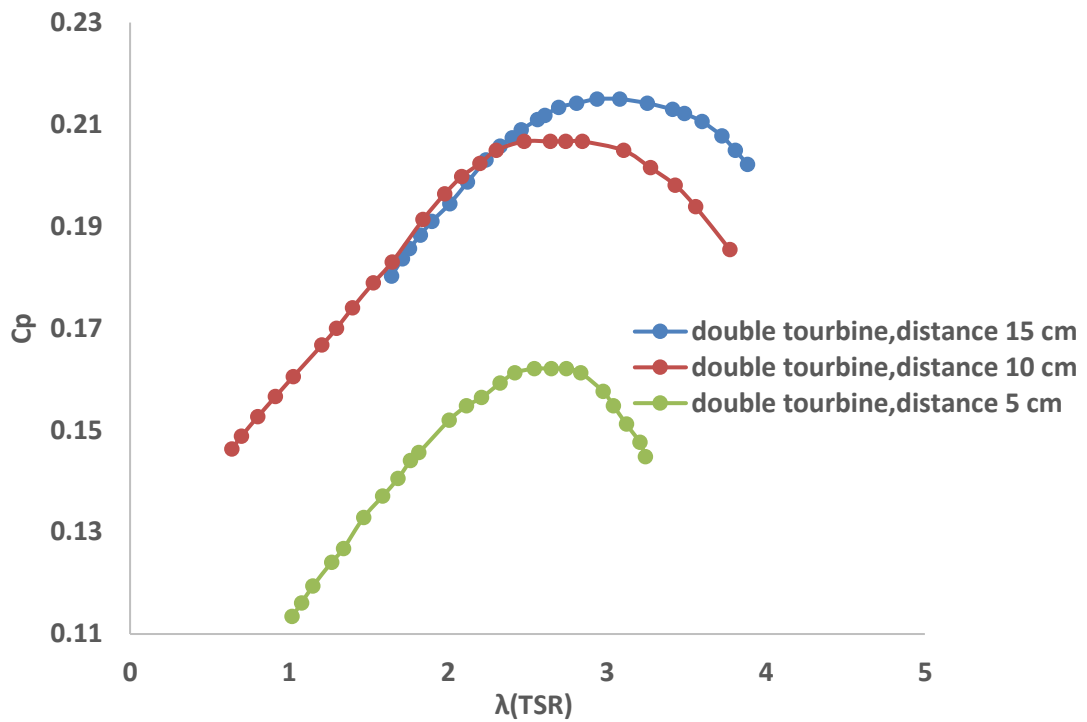


Figure 4.7. Comparison the relationship of a $C_p - \lambda(\text{TSR})$ for double turbine tests.

The results obtained from the dual turbine experiments, as depicted in the accompanying table and figures, clearly underscore its superior performance in Test (A), where the distance between the Savonius and Darrieus blades measures 15 cm. Notably, this test yields higher power values and a superior power coefficient compared to the other test configurations, thus establishing its evident advantage. In contrast, Tests (B) and (C) do not warrant classification as failures, as they still demonstrate satisfactory power output. However, the notably favourable outcomes of the dual turbine in Test (A) position it as the preferred configuration for subsequent experiments. It is pertinent to highlight that the reduced tip speed ratios (TSRs) observed in Tests (B) and (C) are a consequence of the turbine's smaller radius. It is imperative to recognize that TSR is directly proportional to the radius; hence, a diminished radius leads to a reduced TSR.

4.2.5. Comparing the Best Double Turbine with Savonius and Darrieus Turbines

It is imperative to undertake a rigorous comparison between the results and data obtained from the most promising dual turbine test and those from the Savonius and

Darrieus turbine tests. This comparative analysis serves as a pivotal step in evaluating the effectiveness of the proposed model in relation to conventional turbine models. It is essential to underscore that all comparative results have been derived from experiments conducted under identical laboratory conditions. Presented in Table 4.2 and Figure 4.8, these results offer a comprehensive insight into the performance disparities between the various turbine configurations.

Table 4.2. Results and values of the best double turbine and Savonius and Darrieus

Turbine type	Blades rotation speed RPM	The optimum (λ)	Electrical power produced (power available)watt	Power Coefficient Cp
Best double turbine	554.3	3	2.014	0.2149
Savonius	458.8	1.2	1.2936	0.1896
Darrieus	637.39	3.1	1.3662	0.2002

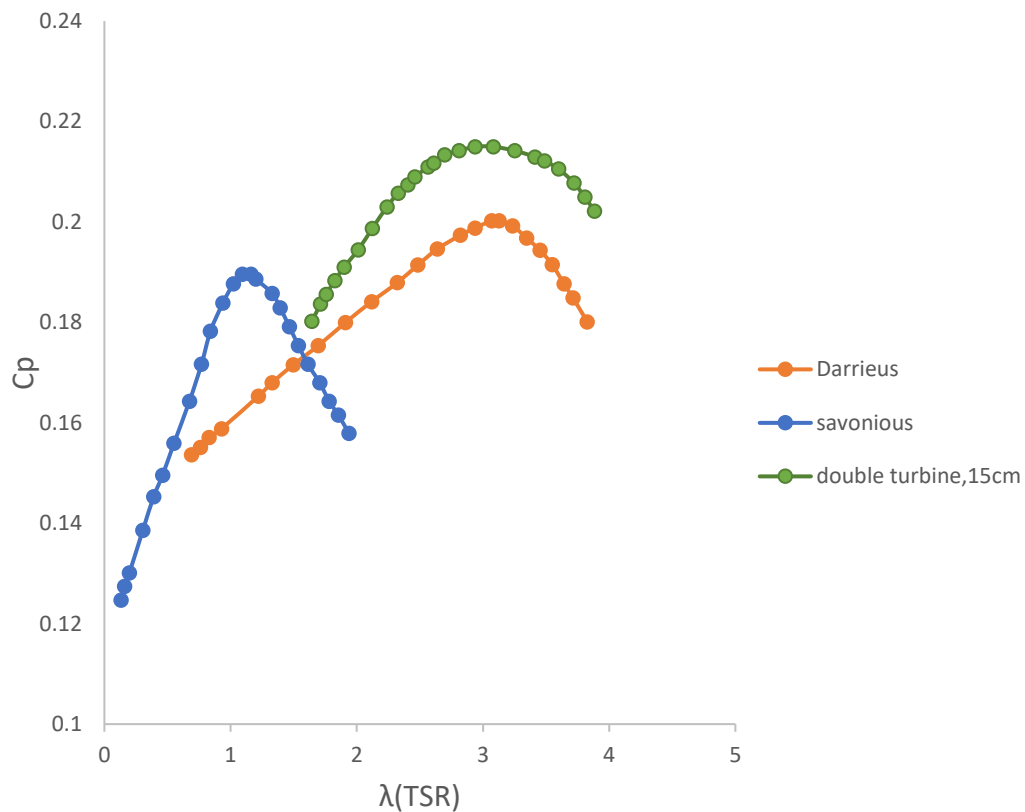


Figure 4.8. Comparison the relationship of a Cp - λ (TSR) for double turbine and Savonius and Darrieus.

The results and findings presented in the table and accompanying figure underscore the distinct superiority of the double turbine configuration when the distance between the Savonius and Darrieus blades measures 15 cm, as compared to the traditional Savonius and Darrieus turbines. This assertion is substantiated by the power values and power coefficient data, which distinctly favour the double turbine in this specific scenario. This observation highlights the effectiveness of geometric optimization in the double turbine, as well as the remarkable synergy between the Savonius and Darrieus blades in this innovative model. These characteristics confer a clear advantage in achieving the highest levels of energy output and meeting the desired objectives. It is worth noting that the tip speed ratio in the double turbine and the Darrieus turbine tests remains comparable, due to the positive relationship between the tip speed ratio and turbine radius. Nevertheless, the double turbine maintains its distinct superiority and preference in energy production.

4.3. RESULT OF EXTERNAL TESTS

The comprehensive assessment of the best double turbine's real-world performance necessitates an evaluation of its performance under typical operating conditions. To gauge the turbine's actual efficiency and capabilities, it is imperative to analyze the results derived from on-site tests conducted under variable external conditions. Given the variability in results contingent on the specific installation location along a highway, optimizing the turbine's positioning becomes a critical factor for achieving optimal outcomes, as shown in Figure 4. 9.

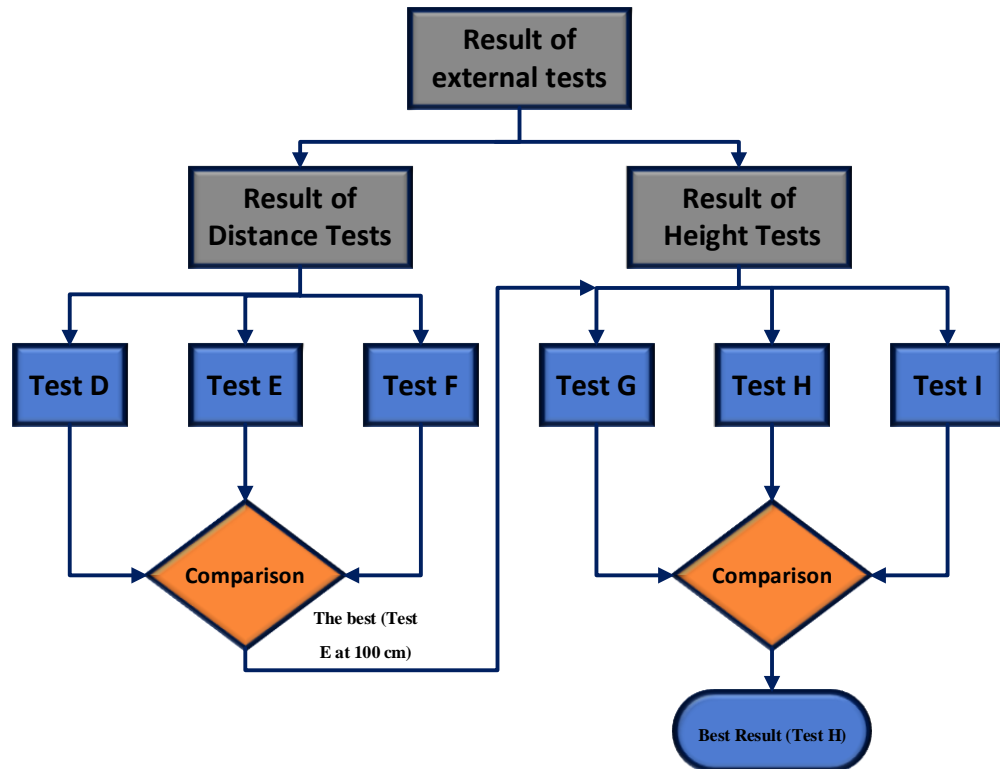


Figure 4.9. Flow Chart of The External Test.

4.3.1. Effect of Turbine Distance Results

The experiment tests focus on the results derived from three distance tests aimed at evaluating the double turbine's performance within an optimal placement relative to the faster side of the highway, ensuring optimal performance. In the initial distance test (Test D), where the turbine was positioned at a distance of 50 cm from the highway and at a height of 50 cm, wind speed measurements ranged from 4.6 to 5.2 m/s. Notably, this test yielded a maximum wind power (P_{max}) of 17.7797 watts, with the turbine blades achieving a peak rotational speed of 705.75 rpm. The maximum tip speed ratio (TSR) reached 4.9491. Furthermore, the data encompassing electrical current and resulting voltages are as follows: the highest electric current recorded was 1.03 Amp, and the maximum voltage measured was 2.91 volts. These findings facilitated the determination of electrical power, culminating in a maximum power output of 2.9391 watts. Subsequently, the power coefficient for the turbine in this particular test was calculated, with the highest value recorded at 0.2222, signifying favorable performance for the double turbine within this location, as depicted in Figure 4.10.

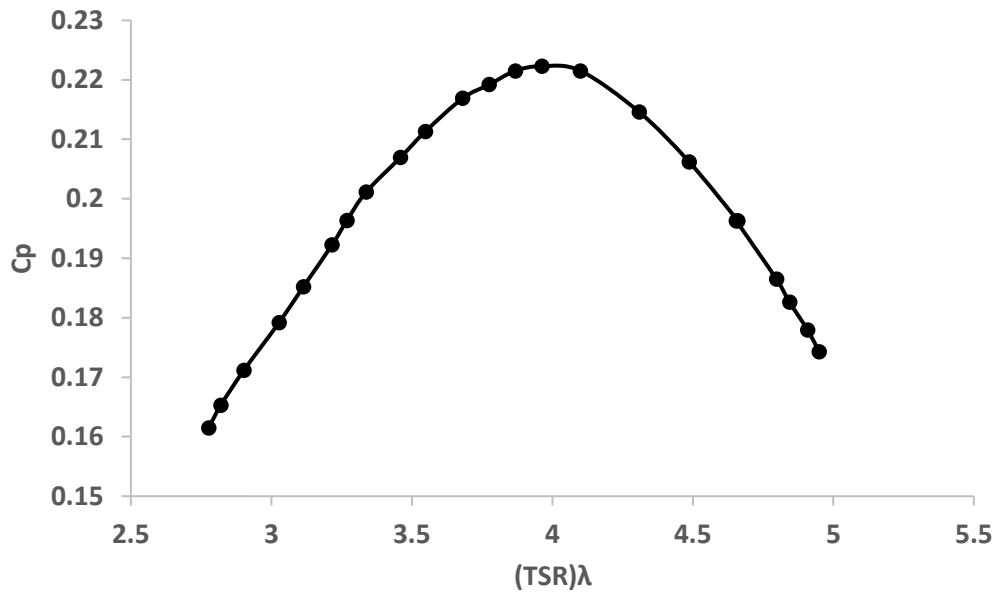


Figure 4.10. $C_p - \lambda(\text{TSR})$ for double turbine in Test D.

Figure 4.10 shows the relationship between the power coefficient and tip speed ratio in the double turbine in testing the distance (50) cm between the double turbine and the highway. It is also clear in it the percentage of increase that occurs in the power coefficient since the beginning of the test and its increase until reaching the maximum value (peak point) when the tip speed ratio is (4) and then the value of the power coefficient begins to decrease until the final time of the test. The values and results obtained in this test for power, power coefficient, and electric current represent good values and competence for the double turbine in this location, and they represent the efficiency and prove the success of the double turbine in this test.

In the second distance test (Test E), which entailed placing the turbine at a distance of 100 cm from the highway with a height of 50 cm, wind speed measurements were meticulously recorded, spanning from 4.6 to 5.5 m/s. This comprehensive evaluation revealed a remarkable maximum wind power (P_{max}) of 21.038 watts, accompanied by the turbine blades reaching a peak rotational speed of 761.6 rpm and a maximum tip speed ratio (TSR) of 5.1354. The data concerning electrical current and voltage in this test showcased a maximum electric current of 1.08 Amp and a peak voltage of 2.99 volts. These observations facilitated the derivation of electrical power,

culminating in a maximum power output of 3.2292 watts. Furthermore, the power coefficient for the turbine within this test was diligently calculated, with the highest recorded value standing at 0.2315, indicative of exceptional performance for the double turbine at this specific location. The results are detailed in Figure 4.11.

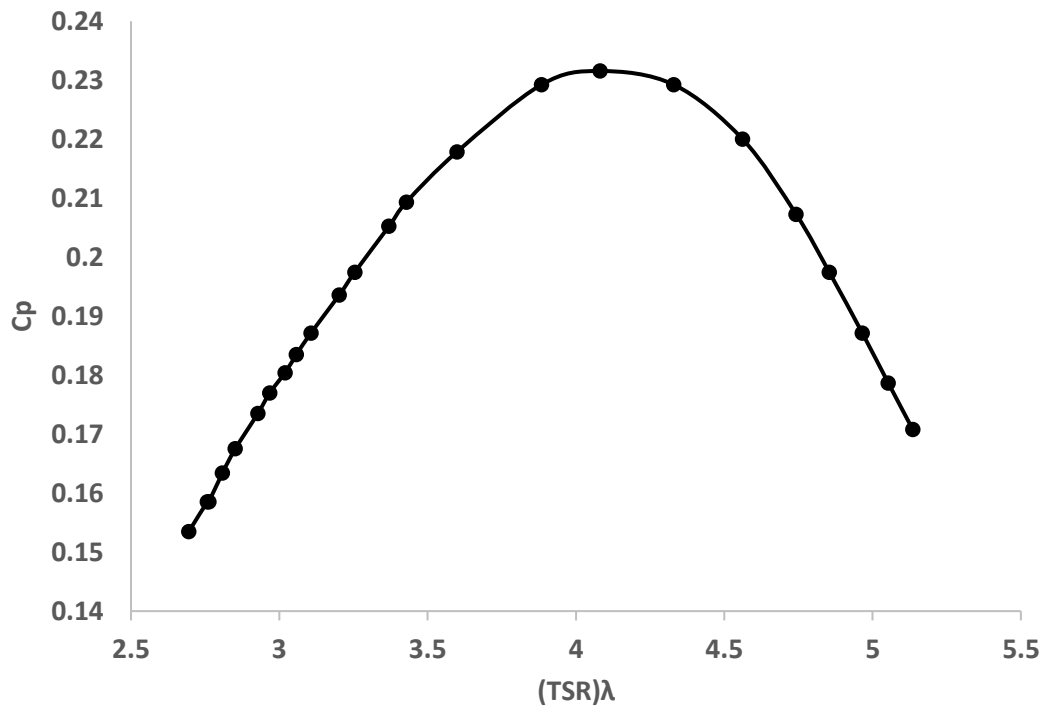


Figure 4.11. Relation between C_p and $\lambda(\text{TSR})$ for double turbine in Test E.

Figure 4.11 shows the relationship between the power coefficient and tip speed ratio in the double turbine in testing the distance (100) cm between the double turbine and the highway. It is also clear in it the percentage of increase that occurs in the power coefficient since the beginning of the test and its increase until reaching the maximum value (peak point) when the tip speed ratio is (4.2) and then the value of the power coefficient begins to decrease until the final time of the test. The values and results obtained in this test for power, power coefficient, and electric current represent very good values and high competence for the double turbine in this location, and they represent the efficiency and prove the success of the double turbine in this test.

In the third distance test (Test F), the turbine was strategically positioned at a distance of 150 cm from the highway, with a consistent height of 50 cm. Meticulous wind speed

measurements, ranging from 4.5 to 4.9 m/s, were conducted. This comprehensive examination revealed a maximum wind power (P_{max}) of 14.8766 watts, with the turbine blades achieving a peak rotational speed of 644.82 rpm and a maximum tip speed ratio (TSR) of 4.6141. The data concerning electrical current and voltage within this test indicated a maximum electric current of 0.94 Amp and a peak voltage of 2.84 volts. These observations facilitated the determination of electrical power, resulting in a maximum power output of 2.6696 watts. Furthermore, the power coefficient for the turbine within this test was diligently calculated, with the highest recorded value reaching 0.2043, signifying commendable performance for the double turbine in this specific location. A detailed presentation of these results can be found in Figure 4.12.

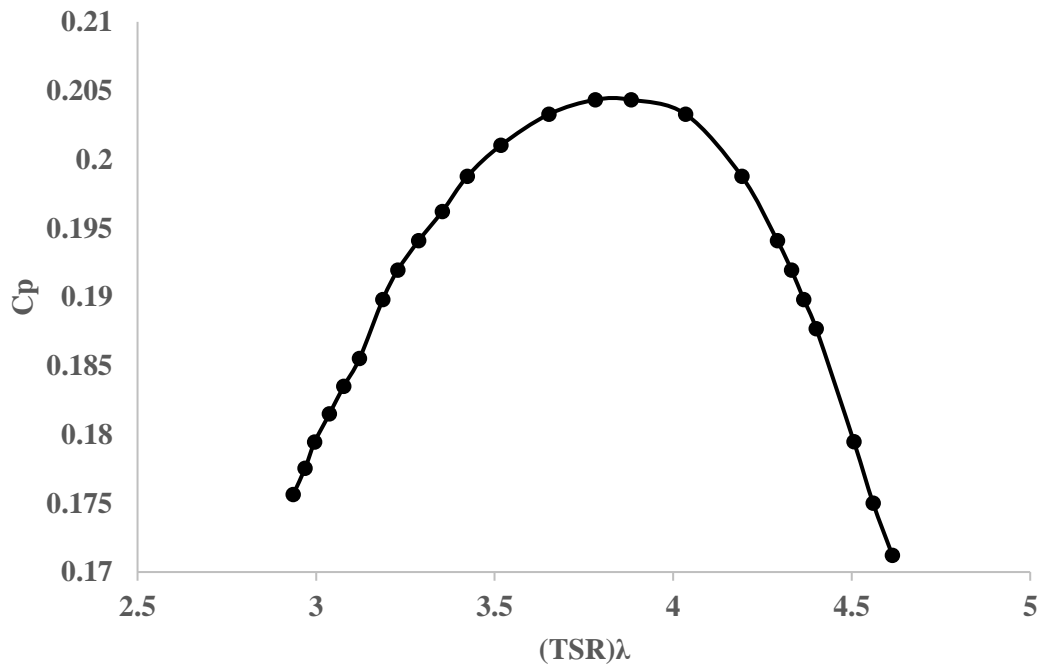


Figure 4.12. Relation between C_p and $\lambda(\text{TSR})$ for double turbine in Test F.

Figure 4.12 shows the relationship between the power coefficient and tip speed ratio in the double turbine in testing the distance (150) cm between the double turbine and the highway. It is also clear in it the percentage of increase that occurs in the power coefficient since the beginning of the test and its increase until reaching the maximum value (peak point) when the tip speed ratio is (3.8) and then the value of the power coefficient begins to decrease until the final time of the test. The values and results obtained in this test for power, power coefficient, and electric current represent good

values and competence for the double turbine in this location, and they represent the efficiency and prove the success of the double turbine in this test.

4.3.2. Comparison Between Distance Tests

In order to discern the most effective placement for the double turbine's performance and enhancing energy production, it is imperative to conduct a comparative analysis of the results obtained from distance tests carried out under varying conditions, encompassing a spectrum of wind vortices generated by the diverse categories of vehicles traversing the highways. The results from these assessments are comprehensively presented in Table 4.3 and Figure 4.13, encapsulating the findings from the distance tests of the double turbine.

Table 4.3. Results and values of distance tests of the double turbine.

Test name	The distance between the double turbine and highway.cm	Blades rotation speed RPM	The optimum (λ)	Electrical power produced (power available)watt	Power Coefficient Cp
Test D	50	705.75	4	2.9391	0.2222
Test E	100	761.6	4.2	3.2292	0.2315
Test F	150	644.82	3.8	2.6696	0.2043

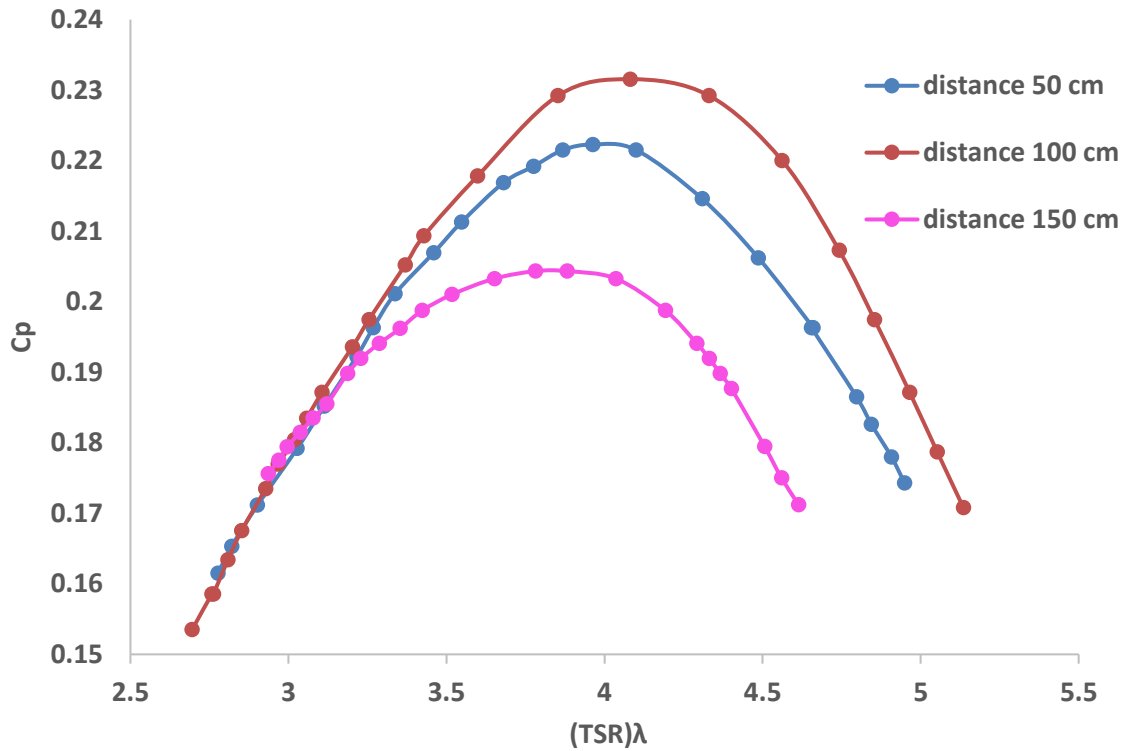


Figure 4.13. Comparison the relationship of a C_p and $\lambda(TSR)$ for double turbine in distance tests.

The results and values in the Table 4.3 and the Figure 4.13 above for distance tests of the best double turbine show that the turbine performs well at all locations. However, through comparison and evaluation, and in order to achieve the best results, highest performance, and efficiency, we found that the results obtained in the second test (Test E), when the distance between the best double turbine and the highway is 100 cm, are the best. This is the dimension that will be adopted in subsequent tests.

4.3.3. Effect of Turbine Height Results

Following the determination of the optimal horizontal positioning of the best double turbine relative to the highway, the subsequent crucial aspect to ascertain is the ideal height at which the turbine should be situated above the ground. While the double turbine demonstrates peak performance when positioned at a distance of 100 cm from the highway, the optimal height has yet to be established. Consequently, a series of tests were executed at three designated heights to amass data and insights for achieving the utmost performance of the double turbine. In the initial height test (Test G), the

best double turbine was placed at an elevation of 50 cm above the ground, maintaining a consistent distance of 100 cm between the turbine and the highway, as derived from the outcomes of the preceding distance tests. Wind speed measurements in this location ranged from 4.6 m/s to 5.2 m/s, resulting in the calculation of wind power (P_{max}), with a maximum of 17.7798 watts. Concurrently, the rotational speed of the turbine blades was meticulously measured, with the maximum recorded at 685.6 rpm. These values enabled the calculation of tip speed ratios (TSR), revealing a peak TSR of 4.8078. A comprehensive set of readings pertaining to electrical current and voltage was acquired, where the highest electric current value was 1.01 Amp, and the maximum voltage value stood at 2.92 volts. An essential parameter of interest, electrical power, was subsequently computed based on these results, with a maximum value of 2.987 watts. This data facilitated the determination of the power coefficient (C_p) for the turbine, with the highest value attaining 0.2253, indicative of commendable performance for the double turbine at this particular elevation as shown in Figure 4.14.

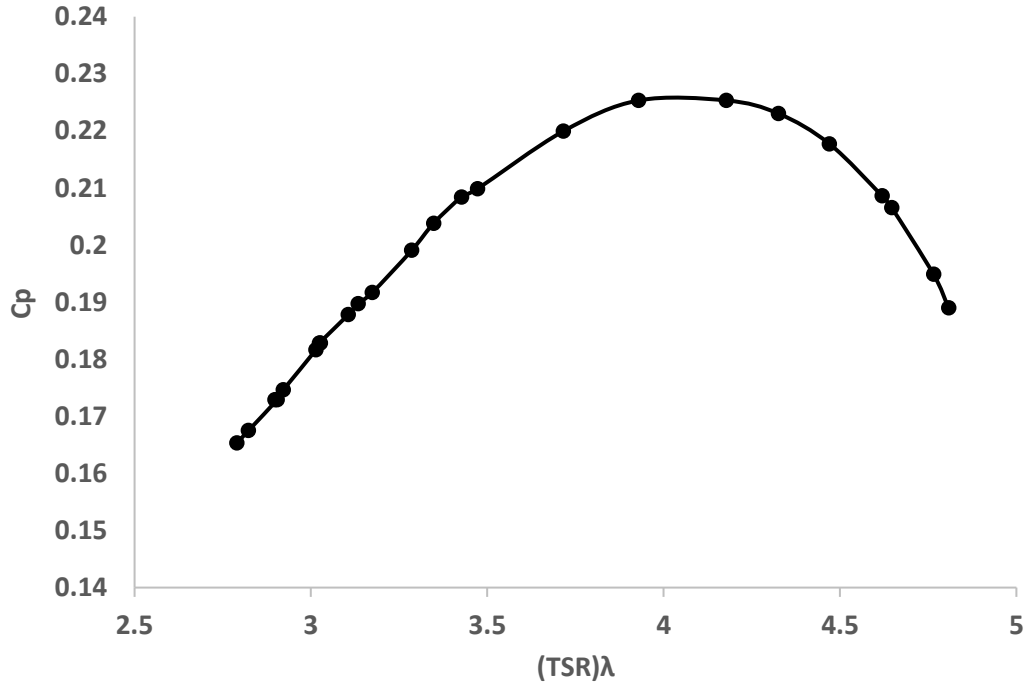


Figure 4.14. Relation between C_p and λ (TSR) for double turbine in Test G.

The Figure 4.14 shows the relationship between the power coefficient and tip speed ratio of a double turbine tested at a height of 50 cm above the ground. The power coefficient is a measure of the efficiency of a wind turbine in converting wind energy into mechanical energy and the tip speed ratio is the ratio of the speed at the tip of the rotor blade to the wind speed. The Figure 4.14 shows that the power coefficient increases with the tip speed ratio until it reaches a peak value at a tip speed ratio of (4). After this point, the power coefficient decreases. This is because the blades are moving too fast and are not able to capture as much wind energy. The percentage increase in the power coefficient from the beginning of the test to the peak value is significant. This demonstrates that the double turbine is very efficient at converting wind energy into mechanical energy. The values and results obtained in this test for power, power coefficient, and electric current are all very good. This indicates that the double turbine is a viable and efficient way to generate electricity from wind energy in this location. In the second height test (Test H), the best double turbine was positioned at an elevation of 100 cm above the ground, maintaining a consistent distance of 100 cm from the highway. Wind speed measurements at this location ranged between 4.6 and 5.4 m/s, culminating in a maximum wind power output of 19.9112 watts. The rotational speed of the turbine blades was diligently monitored during the test, with the highest rotational speed recorded at 794.83 rpm. These measurements facilitated the calculation of the tip speed ratio (TSR), which attained a peak value of 5.2583. A comprehensive dataset pertaining to electrical current and voltage was acquired, with the maximum electric current reaching 1.06 Amp and the highest voltage reaching 2.96 Volts. Electrical power was subsequently computed based on these readings, yielding a maximum power output of 3.108 watts. Furthermore, the power coefficient (C_p) for the turbine was calculated, with the highest recorded value standing at 0.2338, indicative of the commendable performance of the double turbine at this specific elevation. The detailed results are visually presented in Figure 4.15.

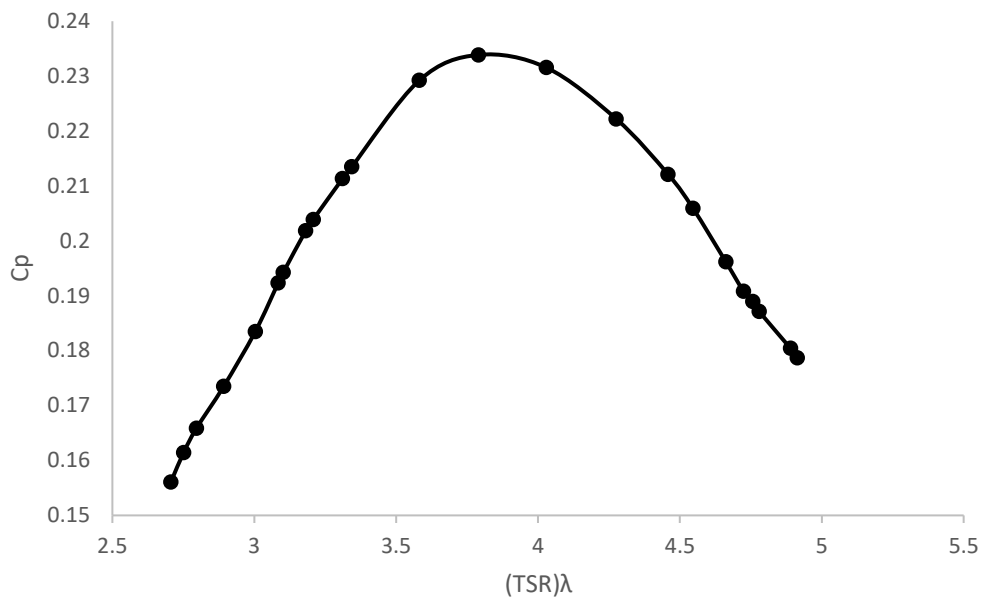


Figure 4.15. Relation between C_p and $\lambda(\text{TSR})$ for double turbine in Test H.

The Figure 4.15 depicts the relationship between the power coefficient and tip speed ratio of a double turbine tested at a height of (100) cm above the ground. The power coefficient is a measure of the efficiency of a wind turbine in converting wind energy into mechanical energy. At the same time, the tip speed ratio is the ratio of the speed at the tip of the rotor blade to the wind speed. The figure shows that the power coefficient increases with the tip speed ratio until it reaches a peak value at a tip speed ratio of (4.1). After this point, the power coefficient decreases because the blades move too fast and cannot capture as much wind energy. The percentage increase in the power coefficient from the beginning of the test to the peak value is significant, demonstrating that the double turbine is very efficient at converting wind energy into mechanical energy.

In the third height test (Test I), the optimal positioning of the best double turbine involved placing it at a height of 150 cm above the ground, maintaining a consistent distance of 100 cm from the highway. Within this setup, wind speed measurements were recorded, ranging from 4.7 to 5.2 m/s, resulting in a maximum wind power output of 17.7797 watts. The rotational speed of the turbine blades was diligently tracked during the test, with the highest recorded rotational speed standing at 612.48 rpm. Utilizing these rotational speed measurements and other pertinent data, the tip speed

ratio (TSR) was computed and reached a value of 4.2108. A comprehensive dataset pertaining to electrical current and voltage was obtained, with the maximum electric current measuring 0.98 Amp and the highest voltage measuring 2.89 Volts. Subsequent calculations yielded an electrical power output of 2.8126 watts. Furthermore, the power coefficient (C_p) for the turbine was determined, and the highest recorded value reached 0.2004, indicative of the commendable performance of the double turbine at this specific height. The detailed results are visually presented in Figure 4.16.

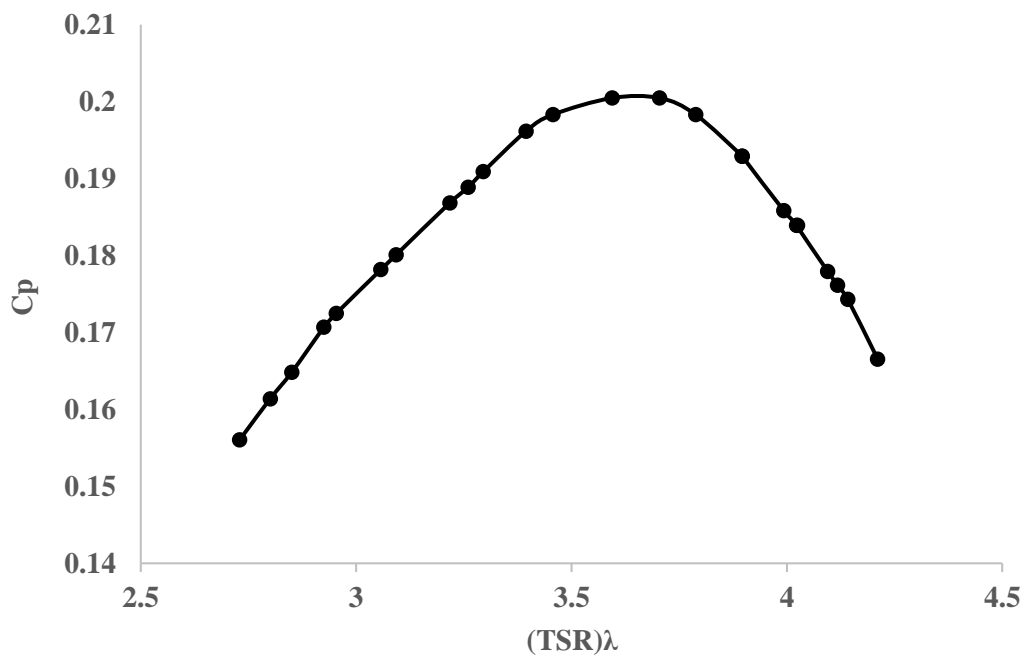


Figure 4.16. Relation between C_p and λ (TSR) for double turbine in Test I.

The Figure 4.16 depicts the relationship between the power coefficient and tip speed ratio of a double turbine tested at a height of (150) cm above the ground. The power coefficient is a measure of the efficiency of a wind turbine in converting wind energy into mechanical energy, while the tip speed ratio is the ratio of the speed at the tip of the rotor blade to the wind speed. This figure shows that the power coefficient increases with the tip speed ratio until it reaches a peak value at a tip speed ratio of (3.6) After this point, the power coefficient decreases because the blades are moving too fast and are not able to capture as much wind energy. The percentage increase in the power coefficient from the beginning of the test to the peak value is significant,

demonstrating that the double turbine is very efficient at converting wind energy into mechanical energy.

4.3.4. Comparison Between Height Tests

To fully evaluate the performance of the double turbine, it is necessary to compare the results of height tests to determine the optimal height at which the double turbine will achieve its peak efficiency. The following Table 4.4 and Figure 4.17 show the results of height tests of the double turbine.

Table 4.4. Results and values of height tests of the double turbine

Test name	The height of the turbine from the ground.cm	Blades rotation speed RPM	The optimum (λ)	Electrical power produced (power available)watt	Power Coefficient Cp
Test G	50	685.6	4	2.987	0.2253
Test H	100	794.83	4.1	3.108	0.2338
Test I	150	612.48	3.6	2.8126	0.2004

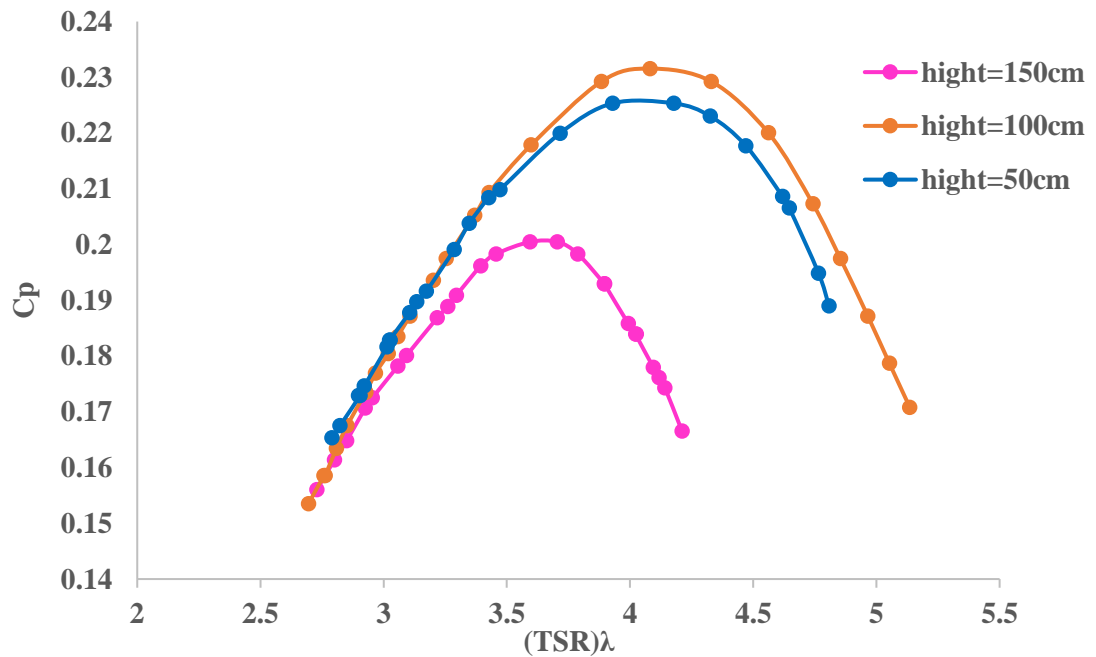


Figure 4.17. Comparison the relationship of a Cp and λ (TSR) for double turbine in height tests.

The results and values in the table and figure above for height tests of the best double turbine demonstrate that the turbine has good efficiency at all locations. To achieve the highest evaluation of the double turbine, the values from the three tests were compared, and it was determined that the double turbine performs best at a height of (100) cm in Test H. Therefore, based on all the tests conducted and the results and values obtained, we conclude that the best performance of the double turbine is achieved when it is placed (100) cm from the highway and (100) cm above the ground.

4.4. RESULTS OF SINGLE TYPE VEHICLE

Having learned about the extensive engineering improvements to the double turbine and its optimal location, now work to discover and evaluate its performance for each type of known vehicle and to calculate the total energy produced by the double turbine in each case of vehicle testing. The main types of vehicles that travel on main roads are trucks, buses, minitrucks, minibuses, saloon cars, and four-wheel drive cars. Therefore, it is necessary to present and discuss the results and values of the total energy produced when each type is tested individually. The double turbine is a promising new technology with the potential to significantly improve the performance and efficiency of different vehicle types. By evaluating its performance in a variety of vehicles, we can gain a better understanding of its potential benefits and limitations. This information can then be used to develop guidelines for the design and implementation of double turbines in different vehicle applications. The double turbine was tested on (Saloon car, Minibus, Minitruck, Bus, and Truck) car at a height of 100 cm and a distance of 100 cm, with the car passing in front of the turbine at a speed of 100 km/h. The necessary values were measured and calculations were performed, which gave the desired results during the 10-second test period. After completing the double turbine test on each vehicle type, it was necessary to compare and contrast the results to clarify the total energy levels and available power for each vehicle. The total energy was calculated by finding the area under the curve using MATLAB program. The Table 4.5 and Fig 4.18 and Fig 4.19 show the results of vehicle tests of the double turbine.

Table 4.5. Data results of the vehicle types test.

Vehicle Type	Maximum wind speed (m/s)	P max (Watt)	I max (AMP)	Voltage (Volt)	Maximum power electric (Watt)	Total energy (Joule)
Saloon car	2.8	2.7758	0.33	1.32	0.4356	3.2747
Minibus	3	3.4141	0.39	1.35	0.5265	3.5888
Mini truck	3.1	3.767	0.4	1.35	0.54	3.6323
Bus	3.4	4.9699	0.45	1.38	0.621	4.1235
Truck	3.6	5.8996	0.48	1.4	0.672	4.57625

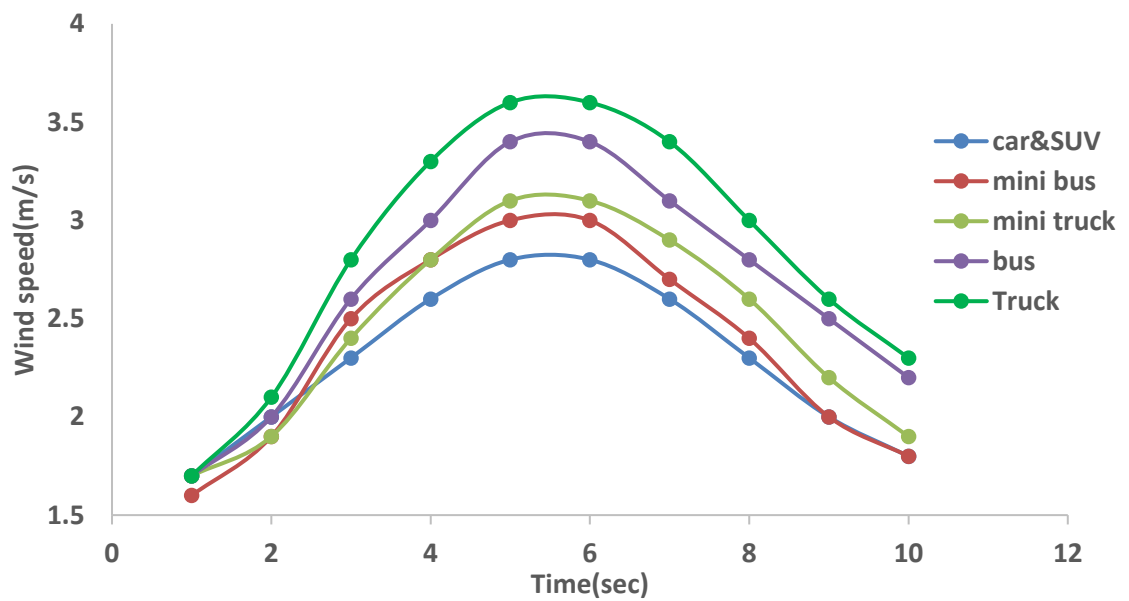


Figure 4.18. Comparison of the relationship of the wind speed and test time for the double turbine in single vehicle tests.

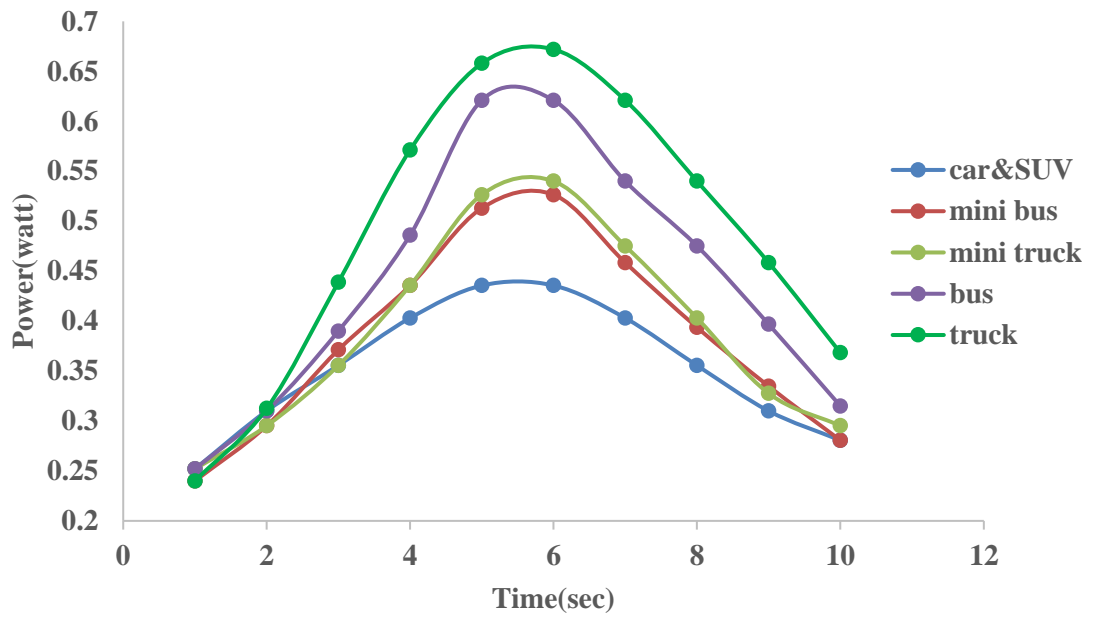


Figure 4.19. Comparison of the relationship of the power and test time for the double turbine in single vehicle tests.

Table 4.5 and Figures 4.18 and 4.19 demonstrably illustrate the turbine's efficiency in terms of power and energy conversion during truck passage tests for single-type vehicles. The data reveals a significant impact of wind vortices generated by the truck's size on the performance of this specific hybrid vertical turbine, and vertical turbines in general. This positive interaction between the turbine blades and the truck-induced wind turbulence is further evidenced by the power and energy results presented.

PART 5

CONCLUSION AND RECOMMENDATIONS

5.1. CONCLUSION OF DOUBLE TURBINE

- The proposed double turbine model exhibits versatility and consistent performance across diverse wind conditions.
- Turbine power is directly proportional to the double turbine's diameter, albeit within an optimal range.
- Maximum efficiency is achieved with a specific blade spacing of (15) cm between the Savonius and Darrieus components, while reduced spacing at (5) cm leads to decreased efficiency.
- A well-constructed iron frame significantly contributes to turbine efficiency by minimizing vibrations.
- The double turbines demonstrate effectiveness as power generators across various locations on the highway, yielding varying yet substantial results.
- The highest efficiency and optimal performance are attained when the double turbine is positioned at a distance of (100) cm from the highway's fastest side and at a height of (100) cm above the ground.
- Placement of the double turbine at a distance of (150) cm from the highway's fastest side results in reduced efficiency and performance.
- Discrepancies between wind speed and rotational speed adversely affect the power coefficient, stemming from either inadequate wind energy absorption or the redirection of wind vortices away from the double turbine.
- These conclusions underscore the potential of the proposed double turbine for harnessing wind energy along highways under varying conditions, emphasizing the importance of precise turbine geometry and positioning for optimal performance.

- In our experiments, probably our measurements were potentially susceptible to inaccuracies due to instrument limitations, environmental disturbances, and vehicle-airflow interactions, along with potential generator performance variations. Despite these uncertainties, observed trends provide strong support for our conclusions.

5.2. RECOMMENDATIONS AND SUGGESTION

- **Enhanced Double Turbine Design:** Consider further refinements to the double turbine's design, focusing on increasing its adaptability to varying wind conditions. This may involve exploring alternative blade configurations and materials to improve efficiency.
- **Optimized Blade Spacing:** Continue investigations into blade spacing, as optimizing this parameter could lead to even greater performance improvements. Conduct additional tests with blade spacings different from the (15) cm to identify potential gains in efficiency.
- **Strengthened Frame Construction:** Invest in the development of more robust and stable iron frames for the double turbines. Enhanced structural integrity will reduce vibrations, leading to increased turbine efficiency and longevity.
- **Turbine Maintenance and Reliability:** Develop maintenance protocols and routines to ensure the long-term reliability of the double turbines. Regular inspection and upkeep can extend their operational lifespan and efficiency.
- **Adding a gearbox or a transmission belt** between the rotating shaft and the motor, or both of them, to the proposed double turbine as it could give better results.
- **Continued Research:** Support ongoing research and development efforts to advance the field of wind energy and improve the efficiency and effectiveness of double turbines. Collaboration with experts and institutions can lead to innovations in turbine technology.
- **Cost-Benefit Analysis:** Perform a comprehensive cost-benefit analysis to evaluate the economic feasibility of deploying double turbines. This should consider initial installation costs, maintenance expenses, and the long-term benefits of energy generation.

REFERENCES

- [1] Y. Kumar *et al.*, "Wind energy: Trends and enabling technologies," *Renewable and Sustainable Energy Reviews*, vol. 53, pp. 209-224, 2016.
- [2] M. Seif, M. A. Warsame, and W. Kasima, "Wind energy: energy sustainability perspective," Department of Technical and Vocational Education (TVE), Islamic University ..., 2013.
- [3] D. Infield and L. Freris, *Renewable energy in power systems*. John Wiley & Sons, 2020.
- [4] M. A. Mac Kinnon, J. Brouwer, and S. Samuelsen, "The role of natural gas and its infrastructure in mitigating greenhouse gas emissions, improving regional air quality, and renewable resource integration," *Progress in Energy and Combustion science*, vol. 64, pp. 62-92, 2018.
- [5] R. Redlinger, P. Andersen, and P. Morthorst, *Wind energy in the 21st century: Economics, policy, technology and the changing electricity industry*. Springer, 2016.
- [6] M. Lutovska, V. Mijakovski, F. Mojsovski, and I. Shesho, *Review of Major Greenhouse gas emissions in Skopje*. 2019.
- [7] J. Liu, H. Lin, and J. Zhang, "Review on the technical perspectives and commercial viability of vertical axis wind turbines," *Ocean Engineering*, vol. 182, pp. 608-626, 2019.
- [8] M. K. Johari, M. Jalil, and M. F. M. Shariff, "Comparison of horizontal axis wind turbine (HAWT) and vertical axis wind turbine (VAWT)," *International Journal of Engineering and Technology*, vol. 7, no. 4.13, pp. 74-80, 2018.
- [9] A. Das and P. K. Talapatra, "Modelling and analysis of a mini vertical axis wind turbine," *International Journal of Emerging Technology and Advanced Engineering*, vol. 6, no. 6, pp. 184-194, 2016.
- [10] A. Rezaeiha, H. Montazeri, and B. Blocken, "Characterization of aerodynamic performance of vertical axis wind turbines: Impact of operational parameters," *Energy Conversion and Management*, vol. 169, pp. 45-77, 2018.
- [11] A. I. Altmimi, M. Alaskari, O. I. Abdullah, A. Alhamadani, and J. S. Sherza, "Design and optimization of vertical axis wind turbines using QBlade," *Applied System Innovation*, vol. 4, no. 4, p. 74, 2021.

- [12] R. N. Jarudkar and Y. P. Deshmukh, "Measurement and analysis for the improvement of efficiency and power of Savonius vertical axis wind turbines without dimples and fins," *Materials Today: Proceedings*, vol. 62, pp. 2016-2020, 2022.
- [13] G. Aboufaires, "Final thesis - ABOUFARES," 2015.
- [14] P. Fuglsang and K. Thomsen, "Site-specific design optimization of 1.5–2.0 MW wind turbines," *J. Sol. Energy Eng.*, vol. 123, no. 4, pp. 296-303, 2001.
- [15] K. Jackson, C. Van Dam, and D. Yen-Nakafuji, "Wind turbine generator trends for site-specific tailoring," *Wind Energy: An International Journal for Progress and Applications in Wind Power Conversion Technology*, vol. 8, no. 4, pp. 443-455, 2005.
- [16] H. Westlund and M. Wilhelmsson, "The socio-economic cost of wind turbines: A Swedish case study," *Sustainability*, vol. 13, no. 12, p. 6892, 2021.
- [17] S. R. Shah, R. Kumar, K. Raahemifar, and A. S. Fung, "Design, modeling and economic performance of a vertical axis wind turbine," *Energy Reports*, vol. 4, pp. 619-623, 2018.
- [18] A. Dhote and V. Bankar, "Design analysis and fabrication of Savonius vertical axis wind turbine," *International Research Journal of Engineering and Technology*, vol. 2, no. 3, pp. 2048-2054, 2015.
- [19] J. B. Damota, J. d. D. R. García, A. C. Casanova, J. T. Miranda, C. G. Caccia, and M. I. L. Galdo, "Analysis of a nature-inspired shape for a vertical axis wind turbine," *Applied Sciences*, vol. 12, no. 14, p. 7018, 2022.
- [20] S. M. Al Absi, A. H. Jabbar, S. O. Mezan, B. A. Al-Rawi, and S. T. Al_Attabi, "An experimental test of the performance enhancement of a Savonius turbine by modifying the inner surface of a blade," *Materials Today: Proceedings*, vol. 42, pp. 2233-2240, 2021.
- [21] M. Nasef, W. El-Askary, A. Abdel-Hamid, and H. Gad, "Evaluation of Savonius rotor performance: Static and dynamic studies," *Journal of Wind Engineering and Industrial Aerodynamics*, vol. 123, pp. 1-11, 2013.
- [22] R. Gupta, B. Deb, and R. Misra, "Performance analysis of a helical Savonius rotor with shaft at 45 twist angle using CFD," *Mechanical Engineering Research*, vol. 3, no. 1, p. 118, 2013.
- [23] M. Mohamed, G. Janiga, E. Pap, and D. Thévenin, "Optimization of Savonius turbines using an obstacle shielding the returning blade," *Renewable Energy*, vol. 35, no. 11, pp. 2618-2626, 2010.
- [24] K. Sobczak, D. Obidowski, P. Reorowicz, and E. Marchewka, "Numerical investigations of the savonius turbine with deformable blades," *Energies*, vol. 13, no. 14, p. 3717, 2020.

- [25] A. Ducoin, M. S. Shadloo, and S. Roy, "Direct Numerical Simulation of flow instabilities over Savonius style wind turbine blades," *Renewable energy*, vol. 105, pp. 374-385, 2017.
- [26] G. Ferrari, D. Federici, P. Schito, F. Inzoli, and R. Mereu, "CFD study of Savonius wind turbine: 3D model validation and parametric analysis," *Renewable energy*, vol. 105, pp. 722-734, 2017.
- [27] O. Yaakob, Y. M. Ahmed, and M. A. Ismail, "Validation study for Savonius vertical axis marine current turbine using CFD simulation," in *The 6th Asia-Pacific Workshop on Marine Hydrodynamics-APHydro2012*, 2012, pp. 3-4.
- [28] E. Kerikous and D. Thévenin, "Optimal shape of thick blades for a hydraulic Savonius turbine," *Renewable energy*, vol. 134, pp. 629-638, 2019.
- [29] D. H. Didane, M. A. Z. S. Anuar, M. F. M. Batcha, K. Abdullah, M. F. M. Ali, and A. N. Mohammed, "Simulation study on the performance of a counter-rotating savonius vertical axis wind turbine," *CFD Letters*, vol. 12, no. 4, pp. 1-11, 2020.
- [30] A. P. Díaz, G. J. Pajaro, and K. U. Salas, "Computational model of Savonius turbine," *Ingeniare. Revista chilena de ingeniería*, vol. 23, no. 3, pp. 406-412, 2015.
- [31] I. Marinić-Kragić, D. Vučina, and Z. Milas, "Computational analysis of Savonius wind turbine modifications including novel scooplet-based design attained via smart numerical optimization," *Journal of Cleaner Production*, vol. 262, p. 121310, 2020.
- [32] M. Kamoji, S. B. Kedare, and S. Prabhu, "Experimental investigations on single stage modified Savonius rotor," *Applied Energy*, vol. 86, no. 7-8, pp. 1064-1073, 2009.
- [33] F. Wenehenubun, A. Saputra, and H. Sutanto, "An experimental study on the performance of Savonius wind turbines related with the number of blades," *Energy procedia*, vol. 68, pp. 297-304, 2015.
- [34] J.-L. Menet, "A double-step Savonius rotor for local production of electricity: a design study," *Renewable energy*, vol. 29, no. 11, pp. 1843-1862, 2004.
- [35] F. Nobuyuki, "On the torque mechanism of Savonius rotors," *Journal of Wind Engineering and Industrial Aerodynamics*, vol. 40, no. 3, pp. 277-292, 1992.
- [36] A. Damak, Z. Driss, and M. Abid, "Experimental investigation of helical Savonius rotor with a twist of 180," *Renewable Energy*, vol. 52, pp. 136-142, 2013.
- [37] C. Jian, J. Kumbernuss, Z. Linhua, L. Lin, and Y. Hongxing, "Influence of phase-shift and overlap ratio on Savonius wind turbine's performance," 2012.

- [38] R. E. Sheldahl, B. F. Blackwell, and L. V. Feltz, "Wind tunnel performance data for two-and three-bucket Savonius rotors," *Journal of Energy*, vol. 2, no. 3, pp. 160-164, 1978.
- [39] M. Nakajima, S. Iio, and T. Ikeda, "Performance of Savonius rotor for environmentally friendly hydraulic turbine," *Journal of Fluid Science and Technology*, vol. 3, no. 3, pp. 420-429, 2008.
- [40] A. Alexander and B. Holownia, "Wind tunnel tests on a Savonius rotor," *Journal of Wind Engineering and Industrial Aerodynamics*, vol. 3, no. 4, pp. 343-351, 1978.
- [41] T. Hayashi, Y. Li, and Y. Hara, "Wind tunnel tests on a different phase three-stage Savonius rotor," *JSME International Journal Series B Fluids and Thermal Engineering*, vol. 48, no. 1, pp. 9-16, 2005.
- [42] U. Saha and M. J. Rajkumar, "On the performance analysis of Savonius rotor with twisted blades," *Renewable energy*, vol. 31, no. 11, pp. 1776-1788, 2006.
- [43] K. Irabu and J. N. Roy, "Characteristics of wind power on Savonius rotor using a guide-box tunnel," *Experimental thermal and fluid science*, vol. 32, no. 2, pp. 580-586, 2007.
- [44] M. Percival, P. Leung, and P. Datta, "The development of a vertical turbine for domestic electricity generation," in *European Wind Energy Conference*, 2004, pp. 22-25.
- [45] P. Ghiasi, G. Najafi, B. Ghobadian, A. Jafari, R. Mamat, and M. F. Ghazali, "CFD-Study of the H-Rotor Darrius wind turbine performance in Drag-Lift and lift Regime: Impact of Type, thickness and chord length of blades," *Alexandria Engineering Journal*, vol. 67, pp. 51-64, 2023.
- [46] M. Zamani, S. Nazari, S. A. Moshizi, and M. J. Maghrebi, "Three dimensional simulation of J-shaped Darrius vertical axis wind turbine," *Energy*, vol. 116, pp. 1243-1255, 2016.
- [47] A. Rezaeiha, I. Kalkman, and B. Blocken, "Effect of pitch angle on power performance and aerodynamics of a vertical axis wind turbine," *Applied energy*, vol. 197, pp. 132-150, 2017.
- [48] Y.-T. Lee and H.-C. Lim, "Numerical study of the aerodynamic performance of a 500 W Darrius-type vertical-axis wind turbine," *Renewable energy*, vol. 83, pp. 407-415, 2015.
- [49] S.-M. Lee and C.-M. Jang, "Performance Evaluation of a Small Darrius Wind Turbine Installed at Duckjeok Island in Korea," in *Fluids Engineering Division Summer Meeting*, 2016, vol. 50299: American Society of Mechanical Engineers, p. V01BT29A006.

- [50] R. Gosselin, G. Dumas, and M. Boudreau, "Parametric study of H-Darrieus vertical-axis turbines using CFD simulations," *Journal of Renewable and Sustainable Energy*, vol. 8, no. 5, 2016.
- [51] M. T. Asr, E. Z. Nezhad, F. Mustapha, and S. Wiriadidjaja, "Study on start-up characteristics of H-Darrieus vertical axis wind turbines comprising NACA 4-digit series blade airfoils," *Energy*, vol. 112, pp. 528-537, 2016.
- [52] C.-C. Chen and C.-H. Kuo, "Effects of pitch angle and blade camber on flow characteristics and performance of small-size Darrieus VAWT," *Journal of Visualization*, vol. 16, pp. 65-74, 2013.
- [53] H. Lei, D. Zhou, Y. Bao, Y. Li, and Z. Han, "Three-dimensional Improved Delayed Detached Eddy Simulation of a two-bladed vertical axis wind turbine," *Energy conversion and management*, vol. 133, pp. 235-248, 2017.
- [54] M. Mohamed, "Aero-acoustics noise evaluation of H-rotor Darrieus wind turbines," *Energy*, vol. 65, pp. 596-604, 2014.
- [55] R. Howell, N. Qin, J. Edwards, and N. Durrani, "Wind tunnel and numerical study of a small vertical axis wind turbine," *Renewable energy*, vol. 35, no. 2, pp. 412-422, 2010.
- [56] J. Weber, S. Becker, C. Scheit, J. Grabinger, and M. Kaltenbacher, "Aeroacoustics of Darrieus wind turbine," *International Journal of Aeroacoustics*, vol. 14, no. 5-6, pp. 883-902, 2015.
- [57] L. Du, R. G. Dominy, and A. Berson, "The prediction of the performance and starting capability of H-Darrieus wind turbines," in *Turbo Expo: Power for Land, Sea, and Air*, 2015, vol. 56802: American Society of Mechanical Engineers, p. V009T46A003.
- [58] A. Rossetti and G. Pavesi, "Comparison of different numerical approaches to the study of the H-Darrieus turbines start-up," *Renewable Energy*, vol. 50, pp. 7-19, 2013.
- [59] R. Patil, L. Daróczy, G. Janiga, and D. Thévenin, "Large eddy simulation of an H-Darrieus rotor," *Energy*, vol. 160, pp. 388-398, 2018.
- [60] R. Bravo, S. Tullis, and S. Ziada, "Performance testing of a small vertical-axis wind turbine," in *Proceedings of the 21st Canadian Congress of Applied Mechanics*, 2007, pp. 3-7.
- [61] L. Du, G. Ingram, and R. G. Dominy, "Experimental study of the effects of turbine solidity, blade profile, pitch angle, surface roughness, and aspect ratio on the H-Darrieus wind turbine self-starting and overall performance," *Energy Science & Engineering*, vol. 7, no. 6, pp. 2421-2436, 2019.
- [62] N. Batista, R. Melício, V. Mendes, M. Calderón, and A. Ramiro, "On a self-start Darrieus wind turbine: Blade design and field tests," *Renewable and Sustainable Energy Reviews*, vol. 52, pp. 508-522, 2015.

- [63] L. Battisti, A. Brighenti, M. R. Castelli, G. Persico, and V. Dossena, "Performance and midspan wake measurements on a H-Darrieus in controlled conditions," in *Journal of Physics: Conference Series*, 2018, vol. 1037, no. 2: IOP Publishing, p. 022041.
- [64] A. Bianchini, F. Balduzzi, G. Ferrara, and L. Ferrari, "Virtual incidence effect on rotating airfoils in Darrieus wind turbines," *Energy Conversion and Management*, vol. 111, pp. 329-338, 2016.
- [65] T. Maeda *et al.*, "Effect of solidity on aerodynamic forces around straight-bladed vertical axis wind turbine by wind tunnel experiments (depending on number of blades)," *Renewable energy*, vol. 96, pp. 928-939, 2016.
- [66] H. M. S. M. Mazarbhuiya, A. Biswas, and K. K. Sharma, "Performance investigations of modified asymmetric blade H-Darrieus VAWT rotors," *Journal of Renewable and Sustainable Energy*, vol. 10, no. 3, 2018.
- [67] A. C. Molina *et al.*, "Combined experimental and numerical study on the near wake of a Darrieus VAWT under turbulent flows," in *Journal of physics: Conference series*, 2018, vol. 1037, no. 7: IOP Publishing, p. 072052.
- [68] A. Sengupta, A. Biswas, and R. Gupta, "Studies of some high solidity symmetrical and unsymmetrical blade H-Darrieus rotors with respect to starting characteristics, dynamic performances and flow physics in low wind streams," *Renewable Energy*, vol. 93, pp. 536-547, 2016.
- [69] H. Dumitrescu, A. Dumitrache, C. Popescu, M. Popescu, F. Frunzulică, and A. Crăciunescu, "Wind tunnel experiments on vertical-axis wind turbines with straight blades," *Renewable Energy and Power Quality Journal*, vol. 1, no. 12, pp. 1001-1004, 2014.
- [70] N. M. Ali, S. Aljabair, and A. Abdul Hassan, "An experimental and numerical investigation on Darrieus vertical axis wind turbine types at low wind speed," *International Journal of Mechanical & Mechatronics Engineering IJMME-IJENS*, vol. 19, no. 06, pp. 97-110, 2019.
- [71] V. Patel, T. Eldho, and S. Prabhu, "Experimental investigations on Darrieus straight blade turbine for tidal current application and parametric optimization for hydro farm arrangement," *International journal of marine energy*, vol. 17, pp. 110-135, 2017.
- [72] A. Benzerdjeb, B. Abed, H. Achache, M. K. Hamidou, and A. M. Gorlov, "Experimental study on blade pitch angle effect on the performance of a three-bladed vertical-axis Darrieus hydro turbine," *International Journal of Energy Research*, vol. 43, no. 6, pp. 2123-2134, 2019.
- [73] A. Gharib-Yosry, E. Blanco-Marigorta, A. Fernández-Jiménez, R. Espina-Valdés, and E. Álvarez-Álvarez, "Wind–water experimental analysis of small sc-darrieus turbine: an approach for energy production in urban systems," *Sustainability*, vol. 13, no. 9, p. 5256, 2021.

- [74] E. Erwin, S. Wiyono, M. Iqbal, and H. M. Yusuf, "The effect of steering tail fin on performance on double pillars hybrid vertical axis wind turbine (Sultan Wind Turbine V-4.5)," *Teknika: Jurnal Sains dan Teknologi*, vol. 18, no. 2, pp. 150-157, 2022.
- [75] D. Didane, S. Maksud, M. Zulkafli, N. Rosly, S. Shamsudin, and A. Khalid, "Experimental Study on the Performance of a Savonius-Darrius Counter-Rotating Vertical Axis Wind Turbine," in *IOP Conference Series: Earth and Environmental Science*, 2019, vol. 268, no. 1: IOP Publishing, p. 012060.
- [76] K. M. Krishna, S. Prathap, and K. L. Chandra, "Hybrid Power Generation System using Solar and Wind Energy," *International Journal of Engineering Research*, vol. 5, no. 03, 2016.
- [77] T. Salih, Y. Wang, and M. A. A. Adam, "Renewable micro hybrid system of solar panel and wind turbine for telecommunication equipment in remote areas in Sudan," *Energy Procedia*, vol. 61, pp. 80-83, 2014.
- [78] A. T. Nugraha and D. Priyambodo, "Prototype hybrid power plant of solar panel and vertical wind turbine as a provider of alternative electrical energy at Kenjeran beach Surabaya," *Journal of Electronics, Electromedical Engineering, and Medical Informatics*, vol. 2, no. 3, pp. 108-113, 2020.
- [79] B. Prashanth, R. Pramod, and G. V. Kumar, "Design and development of hybrid wind and solar energy system for power generation," *Materials Today: Proceedings*, vol. 5, no. 5, pp. 11415-11422, 2018.
- [80] H. Sun, X. Luo, and J. Wang, "Feasibility study of a hybrid wind turbine system—Integration with compressed air energy storage," *Applied Energy*, vol. 137, pp. 617-628, 2015.
- [81] B. S. Borowy and Z. M. Salameh, "Optimum photovoltaic array size for a hybrid wind/PV system," *IEEE Transactions on energy conversion*, vol. 9, no. 3, pp. 482-488, 1994.
- [82] Q. Huang, Y. Shi, Y. Wang, L. Lu, and Y. Cui, "Multi-turbine wind-solar hybrid system," *Renewable Energy*, vol. 76, pp. 401-407, 2015.
- [83] A. Haddad, M. Ramadan, M. Khaled, H. S. Ramadan, and M. Becherif, "Triple hybrid system coupling fuel cell with wind turbine and thermal solar system," *International journal of hydrogen energy*, vol. 45, no. 20, pp. 11484-11491, 2020.
- [84] A. Al-Aqel, B. Lim, E. M. Noor, T. C. Yap, and S. Alkaff, "Potentiality of small wind turbines along highway in Malaysia," in *2016 International Conference on Robotics, Automation and Sciences (ICORAS)*, 2016: IEEE, pp. 1-6.
- [85] S. Rana, B. Roy, B. B. Saha, and S. Ghosh, "Energy Harvesting from Highway Traffic Vehicles Movement via VAWT," 2022.

- [86] E. H. Bani-Hani, A. Sedaghat, M. Al-Shemmary, A. Hussain, A. Alshaieb, and H. Kakoli, "Feasibility of highway energy harvesting using a vertical axis wind turbine," *Energy Engineering*, vol. 115, no. 2, pp. 61-74, 2018.
- [87] K. Mithun Raj and S. Ashok, "Design and simulation of a vertical axis wind turbine for highway wind power generation," *International Journal of Electrical and Electronics Engineers*, vol. 7, no. 01, pp. 251-259, 2015.
- [88] S. Santhakumar, I. Palanivel, and K. Venkatasubramanian, "A study on the rotational behaviour of a Savonius Wind turbine in low rise highways during different monsoons," *Energy for Sustainable Development*, vol. 40, pp. 1-10, 2017.
- [89] S. Hussain, "Wind Turbine for Power Generation and Storage by Vehicular Movement on Highways with IoT," *Turkish Journal of Computer and Mathematics Education (TURCOMAT)*, vol. 12, no. 13, pp. 311-318, 2021.
- [90] S. A. Kulkarni and M. Birajdar, "Vertical axis wind turbine for highway application," *Imp. J. Interdiscip. Res.*, vol. 2, no. 10, pp. 1543-1546, 2016.
- [91] M. Z. Mazlan, F. M. Zawawi, T. Tahzib, K. Ismail, and S. Samion, "Performance analysis of highway wind turbine enhanced with wind guide vanes using the Taguchi method," *CFD Letters*, vol. 13, no. 3, pp. 25-42, 2021.
- [92] S. Toudarbari, M. J. Maghrebi, and A. Hashemzadeh, "Evaluation of Darrieus wind turbine for different highway settings using CFD simulation," *Sustainable Energy Technologies and Assessments*, vol. 45, p. 101077, 2021.
- [93] T. Morbiato, C. Borri, and R. Vitaliani, "Wind energy harvesting from transport systems: A resource estimation assessment," *Applied Energy*, vol. 133, pp. 152-168, 2014.
- [94] P. Fuglsang *et al.*, "Site-specific design optimization of wind turbines," *Wind Energy: An International Journal for Progress and Applications in Wind Power Conversion Technology*, vol. 5, no. 4, pp. 261-279, 2002.
- [95] M. Stiebler, *Wind energy systems for electric power generation*. Springer Science & Business Media, 2008.
- [96] L. Pearce Williams, "Faraday's discovery of electromagnetic induction," *Contemporary Physics*, vol. 5, no. 1, pp. 28-37, 1963.
- [97] E. Hermans, F. Van den Bossche, and G. Wets, "Uncertainty assessment of the road safety index," *Reliability Engineering & System Safety - RELIAB ENG SYST SAFETY*, vol. 94, 11/08 2008, doi: 10.1016/j.ress.2008.09.004.
- [98] S. Roy and U. K. Saha, "An adapted blockage factor correlation approach in wind tunnel experiments of a Savonius-style wind turbine," *Energy Conversion and Management*, vol. 86, pp. 418-427, 2014.


APPENDIX A.

A: The tachometer




Technical data					
Basic function	Range	Basic accuracy			
		DT-2234A	DT-2234B	DT-2234C	DT-2235B
Photoelectric rotation speed	2.5~9999RPM(r/min)	$\pm(0.05\%+1\text{digit})$	$\pm(0.05\%+1\text{digit})$	$\pm(0.05\%+1\text{digit})$	
Contact rotation speed	0.5~19,999RPM (r/min)				$\pm(0.05\%+1\text{digit})$
Special function	DT-2234A	DT-2234B	DT-2234C	DT-2235B	
Measuring way	LED photoelectric	LED photoelectric	Laser photoelectric	touched	
Resolution	0.1RPM (2.5~999.9RPM) 1RPM(over 1000RPM)	0.1RPM (2.5~999.9RPM) 1RPM(over 1000RPM)	0.1RPM (0.5~999.9RPM) 1RPM(over 1000RPM)	Contact rotation speed: 0.1RPM (0.5~999.9RPM) 1RPM (over 1000RPM)	
Sampling time	0.5s(over 120RPM)	0.5s(over 120RPM)	0.5s(over 120RPM)	0.5s(over 120RPM)	
Range selection	Auto switch	Auto switch	Auto switch	Auto switch	
Effective distance	50mm~250mm	50mm~250mm	50mm~250mm		
Power Consumption	Max. 40mA	Max. 40mA	Max. 45mA	Max. 45mA	
Memory	Auto memory Max./Min. last value	Auto memory Max./Min. last value	Auto memory Max./Min. last value	Auto memory Max./Min. last value	
Time Base	6MHz Quartz crystal	6MHz Quartz crystal	6MHz Quartz crystal	6MHz Quartz crystal	
BatteryAccuracy of time base	10×10^{-6} (0°C~50°C)	10×10^{-6} (0°C~50°C)	10×10^{-6} (0°C~50°C)	10×10^{-6} (0°C~50°C)	
Battery	4X1.5V AA Size Battery	4X1.5V AA Size Battery	4X1.5V AA Size Battery	4X1.5V AA Size Battery	
Size	160mm×72mm×37mm	184mm×76mm×30mm	184mm×76mm×30mm	184mm×76mm×30mm	
Max. display	99999	99999	99999	99999	
LCD size	5digits 18mm	5digits 18mm	5digits 18mm	5digits 18mm	

B: The Anemometer



MODEL: GM816

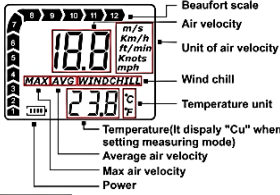
**Anemometer
Instruction manual**



A. FUNCTION

- Air Velocity & Temperature Measurement;
- Max/Average/Current air velocity measurement;
- C/F Temperature unit selection;
- Five units of air velocity:
M/s, Km/h, ft/min, Knots, mph
- Beaufort scale;
- Backlight display;
- Manual/Auto power shut off;
- Wind chill indication;
- Low battery indication.

B. LCD Display



C. Operation

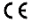

- Turn on:** Press "MODE" button for 2 seconds to turn on the unit. LCD will display Air velocity, temperature and battery icon. LCD backlight will last for 12 seconds.
- Set unit of air velocity and measuring mode:**
Press "MODE" button more than 3 seconds until "m/s" starts to blink. Press "SET" button to select desired air velocity unit. To confirm the unit, press "MODE" button. For setting MAX/AVG/CU mode, press "SET" button again and again until CU/MAX/AVG blink, then press "MODE" button to confirm.
 - The setting will be stored when turn off the unit. But if you change the battery, the setting will go back to the factory preset.
 - Unit of Air velocity: m/s, Km/hr, ft/min, Knots, mph
 - Measuring mode: CU: current air velocity
MAX: max air velocity AVG: average air velocity

- Set temperature unit:**
Temperature switch key (C/F) conceal in the rear cabinet, please use a little push-pin to press the key for C/F conversion.
- Backlight display:** The backlight will be activated for 12 seconds by press any key
- Measurement:** when the wind vane (impeller) turns, LCD will instant display wind speed, temperature and beaufort scale. When temperature below 0 °C, "WIND CHILL" will be shown on the LCD.
- Turn off:** Press "MODE" + "SET" buttons at the same time to turn off the unit.
- Auto power shut off:** The unit will be shut off without any operation for 14 minutes
- Change battery:** When the symbol "⎓" shown on the LCD, please change the battery.

D. Specification

A. Air velocity				
Unit	Range	Resolution	Threshold	Accuracy
M/s	0-30	0.1	0.1	±5%
ft/min	0-5680	19	39	
Knots	0-55	0.2	0.1	
Km/hr	0-90	0.3	0.3	
Mph	0-65	0.2	0.2	
B. Temperature				
Unit	Range	Resolution	Accuracy	
°C	-10°C→+45°C	0.2	±2°C	
°F	14°F→113°F	0.36	±3.6°F	
Battery	CR2032 3.0V (Included)			
Thermometer	NTC thermometer			
Operating temperature	-10°C→+45°C(14°F→113°F)			
Operating humidity	Less than 90%RH			
Store temperature	-40°C→+60°C(-40°F→140°F)			
Current consumption	Approx. 3mA			
Weight	52g			
Dimension	40x18x105mm			

Specific Declarations:
Our company shall hold no any responsibility resulting from using output from this product as an direct or indirect evidence.
We reserves the right to modify product design and specification without notice.

C: The Clamp Meters



MASTECH®

DIGITAL CLAMP METERS

DIGITAL AC CLAMP METER

M266/M266C/M266F

M266

JAW SIZE
Φ50mm/2.0"

VOLTAGE AC 750V
DC 1000V

CURRENT
AC 1000A

V A Ω
Hz

M266C

JAW SIZE
Φ50mm/2.0"

VOLTAGE AC 750V
DC 1000V

CURRENT
AC 1000A

V A Ω
°F/°C Hz

M266F

JAW SIZE
Φ50mm/2.0"

VOLTAGE AC 750V
DC 1000V

CURRENT
AC 1000A

V A Ω
Hz

Features:

- Jaw Size: Φ50mm/2.0"
- Tests AC/DC Voltage, AC Current, Resistance and Frequency
- Type-K Thermocouple Contact Temperature Measurement (M266)
- Diode Check and Continuity Test
- Data Hold

EMC LVD CE ETL CAT.II 1000V CAT.III 600V RoHS

Specifications	Range	M266	M266C	M266F
		Accuracy		
DC Voltage	200mV		±(0.5%+1)	
	2V/20V/200V		±(0.5%+3)	±(0.5%+3)
	1000V	±(0.8%+3)	±(0.8%+3)	±(0.8%+3)
AC Voltage	200V		±(1.0%+5)	±(1.0%+5)
	750V	±(1.2%+5)	±(1.2%+5)	±(1.2%+5)
	20A	±(2.5%+5)	±(2.5%+5)	±(2.5%+5)
AC Current	1000A	±(3.0%+10)	±(3.0%+10)	±(3.0%+10)
	200Ω/20kΩ			
	200Ω/2kΩ/20kΩ/200kΩ/2MΩ	±(1.0%+8)		±(1.0%+8)
Resistance	200Ω/20kΩ/2MΩ		±(1.0%+8)	
Frequency	2kHz			±(2.0%+5)
Temperature(°C)	0°C-750°C		±(2.0%+2)	
Temperature(°F)	32°F-1400°F		±(2.0%+4)	
Features				
Display	counts	2000	2000	2000
Jaw Opening		Φ50mm/2.0"	Φ50mm/2.0"	Φ50mm/2.0"
Insulation Test	With optional 500V insulation tester unit	●	●	●
Diode	2.7V	●	●	●
Continuity Buzzer	<50Ω	●	●	●
Data Hold		●	●	●
General				
Power Supply	1×9V 6F22 Battery	●	●	●
Product Size	235mm×96mm×46mm/ 9.25"×3.8"×1.8"	●	●	●
Product Weight	268g/0.59lb	●	●	●
Safety Rating	CAT. II 1000V CAT. III 600V	CE ETL	CE ETL	CE ETL

83



Laser Rangefinders from Bosch

More range, more functionality



Type	GLM 30 Professional	GLM 40 Professional	GLM 500 Professional	GLM 50 C Professional	GLM 80 Professional	GLM 100 C Professional	GLM 150 C Professional	GLM 250 VF Professional
Measuring range	0.15-30 m	0.05-40 m	0.05-50 m	0.05-50 m	0.05-80 m	0.05-100 m	400 feet/ 150 m	0.05-250 m
Typical measuring accuracy	± 2 mm	± 1.5 mm	± 0.2 mm	± 1.5 mm	± 1.5 mm	± 1.5 mm	± 1.5 mm	± 1.0 mm
Lowest indication unit	-	1 mm	0.1 mm	0.1 mm	-	-	-	-
Battery service life, (approx.)								
- Individual measurements	5000	5000	10,000	10,000	25,000	25,000	25,000	30,000
- Continuous measurements	-	-	-	-	-	-	-	5 h
Power supply batteries	2 x 1.5 VLR03 (AAA)	2 x 1.5 VLR03 (AAA)	2 x 1.5 VLR03 (AAA)	2 x 1.5 VLR03 (AAA)	1 x 3.7 V Li-on battery (1250 mAh)	1 x 3.7 V Li-on battery (1250 mAh)	3 x quality AA Alkaline batteries	4 x 1.5V (AAA) batteries
Dust and splash protection / Display	IP 54	IP 54	IP 54	IP 54	IP 54	IP 54	2.8 inch IPS colour display	IP 54
Automatic switch off after (approx.)	5 min. (tool)	20 s (laser) 5 min. (tool)	5 min.	5 min.	5 min.	5 min.	5 min.	5 min.
Units of measure	m, ft, inch	m, ft, inch	m/cm, ft/inch	m/cm, ft/inch	m/cm/mm	m/cm/mm	m/cm/mm	m/cm/mm
Dimensions (L/W/H)	105mm x 41mm x 24mm	105mm x 41mm x 24mm	106mm x 45mm x 24mm	106mm x 45mm x 24mm	111mm x 51mm x 30mm	111mm x 51mm x 30mm	111mm x 51mm x 30mm	120mm x 66mm x 37mm
Weight	0.1kg	0.1kg	0.1kg	0.1kg	0.14kg	0.14kg	0.14kg	0.24kg
Comes complete with	2 x 1.5 VLR03 (AAA) batteries, manufacturer's certificate	2 x 1.5 VLR03 (AAA) batteries, manufacturer's certificate	2 x 1.5 VLR03 (AAA) batteries, manufacturer's certificate	2 x 1.5 VLR03 (AAA) batteries, manufacturer's certificate	1 x 3.7 V Li-on batteries, manufacturer's certificate	Protective case, micro USB, charger, micro USB data cable, manufacturer's certificate	Protective case, micro USB, charger, micro USB data cable, manufacturer's certificate	4 x 1.5V (AAA) batteries, carrying strap, protective pouch, manufacturer's certificate
Laser class	2	2	2	2	635 Nm, < 1mW	2	2	2
Laser diode	635 Nm, < 1mW	635 Nm, < 1mW	635 Nm, < 1mW	635 Nm, < 1mW	-	635 nm/ < 1 mW/2	635 nm/ < 1 mW/2	635 nm/ < 1 mW/2
Incline measurement	-	-	-	-	-	± 60°vertical/360° horizontal (4 x 90°)	± 60°vertical/360° horizontal (4 x 90°)	± 60°vertical/360° horizontal (4 x 90°)
Accuracy of incline measurement	-	-	-	-	-	± 0.2°	± 0.2°	± 0.2°
Tripod thread	-	-	1.4"	1.4"	-	-	Plastic, 1/4 inch	Plastic, 1/4 inch
Camera	-	-	-	-	-	-	+ Zoom	+ Zoom
Connectivity	-	-	-	Bluetooth smart (low Energy)	-	Bluetooth smart (low Energy)	Bluetooth smart (low Energy)	Bluetooth smart (low Energy)
Memory capacity	-	10 measurements	20 measurement	30 measurements	20 measurement	50 measurements + 1 Constant	50 measurements	50 measurements
Integrated telescopic viewfinder	-	-	-	-	-	-	-	Yes

D: The Distance measurement



Laser Rangefinders from Bosch More range, more functionality



Type	GLM 30 Professional	GLM 40 Professional	GLM 500 Professional	GLM 50 C Professional	GLM 80 Professional	GLM 100 C Professional	GLM 150 C Professional	GLM 250 VF Professional
Measuring range	0.15-30m	0.05-40m	0.05-50m	0.05-50m	0.05-80m	0.05-100m	400 feet/150m	0.05-250 m
Typical measuring accuracy	± 2 mm	± 1.5 mm	± 0.2 mm	± 1.5 mm	± 1.5 mm	± 1.5 mm	± 1.5 mm	± 1.0 mm
Lowest indication unit	-	1 mm	0.1 mm	0.1 mm	-	-	-	-
Battery service life, (approx.)								
- Individual measurements	5000	5000	10,000	10,000	25,000	25,000	25,000	30,000
- Continuous measurements	-	-	-	-	-	-	-	5 h
Power supply batteries	2 x 1.5 V LR03 (AAA)	2 x 1.5 V LR03 (AAA)	2 x 1.5 V LR03 (AAA)	2 x 1.5 V LR03 (AAA)	1 x 3.7 V Li-ion battery (1250 mAh)	1 x 3.7 V Li-ion battery (1250 mAh)	3 x quality AA Alkaline batteries	4 x 1.5 V (AAA) batteries
Dust and splash protection / Display	IP 54	IP 54	IP 54	IP 54	IP 54	IP 54	2.8 inch IPS colour display	IP 54
Automatic switch off after (approx.)	5 min. (tool)	20 s (laser) 5 min. (tool)	5 min.	5 min.	5 min.	5 min.	5 min.	5 min.
Units of measure	m, ft, inch	m, ft, inch	m/cm, ft/inch	m/cm, ft/inch	m/cm/mm	m/cm/mm	m/cm/mm	m/cm/mm
Dimensions (L/W/H)	105mm x 41mm x 24mm	105mm x 41mm x 24mm	106mm x 45mm x 24mm	106mm x 45mm x 24mm	111mm x 51mm x 30mm	111mm x 51mm x 30mm	111mm x 51mm x 30mm	120mm x 66mm x 37mm
Weight	0.1kg	0.1kg	0.1kg	0.1kg	0.14kg	0.14kg	0.14kg	0.24kg
Comes complete with	2 x 1.5 V LR03 (AAA) batteries, manufacturer's certificate	2 x 1.5 V LR03 (AAA) batteries, manufacturer's certificate	2 x 1.5 V LR03 (AAA) batteries, manufacturer's certificate	2 x 1.5 V LR03 (AAA) batteries, manufacturer's certificate	1 x 3.7 V Li-ion batteries, manufacturer's certificate	Protective case, micro USB, charger, micro USB data cable, manufacturer's certificate	Protective case, micro USB, charger, micro USB data cable, manufacturer's certificate	4 x 1.5 V (AAA) batteries, carrying strap, protective pouch, manufacturer's certificate
Laser class	2	2	2	2	635 nm, < 1mW	2	2	2
Laser diode	635 nm, < 1mW	635 nm, < 1mW	635 nm, < 1mW	635 nm, < 1mW	-	635 nm/ < 1 mW/2	635 nm/ < 1 mW/2	635 nm/ < 1 mW/2
Incline measurement	-	-	-	-	-	± 60° vertical/360° horizontal (4 x 90°)	± 60° vertical/360° horizontal (4 x 90°)	± 60° vertical/360° horizontal (4 x 90°)
Accuracy of incline measurement	-	-	-	-	-	± 0.2°	± 0.2°	± 0.2°
Tripod thread	-	-	1.4"	1.4"	-	-	Plastic, 1/4 inch	Plastic, 1/4 inch
Camera	-	-	-	-	-	-	+ Zoom	+ Zoom
Connectivity	-	-	-	Bluetooth smart (low Energy)	-	Bluetooth smart (low Energy)	Bluetooth smart (low Energy)	Bluetooth smart (low Energy)
Memory capacity	-	10 measurements	20 measurement	30 measurements	20 measurement	50 measurements + 1 Constant	50 measurements	50 measurements
Integrated telescopic viewfinder	-	-	-	-	-	-	-	Yes

CURRICULUM VITAE

Osama Ahmed KAZAL, mechanical engineer, graduated from the College of Engineering, Al-Mustansiriya University, Iraq. he obtained her bachelor's degree in 2008. he is currently studying for a master's degree at Karabük University in the field of mechanical engineering